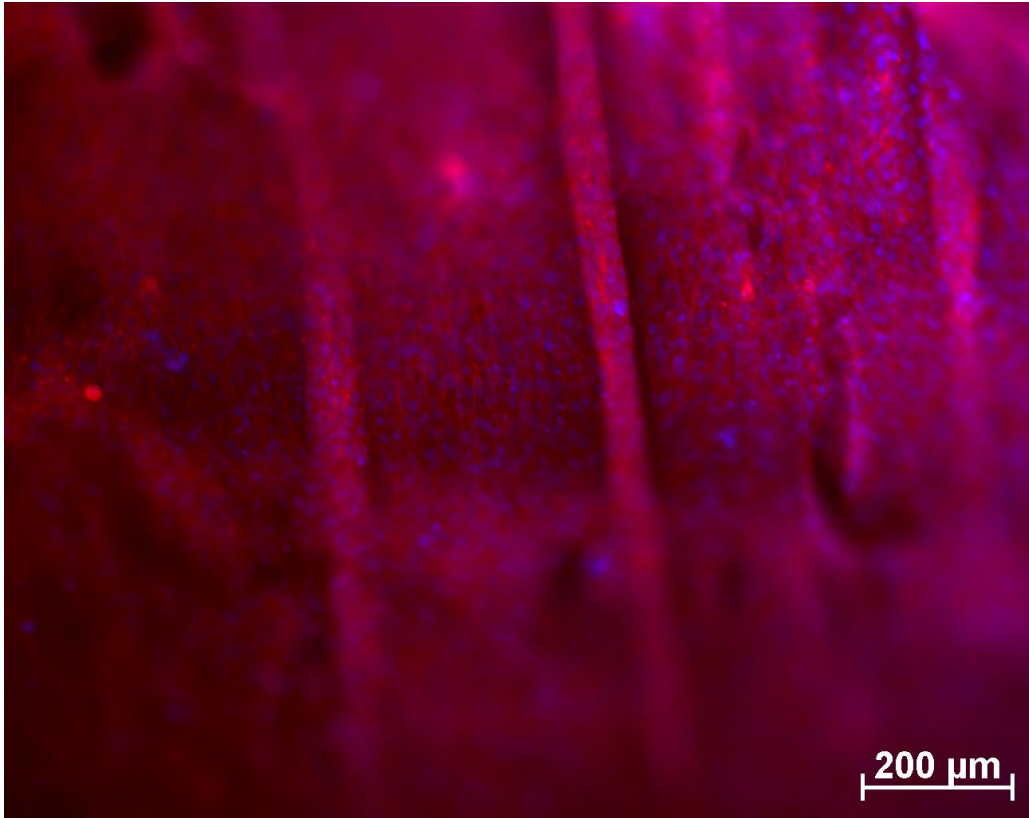




CHALMERS
UNIVERSITY OF TECHNOLOGY



Skeletal Muscle Differentiation in 3D Capillary Gels

Development of a Novel Bioreactor

Master's thesis in Biomedical Engineering

FELIX KLOSE

THESIS FOR THE DEGREE OF MASTER OF
SCIENCE

Skeletal Muscle Differentiation in 3D Capillary Gels

Development of a Novel Bioreactor

FELIX KLOSE



CHALMERS
UNIVERSITY OF TECHNOLOGY

Department of Applied Physics
CHALMERS UNIVERSITY OF TECHNOLOGY
Gothenburg, Sweden 2016

Skeletal Muscle Differentiation in 3D Capillary Gels

Development of a Novel Bioreactor

FELIX KLOSE

© FELIX KLOSE 2016

Cover Illustration:

C2C12 cell culture on capillary RGDA:alginate 1:5 after 8 days of culture

Layout and Design:

Felix Klose

Printed by:

Chalmers Reproservice
Gothenburg, Sweden, 2016

Abstract

Skeletal muscle tissue contributes to many functions in the human body such as locomotion and maintaining the body temperature. Tissue engineering could open up possibilities of grafting muscle tissue *ex vivo* and make way for new autologous treatments mitigating pathological muscle loss. Additionally, skeletal muscle tissue of mammal origin is one of the main nutritional protein sources in the western diet. Also here the production of skeletal muscle tissue *ex vivo* could provide measures to reduce environmental strains due to conventional live-stock production and produce food in a more resource efficient manner. Until a market maturity is achieved, methods have to be found to produce cells in high enough numbers and the differentiation has to be ensured to allow for functional tissue for medical applications and nutritionally valuable food. Additionally, the production of larger tissue-engineered constructs is challenging due to the absence of a perfusion network bringing the nutrients and oxygen deep into the constructs.

The aim of the project is to grow parallel aligned muscle fibres in a three dimensional scaffold with the help of a perfusion bioreactor. The approach was to grow and differentiate C2C12 mouse myogenic progenitor cells inside capillary alginate gels. It was hypothesized that the parallel aligned capillary structure inside the gels could help the alignment of the muscle fibres and prospectively be used in generating muscle constructs closer to physiological muscle found in mammals. In order to promote cell attachment to the gels, different modifications of the alginate gel have been performed. Bulk modifications have been achieved by mixing pure alginate solutions with pre-coupled RGD-alginate or gelatin solutions prior to crosslinking. Furthermore, surface modifications have been performed via collagen coatings or carbodiimide coupling of RGD peptides to the surfaces of crosslinked alginate gels.

Cell cultures were performed on the surface of samples cut from these gels to evaluate the attachment improvement of the various modifications and to study the influences of the capillaries on alignment of the cells. In addition to the cultures the scaffolds have been investigated by light and confocal microscopy. For three dimensional cell cultures a perfusion bioreactor has been designed. Computer-based simulations have been performed for *in silico* evaluations of the flow and oxygen distribution inside the bioreactor and the capillaries of the alginate gels. Eventually, the bioreactor and the RGD:alginate bulk modified gels were combined in 3D culture experiments to characterize the culture setup in different operational modes, to formulate protocols and to test the feasibility of the experimental setup for cell growth and differentiation.

As a result of this project, a bioreactor system has been developed allowing for future investigations of capillary alginate gels as a culturing scaffold for skeletal muscle progenitor cells. The bulk modification with RGD-alginate seems to be most beneficial in growing high cell numbers and achieving good attachment quality of the cells to the alginate gels. Optimization of the sterilization techniques in concert with improved modifications of the alginate scaffold to better present the functional groups to the cells could lead to more promising results of the cell cultures. CaCl_2 is recommended to be replaced by another crosslinking agent because the gels crosslinked with Ca^{2+} do not have the necessary structural integrity throughout the cell culture. A switch to covalently bound gels and more careful tailoring of the scaffold properties, e.g. elastic modulus, stress relaxation behaviour, could improve the outcome of the cell cultures. This project serves as a basis for future advancements in culturing skeletal muscle cells *in vitro* for nutritional as well as medical applications.

Keywords

Tissue engineering, C2C12 muscle cells, capillary alginate, scaffold, modifications, bioreactor, 3D cell culture, simulations

Acknowledgements

First of all, I would like to thank my supervisors Julie Gold and Patric Wallin for giving me the opportunity to pursue my master thesis in the topic of my choice and giving me the freedom to follow my own curiosity during this last year. For giving me the support I needed and having a friendly ear for me, even when their own time was running low. Thank you for the many hours of nice discussions and being committed way beyond your supervising duties.

The next thanks goes to Anna Ström (Chemistry and Chemical Engineering, Chalmers) and Erich Schuster (SIK, SP Sverige) my collaborators for their help and insights into the chemistry of capillary alginate gels. Furthermore, thanks for spending some of your valuable measurement time on my gelatin:alginate. All your help is greatly appreciated.

Of course a special thanks to the group of biological physics for not only supporting me with my technical problems but for keeping the spirits up throughout the project. I enjoyed the Fikas a lot and the many inspiring discussions we shared. Especially I would like to thank Hudson Pace and Noomi Altgårde for helping me with my surface coupling and other chemical endeavours. To Karin Norling who supported me in my project together with a student group of the tissue engineering course and for letting me co-supervise the group as well. And again a bid thanks to all the unmentioned members of the group.

Furthermore, I would like to mention Bo Peng, Elin Pernevik and Yovanna Gonzalez who started the student project together with me that would be the starting point for this great project. Thank you for the project work, the countless hours in the computer cabinet and all the fun moments we shared.

A special thanks goes to my family who strongly encouraged me and had my back at any given time to let me stay focused on my studies and work. Your help in fighting with offices and car problems ensured my years in Sweden. Thanks for the nice visits during the past two years and for the ones to come. Know that you are always welcome to pay a visit. With this a special thanks goes to my beloved mother who always encouraged me to push for the best, supported me with her everlasting bright and optimistic nature and taught me to stay positive through all the tough times.

The next big thanks goes to the person that reminded me to relax, when I just got too heated up about my project. Especially during the report writing, that reminder was necessary when fighting with formatting issues or while trying to keep it all together. Thank you Orlando, for your ongoing support and how you carry me through those sometimes hectic states of mind. Your ability to calm me down and get my mind off my work is amazing and I love you for it. Thank you.

I want to thank my many friends, the ones back in Germany, the new ones I had the pleasure to get to know here in Sweden and the other ones scattered all over the world. Thank you for being there for me when I needed moral support and also helping me to keep me free from bureaucratic hurdles throughout the years. Thank you for the great times during Afterwork, all the other nice times spend together and all the nice times to come in the future.

Again a big thanks to everybody, that made my learning experience here at Chalmers and my thesis project an amazing experience. This thesis is going to be the stepping stone into the next chapter of my academic career. It convinced me to take the plunge into doctoral studies and I am thrilled for the things to come. All those people that supported me and made this exciting journey possible, I want them to keep in mind that every single contribution from their side enables me to pursue my wish in becoming a doctoral student and to venture further into the next big adventure called research.

Table of Contents

Table of Abbreviations	XI
1 Introduction	1
2 Objective & Purpose	3
3 Background	5
3.1 Muscle Tissue	5
3.1.1 Physiological Basics of Muscle Tissue	5
3.1.2 Challenges and Applications for In Vitro Grown Muscle	7
3.2 Bioreactors	9
3.3 Scaffolds	10
3.3.1 Alginate as Scaffolding Material	10
3.3.2 Modifications for Improved Cell Attachment	11
3.4 Cells	12
3.4.1 Choosing the right cell line – C2C12 cell line	12
3.4.2 Cell-Environment Interactions	14
3.5 Sterility	16
3.6 Measurement Techniques	17
3.6.1 Light Microscopy	17
3.6.2 Immunostaining	19
3.6.3 Fluorescence Microscopy	20
3.6.4 Confocal Microscopy	23
4 Materials & Methods	25
4.1 Approach	25
4.2 Bioreactor	26
4.2.1 Simulations	26
4.2.2 Design and Manufacturing	29
4.2.3 Leakage Experiments and Flow Through	31
4.3 Scaffolds	31
4.3.1 Alginate Gel Formation	31
4.3.2 Formation of Capillary Alginate Gels	31
4.3.3 Modification of Alginate Gels	32
4.3.4 Sterilization	35
4.4 Cells	36
4.4.1 Flat Gel Experiments	36
4.4.2 PDMS dish Cell Cultures	38
4.4.3 3D Cell Cultures	43
4.4.4 Staining & Fixation	47

5 Results	49
5.1 Bioreactor	49
5.1.1 Simulations	49
5.1.2 Leakage and Operability of the Bioreactor	52
5.2 Scaffold	54
5.2.1 Alginate	54
5.2.2 Gelatin:Alginate	56
5.2.3 RGD Modified Alginate	57
5.2.4 Sterilization	58
5.3 Cells	59
5.3.1 Flat Gel Experiments	59
5.3.2 PDMS Dish Experiments	62
5.3.3 3D Cell Seeding	67
5.3.4 3D Cell Cultures	70
6 Discussion	73
6.1 Bioreactor	73
6.1.1 Simulations	73
6.1.2 Design of the Bioreactor	74
6.2 Scaffold	76
6.2.1 Alginate a Feasible Scaffolding Material?	76
6.2.2 Scaffold Modifications	78
6.2.3 Optimization of the Protocols	80
6.3 Cells	80
6.3.1 Culturing Techniques	80
6.3.2 Operations Mode	82
6.3.3 Sterility during the cell culture	83
7 Summary and Conclusions	85
8 Future Outlook	87
Bibliography	89

Appendices	95
1 List of Materials	95
2 PDMS Protocol	96
3 Sterilization Protocol	97
4 Capillary Alginate Protocol	98
5 Two-Step coupling of Proteins Using EDS and NHS or Sulfo-NHS	99
6 Collagen Coating Protocol	100
7 NucBlue Protocol	101
8 Cell Seeding Protocol	102
9 Cell Passaging Protocol	103
10 Cell Counting Protocol	104
11 Cell Fixation Protocol	105
12 Cell Staining Protocol	106
13 MHC Staining Protocol	107
14 3D Cell Seeding Protocol	108
15 SAXS results	111
16 Estimation of the Relative Amount of Surface Interaction	112
17 Estimating the cell numbers for a confluent seeding	114
18 Gantt Schedules	115
19 Questions to be Addressed	117
20 Overview Mind map	118

Table of Abbreviations

A

ABS: Acrylonitrile Butadiene Styrene.

C

CNS: Central Nervous System.

D

DAPI: 4',6-diamidino-2-phenylindole.

DM: Differentiation Media.

DMEM: Dulbecco's Modified Eagle Medium.

E

ECM: Extra Cellular Matrix.

EDC: 1-Ethyl-3-(3-dimethylamino propyl)carbodiimide.

EDTA: Ethylenediaminetetraacetic acid.

EtO Sterilization: Ethylene Oxide Sterilization.

F

FAC: Focal Adhesion Complex.

FBS: Fetal Bovine Serum.

G

GAG: Glycosaminoglycan.

G-Block: Gulluronic Block.

GF: Growth Factor.

GHG: Greenhouse Gas.

GM: Growth Media.

GP: Glycoprotein.

H

HEPES buffer: 4-(2-hydroxyethyl)-1-piperazineethanesulfonic acid buffer.

HS: Horse Serum.

I

iPS Cells: induced pluripotent stem cells.

L

LAF bench: Laminar-Air-Flow bench.

M

M-Block: Mannuronic Block.

MES buffer: 2-(N-morpholino)ethanesulfonic acid buffer.

MHC: Myosin Heavy Chain.

MRD: Minimum Resolvable Distance.

N

NA: Numerical Aperture.

P

PBS buffer: Phosphate-buffered saline buffer.

PDMS: Polydimethylsiloxane.

PG: Proteoglycan.

R

RGD: Arginylglycylaspartic acid.

RP: Rhodamine Phalloidin.

RT: Room Temperature.

S

SC: Stem Cell.

SMT: Skeletal Muscle Tissue.

Sulfo-NHS/sNHS: N-hydroxysulfosuccinimide.

T

TE: Tissue Engineering.

U

UV light: Ultraviolet light.

V

VEGF: Vascular Endothelial Growth Factor.

W

w/w: weight to weight.

Introduction

Muscle tissue is divided into cardiac, smooth or skeletal muscle tissue. All three of them share certain traits but each of them is specialized for specific functions in the human body (Tortora & Derrickson 2012). Unfortunately, muscle tissue is limited to a small amount of regenerative capacity which increases the potential impact that tissue engineering could have in tackling diseases leading up to functional and volumetric muscle loss (Bian & Bursac 2008). In addition to this, a growing interest in developing alternative techniques of producing animal-based protein for human consumption is leading companies and researchers into the area of skeletal muscle tissue engineering (Post 2012). Therefore, studies on mammalian skeletal muscle tissue can both support the medical advancement and be utilized by the food processing industry. With the help of cell culture experiments and the detailed characterization of the skeletal muscle tissue the underlying mechanisms for tissue regeneration, maintenance and homeostasis are unravelled piece by piece. These findings are put together to get a grasp of the complex system and to make way for future applications.

In the medical field the amount of prospective applications for grafted skeletal muscle tissue could be tremendous due to the many functions the tissue performs in the human body, like locomotion, stabilizing the body posture, circulating fluids and even contribution to the regulation of the body temperature (Tortora & Derrickson 2012). The prospective applications could include the mitigation of muscle loss for example in therapies for facial reconstruction (Yan et al. 2007) or to bring back muscular functions that have been lost in traumatic events (Bian & Bursac 2008). If understood sufficiently the regenerative treatment of skeletal muscle tissue could provide autologous therapies reducing the risk of tissue rejection (Ellis et al. 2005) and amplify the results of today's approaches like satellite cell injection (Tedesco et al. 2010). Apart from the direct patient centred applications a high demand for basic and reliable human tissue models is arising in the pharmaceutical industry. The prospect of testing drugs directly on the specific tissue or to assemble whole simulations of a functioning metabolic system in a lab-on-a-chip fashion could open the way for a more streamlined process of drug development. Applications to produce therapeutic proteins are also imaginable (Kosnik et al. 2003). Not only therapeutic, but also nutritional proteins get more and more into the focus of research. Producing meat is an expensive process and puts heavy loads on the environment with respect to land mass, water usage and greenhouse gas emissions. Furthermore, it is fairly ineffective with respect to overall resource input against protein output. One alternative could be the production of in vitro meat. No whole organisms would have to be maintained for only a small amount of desirable meat products and the resources could be transformed more effectively. The overall high level of effectiveness in producing meat in an in-vitro fashion would be a favourable change for sustaining the growing population and could reduce the impact on the environment tremendously. (Tuomisto & de Mattos 2011; Post 2012).

When seeing the vastness of promises and prospective applications, one can understand that it is a reasonable choice to invest in understanding the growth of skeletal muscle tissue. Ways of feasibly growing and cultivating skeletal muscle cultures ex vivo have yet to be unravelled, and many future challenges have to be taken on like vascularization, enervation, growing three dimensional specimens and developing robust protocols. This project aims to take on some of these challenges on a small scale to receive more insights into the generation of skeletal muscle tissue ex vivo.

The Story Line

This project was set out to develop a method with which it would be possible to grow muscle cells outside of a natural host. Growing muscle as a tissue is gaining importance because it could provide us with a future food source and even help patient that suffered from muscle or functional loss. For growing a piece of functioning muscle tissue it is important to not only increase the amount of cells in the culture but to support the cells in their specialization process to gain in functionality, this process is referred to as differentiation. During this process the cells will start to merge together and form long fibres in their drive to become muscle fibres that can bear load and contract. For this process of gaining function, several proteins have to be expressed by the cells. Among the building blocks of those proteins are some indispensable nutrients for the human nutrition, therefore it gains a load of attention from the cultured meat community.

As aforementioned the cells will form into long fibres and eventually will start to align to each other or the substrate. Thus the substrate gives us the opportunity to control the development of the cells. One of those substrate materials is alginate hydrogel, which is harvested from brown sea weed. It is known for its easy handling and can be easily moulded into the desired shape. It is usually sold and shipped in dry powdery state and results in a thick solution when dissolved in water. This solution is the basis for the gelation process which we usually perform with the help of salt solution (calcium chloride). With the help of the salt the formerly separated chains of the alginate can be connected to form a network. A special technique used in this project allows to produce parallel aligned capillaries in the alginate. It was hypothesized that this conformation could assist the cells in their aligning process to form fibres.

The capillary alginate has good structural properties for housing cells and also the mechanical properties can be tailored with the help of different methods, concentrations and salts. One challenge is increasing the attractivity for the cells to hold on to the surface (attachment) and for giving them an opportunity to spread out over the substrate, as this is not usually provided by the pure alginate. The attachment is important for the cells and stimulates processes inside the cell for increasing the well-being of the cell. Also as mentioned before, the cells need to work together in building the typical muscle fibres. For that it is necessary that the cells find together in preparation of the merging process. A good substrate with good opportunities for attachment can support the cell when it probes their surroundings for other cells. What we can do for example is mix in bioactive materials that can be found in the natural surroundings of the cells or we bind these materials to the surface of the gel.

After having the cell cultures on the one hand and the alginate gel as a scaffold we need a confined environment that we can place them in together. For that so-called bioreactors are developed closely to the needs of the cell culture. In this project we aimed for achieving a flow through the capillaries where the cells sit. This should support them with the necessary nutrition, oxygen and other important factors that we mix into the medium. In the natural cell environment, a closely knit network of small blood vessels is found which can provide those compounds deep into the tissue. When trying to grow larger constructs of muscle cells, we often do not have that network so that after a certain size the cells in the middle of the constructs start to suffocate or starve. Therefore, the combination of capillaries with flow is supposed to assist the culture deep into the construct. The bioreactors are often placed in incubators. Those incubators give a sterile environment, with a fixed mixture of air, humidity and temperature. Thus both incubator and bioreactor can work in concert to build up stable surrounding conditions.

From this outset the three main components of the system are the bioreactor, the alginate scaffold and the cell culture. When those three parts are put together, with every component being carefully designed, characterized and optimized a cell culture with differentiation towards functioning muscle tissue might be achieved.

Objective & Purpose

Hypothesis

It was hypothesized that alginate scaffolds with their specific properties like simple crosslinking methods, easy handling and scaffold tailoring and bio inertness offer a suitable environment for cell culturing. The ability to form capillaries into the hydrogel supports that claim even further by mimicking the spatial conditions of the extracellular matrix (ECM). With the help of a flow-through bioreactor a culturing of skeletal muscle progenitor cells in the capillaries should be enabled, thus tackling the challenges of suffocation in three dimensional cultures. Carrying that idea even further, a differentiation of the skeletal muscle cells to successfully form myosin heavy chains (MHC) should be enabled. The hope is that this could lead to the formation of skeletal muscle tissue with the help of vascularization from co-cultured endothelial cells and the breakdown of the biodegradable alginate.

Aims

The goal is to create a functioning culture environment allowing for the usage of three dimensional capillary alginate scaffolds for the cultivation of C2C12 cells. It is aimed for prolonged culture times, proliferation and differentiation of the cells to form vital cultures and mature muscle fibres in or on the alginate scaffolds. The development of a functioning platform includes a working bioreactor defined geometrically, by specific flow parameters and a robust concept. Furthermore, producing promising alginate scaffolds that can serve the hypothesized perks, like sufficient nutrient and oxygen transport to the culture and giving the desired parallel aligned capillaries. With the help of modifications, the effectiveness of the alginate with regards to cell attachment should be increased and the cell cultures controlled better. The desired outcome of this project would be a robust foundation comprising the culture system, the necessary body of knowledge about culture techniques, the basic protocols and results that stimulate future cell experiments.

Limitations

At the beginning of the project simulations were performed to guide in the design of the bioreactor. Estimations about the flow profile and oxygen were of importance during that step. The simulations are supposed to be used as a tool for assisting the design process of the bioreactor. Furthermore, they can give some indications of the conditions inside the culture chamber. A detailed simulation of the culture conditions is not the prioritized aim of the modelling, but it could provide the beginnings for a project focusing on the simulations alone.

The main goal of the project was feasibility and realisation of cell culturing instead of minutely detailed analysis of the single factors on the culture. With that the focus was not to probe for the most efficient solution of every single method before progressing but rather trying to find a realisation that has shown to be feasible to improve the specific properties. Eventually the cell viability and maturation of the cell culture are often the ultimate measure for this project, thus it relies on a solid amount of qualitative data.

The alginate scaffold development is important as long as it is serving the purpose of helping the cell culture. That means for the project that it was not the goal to test a multiplicity of properties of the alginate to characterize them fully like for example diffusion characteristics, degradation time or

mechanical properties. These would only be performed if the expected results would help to improve the cell attachment and the success of cell culturing on the scaffold. If there are indications during the project that specific parameters are necessary to achieve a better attachment and survival of the cell culture the necessary parameters would be investigated more closely. On the one hand how we could control the parameters and on the other hand what would be the optimal range the cells prefer for the planned maturation processes. This emphasizes the iterative character of this work as it takes on one challenge after the other instead of finding a theoretically optimal path before going into culture experiments.

The project is designed to pick up several loose ends and combine them as a prove-of-concept project. It is composed of three main stages, which are the bioreactor design, the scaffold development and cell culture methods. These have to be combined to allow for future more in-depth culture experiments. Thus additional characterizations and detailed optimizations are to be performed after achieving the first solid experimental stage. With this advanced cell experiments including co-culture of endothelial cells, degradation of the alginate or the formation of a more tissue like construct are out of beyond the scope at the current state of the project.

Background

3.1 Muscle Tissue

3.1.1 Physiological Basics of Muscle Tissue

Muscle tissue accounts for up to 50 weight percent of the human body (Tortora & Derrickson 2012) and is found in the form of three different phenotypes, the smooth, the cardiac and the skeletal muscle tissue (SMT). The smooth muscle cells are lining the inner organs and the cardiac muscle can be found at the heart muscle. Indicated by the name SMT can be found in close proximity to the skeletal system tightly linked via tendons. Besides location further classifications are made according to striation pattern or form of innervation. SMT is likewise known as striated muscle due to the distinct pattern found on the muscle fibres, smooth muscle is classified as non-striated muscle tissue and some sources speak of semi-striated muscle tissue (The Anatomical Travelogue LLC. 2014) when it comes to cardiac muscle. Voluntary muscle activity is only possible with SMT but the smooth and cardiac tissue can only be controlled involuntary either by the central nervous system (CNS) or peripheral innervation, as well as endocrine exposure. (Tortora & Derrickson 2012)

The SMT in collaboration with tendons and bones form the mechanical part of the locomotive system. Which allows for generation of movement and the maintenance of posture. Furthermore, it contributes to the temperature control of the body by performing exercise-associated thermogenesis (e.g. shivering) and aids in the transport of fluids like lymph and blood. (Tortora & Derrickson 2012)

Figure 1 shows the different compartments of skeletal muscle tissue. The smallest building block is the muscle fibre comprised of fused muscle cells organized in muscle fibrils. The fibres get aggregated in fascicles and several of those will make up the main part of the internal lumen wrapped up by a layer called the perimysium. The outer lining of the muscle is governed by the epimysium. This whole bundle of compartments is interspersed by a highly branched blood vessel system to provide oxygen and nutrition deep into the tissue. These aforementioned compartments allow for a good transduction of mechanical forces along the longitudinal axis of the muscle. Tendons connecting the muscle to the bone make up a strong conductor of the mechanical motion for physiological dislocation.

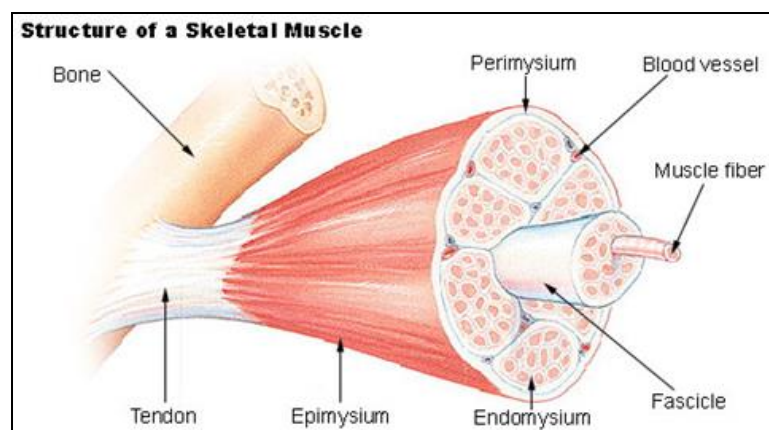


Figure 1: Structure of a skeletal muscle (National Cancer Institute 2014)

When working at the cellular level one has to investigate the details of the immediate environment like cell organisation, structure and ECM. Myogenesis is the process of new muscle formation and usually occurs simultaneous with embryonic bone formation (Crawford 1954). During this process progenitor cells fuse together forming multi nucleated muscle fibres and build up the microstructure; depicted in Figure 2 A. When SMT is formed, three major steps are distinguished: Proliferation of myoblasts; Differentiation of myoblasts and early stage fusion into myotubes containing around 10 nuclei; Formation of myofibres by fusing the smaller myotubes together. Achieving the last stage in-vitro is still challenging and often only leads to small and weak fibres. (Neville et al. 1997)

The microstructure of the muscle fibres gives the SMT its distinct optical pattern and leads to the classification as striated muscle tissue. As shown in the top of Figure 2 A along the longitudinal axis of a myofibrils sarcomeres and the Z disc are found in an alternating fashion. The sarcomeres itself, as functional unit enabling the contraction of the muscle, is divided into a brighter I band and darker A band causing the previously mentioned striated appearance. Multiple sarcomeres are linked to each other in a "zig-zagging" (Tortora & Derrickson 2012) fashion by the Z disc, a protein dense region strongly connecting the neighbouring sarcomeres. By binding of the myosin heads of the thick filament to the actin of the thin filament structural crossbridges are formed. A pulling motion by twisting these crossbridges is enabled, thus leading to muscle contraction. In a fully contracted muscle the H zone will be covered by the overlapping thin filament (Tortora & Derrickson 2012).

The ECM (Figure 2 B) is an important part as it "ensures a functional link between the skeletal muscle cell and the bone" (Kjær 2004) and creates the specific mechanical properties of the SMT. The main constituent of the ECM is collagen type I and II making up the fibrous cell environment it provides stability and acts as a force transmitter through the tissue. Glycosaminoglycans (GAGs) and Proteoglycans (PGs) are specified as the ground substance which can present growth factors (GFs) to the cells. Glycoproteins (GPs) like fibronectin or laminin are structural linkages between the cells and the fibrous proteins e.g. collagen. Supported by the ECM components, GF and enzymes will take on the intercellular messaging in the tissue. (Gillies & Lieber 2011; Temenoff & Mikos 2008)

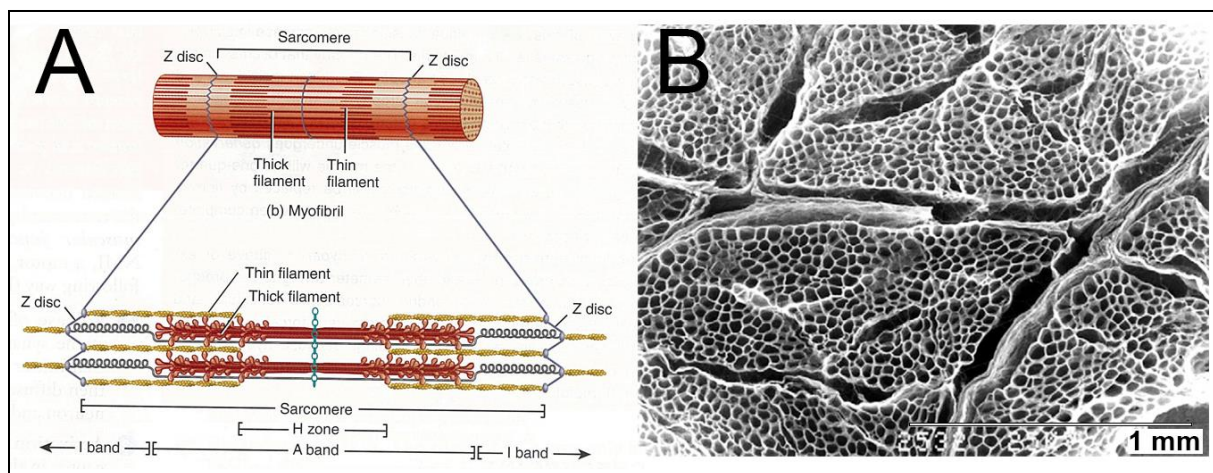


Figure 2: A) Sarcomere structure (Tortora & Derrickson 2012) B) SEM image of the collagen ECM in bovine skeletal muscle after NaOH-digestion (Trotter & Purslow 1992)

3.1.2 Challenges and Applications for In Vitro Grown Muscle

Tissue engineering (TE) has emerged as a field that aspires to grow tissues outside of the living organism in lab conditions (in vitro). Potentially making way for new therapeutic applications like already used skin grafting from foreskin to treat burn victims (Naughton & Tolbert 1996) or other methods in which scaffolds are seeded with autologous cells to re-grow lost or missing organs (Olausson et al. 2014). As introduced in the previous Chapter there are different types of muscle tissue making up the human body. All those areas could benefit greatly from tissue engineering applications. The gap between supply and demand in the food and medical care sector enforced by the faster growing population is creating a niche where tissue engineering could provide solutions (Ehrlich & Holdren 1971; Abouna 2008).

According to doctor Anthony Atala Director of the Wake Forest Institute for Regenerative Medicine “Every 30 seconds a patient dies from a disease that could be treated with tissue replacement” (Atala 2013). From this dramatic phrasing one of the main motivators for realizing clinical applications in tissue engineering is clear. When looking deeper at the potential of skeletal muscle tissue engineering the apparent needs that could be addressed are volumetric as well as functional loss of muscle tissue (Yan et al. 2007; Bian & Bursac 2008). These approaches could go beyond the current limitations of satellite cell injection in which we are strictly limited to the regenerative capacity of the cells (Tedesco et al. 2010). The hope is to find a way of sufficiently manipulating the cells to form a complete tissue outside of the host, or at least form a construct that enables the full reconstruction inside of the patient’s body, like the Dermagraft products (Organogenesis Inc. 2015; Naughton & Tolbert 1996). Pharmaceutical companies are getting increasingly interested in developing stages containing tissue engineered constructs to test the metabolisation of novel drugs. The ideas here range from single organ models up to four-organ-chip approaches trying to model the whole metabolic chain (No et al. 2015; Maschmeyer et al. 2015). Given the background that the cost of drug development has increased over the course of the last decades and that prognoses hint to continue that trend depending on the impact of new biomedical applications (DiMasi et al. 2003). In a very recent news the FDA approved an anthrax vaccine called BioThrax developed by Emergent BioSolutions Inc. (Emergent BioSolutions Inc. 2015). This drug was approved under the “Animal Rule” set in place to allow for approval of drugs against rare or too lethal conditions that have not been fully tested in clinical trials (FDA - U.S. Food and Drug Administration 2015). With the progression of tissue engineering it might be possible in the future to create disease models with human cells on a chip to assess the efficacy of the drugs closer to the area of application.

Stepping aside from the therapeutic applications a growing interest in novel food manufacturing is motivating researchers and companies to join forces in investigating future sources for human protein nutrition (Mark J. Post 2014; Huis et al. 2013). The growth in population and the increase in livestock consumption is challenging the conventional ways of meat production (Sun et al. 2015), as more and more people realize that an upscaling of the current methods will have severe impacts on the environment and the human population (Mattick & Allenby 2012; Tuomisto & de Mattos 2011).

Figure 3 shows the different areas in which meat production has the largest impact. Those different impacts are intertwined with each other in such a way that their individual impacts on the environment are amplifying each other. For example the GHG emission is on the one hand caused by the livestock production itself and roughly one third of the livestock related GHG emissions is caused due to deforestation (Datar & Betti 2010). Thus the land use and GHG emission effect each other directly and the regulating capacities of the forest are lost in the process additionally (Tuomisto & de Mattos 2011). Manure management has another huge impact on the emissions overall and often affect the amounts of usable fresh water additionally (Datar & Betti 2010).

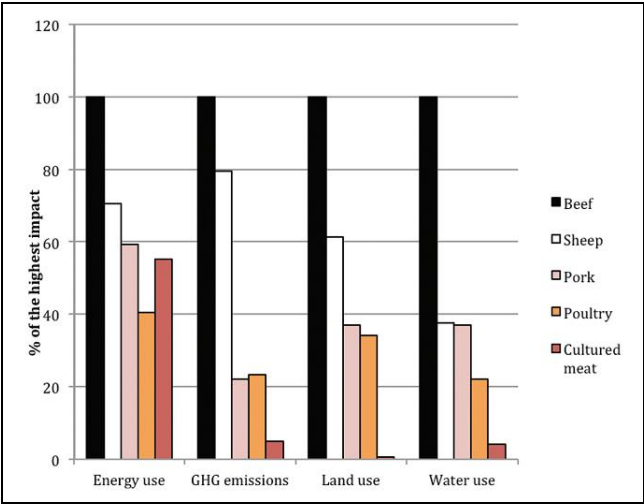


Figure 3: Estimated impacts on Energy use, greenhouse gas (GHG) emission, land and water use of the different production methods of meat (Tuomisto & de Mattos 2011)

After that short introduction to the impacts of livestock production and its associated problems, one has to look at the factors that challenge the development of cultured meat solutions. One of the first and profound problems would be the acceptance struggle in communicating this form of meat production to the general public (Marcu et al. 2015). With this the so-called Yuck-Factor is expressing the ambivalence of the society towards “unnatural” approaches (Mark J Post 2014). Without educating the consumers only small niche markets would open up towards cultured meat solutions. The next challenges lie within the technical realisation to evolve from small scale production as shown in prove-of-concept realisations like cultured meat burger (Mark J Post 2014) towards a fully established and approved processing chain. For this the future research will have to deal with scalability (Rafiq et al. 2013), processing techniques ensuring quality for approval (Mattick & Allenby 2012), to refrain from using animal supplements like serum (Brunner et al. 2010) and find stable and feasible culture protocols as a whole to also address the wide variety of meat products offered.

When this would be realised the prospects for the future could be bright as the reduction of the previously discussed strains on the environment could be initiated and other promises of health benefits might be realisable. Realising cell cultures without antibiotics which is widely used in livestock production could dampen the distribution of multiresistant bacteria (Post 2012). Others hope for functionalizing the meat to address cardiovascular problems caused by the high consumption of meat through increasing protein content, lowering fat content or even substitute with beneficial fatty acids (Hopkins & Dacey 2008). Closing with the words of Mattick & Allenby who wrote:

“Regardless, due to the potential impacts, now is the time to begin developing a framework in which to monitor and adaptively manage its development, commercialization, and diffusion.”

3.2 Bioreactors

Bioreactors in TE serve as an artificial environment to ensure constant and controllable conditions "to either maintain a whole muscle organ ex vivo indefinitely or promote the differentiation of cells and the maturation of both intra and extracellular structures resulting in the generation of an organized tissue" (Dennis et al. 2009). Controllability is key for a successful bioreactor as it either maintains the culture, sends out specific stimuli or completely changes operational modes (van Blitterswijk, Clemens Thomsen et al. 2008). This enclosed environment is achieved and influenced by tightly controlling parameters such as pH, temperature, pressure, flows, or concentrations of diluted species (van Blitterswijk, Clemens Thomsen et al. 2008). The strive towards an almost native environment is usually the goal of a good bioreactor system, thus bioreactors gain a lot of complexity and are being closely tailored to the needs of the cell culture.

Dennis et al. make the point that the understanding of muscle is not sufficient enough to unravel precisely what properties are required when designing a muscle tissue bioreactor (Dennis et al. 2009). Upon this over the last decades critics argued that it is "cumbersome and unnecessary" (Abbott 2003) to do 3D cultures, thus it seems to be challenging to establish feasible 3D bioreactors. According to van Blitterswijk et al. these cultures have more biological significance than common petri dish cultures, so while challenging they are more rewarding (van Blitterswijk, Clemens Thomsen et al. 2008).

To take on those tasks key parameters should be included in designing a bioreactor for muscle tissue growth:

- potential failure modes and countermeasures
- means to probe and monitor muscle development non-destructively
- algorithms to guide the developing muscle along a series of developmental milestones

Figure 4 shows a schematic of a flow-through bioreactor allowing for culture inside of a porous scaffold. A way of controlling the surrounding conditions with regard to temperature and oxygen supply is to place bioreactors in an incubator. The incubator will establish an environment with a constant temperature, humidity and air constitution. PDMS is often chosen as moulding material for fluidic channel as it is easy to handle and allows for easy transport of oxygen via diffusion.

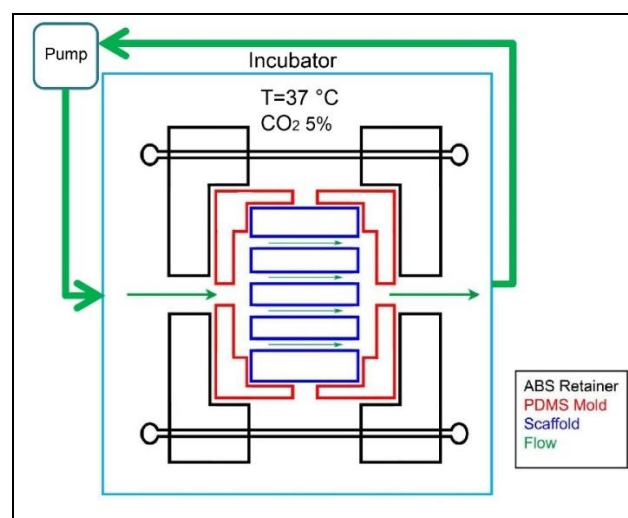


Figure 4: Schematic of a flow through bioreactor (Peng et al. 2014)

3.3 Scaffolds

3.3.1 Alginate as Scaffolding Material

Alginate has emerged as a common scaffold material in the field of TE during recent years. Belonging to the natural polysaccharides it found its way into "medical applications due to [...] biodegradability, biocompatibility" (Baysal et al. 2013), bioactivity properties and "its structural similarity to the natural ECM" (Drury et al. 2004). Natural polymers, like alginate, can be controlled and tailored to the demands of specific applications by means of processing or by invoking specific changes to the polymeric structure (Drury et al. 2004). Furthermore, it is widely accessible and simple to process (Baysal et al. 2013).

Alginate is comprised of two functional units, the mannuronic (M-Block) and the guluronic (G-Block) blocks, when brought in contact to a crosslinking agent these reactive blocks with their respective carboxylic group will start to align around the crosslinker in the so-called egg-box model; as seen in Figure 5. These crosslinking agents can be divalent cations like Cu^{2+} , Ca^{2+} , Ba^{2+} and Sr^{2+} (Rowley et al. 1999). By aligning the previously loosely distributed polymer chains into double strains a solidification into hydrogels is performed. One common application is the formation of small alginate calcium beads as a drug envelope or as scaffolding materials (Murata 2000; Tanaka et al. 1984).

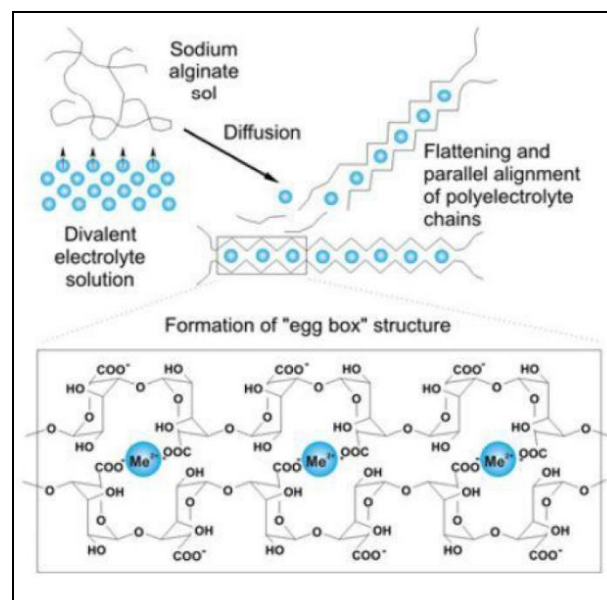


Figure 5: Crosslinking process of alginate gel (Pawar 2010)

Being a polymer the manufacturing possibilities are very broad and one way proposed by Thiele et al. allows for the formation of capillary alginate by directed crosslinking (Thiele & Hallich 1957). CaCl_2 solution is introduced to the alginate solution and by guiding the crosslinking process through the gel from top to bottom self-assembled capillaries are achieved. In Figure 6 on the left side we can see the prepared beaker that is filled with the alginate solution and also the walls of the beaker are pre-treated with the alginate solution. This pre-treatment allows for a better adhesion of the solution to the beaker walls. With this a small amount of the crosslinking solution can be balanced on top of the alginate solution and form a primary membrane of alginate hydrogel on top. After the formation of that first gel phase more CaCl_2 solution can be poured on top. The next process is described by Thiele and Hallich as drop like separation between fluid and gel where small drops build at the interface between gel and CaCl_2 -solution. These drops will take up more of the redundant water during the crosslinking process. They will not mix with the sol and progress through the gel in front of the gelation process, thus imprint

the capillary structure in the hydrogel (Thiele & Hallich 1957). Willenberg et al. explains that the ionotropic gel formation stems from fluid instabilities invoked by friction due to the contraction of the polymers at the front of the newly formed gel (Willenberg et al. 2006). A hydrogel based on alginate interspersed with these characteristic capillaries, as seen in Figure 6, could bridge the structural gap between physiological and synthetic ECM even further. It would allow for an aligned organization of the cells along the capillaries. In three dimensional cultures a lot of contact points can be developed to the surrounding matrix but also to other cells theoretically all around the cell (Yan et al. 2007). These environmental cues are beneficial for cell development and as we know from Chapter 3.1 in order to form viable muscle tissue cell fusion has to occur. Thus a well-designed scaffold can greatly influence the results of the cell culture.

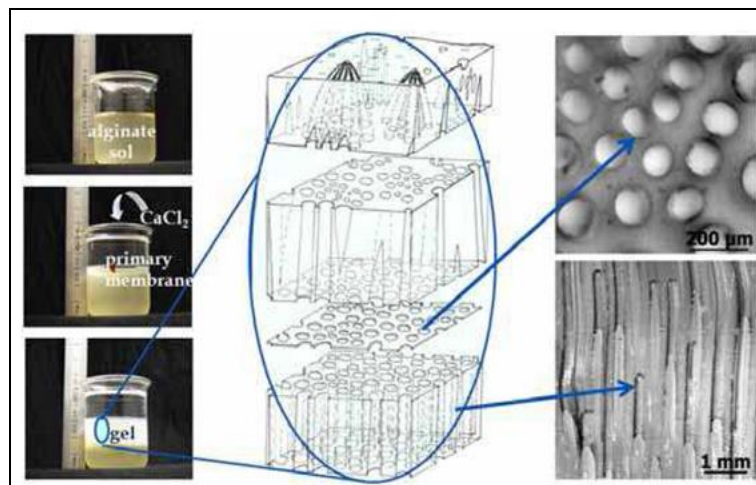


Figure 6: Formation of alginate capillaries (Despang et al. 2011)

3.3.2 Modifications for Improved Cell Attachment

For setting up three dimensional cell cultures scaffolds are the first choice to spatially organize the cells and invoke reactions lacking in petri dish cultures. Many different materials and manufacturing methods allow us to create structures favourable for close to native cell organization but often the important triggers found in the native ECM are missing. At this point material modifications come into play to compensate for the lack of these signals. Therefore, an important factor in scaffold design are the surface properties which should support cell attachment, migration, proliferation, differentiation as found in the native environment (van Blitterswijk, Clemens Thomsen et al. 2008).

When looking at the ECM we can see a plethora of different materials working together as a compound supporting the viability of the cells (Gillies & Lieber 2011). On the way to create suitable scaffolds multiple approaches have emerged; some try to use the native ECM-Material as a basis (Methe et al. 2013), and other approaches deliver just enough stimuli to the cell culture to achieve a long viability and to trigger an auto-assembly of the necessary ECM components by the cells (van Blitterswijk, Clemens Thomsen et al. 2008). Eventually, it comes down to the cell type that is to be cultured in the scaffold, as specific pre-requisites have to be met for different cell families.

This project deals with the natural polymer alginate in the form of hydrogels. Alginate is described as a very inert material that means by definition that it does not invoke any responses or interact with biological tissue (Blokhuis et al. 2000). This stems from the absence of functional groups responsible for attachment and spreading in the native cell environment. To compensate for that lack of interaction material modifications are performed. Common modification methods are bulk or surface modification. In a bulk modification functional groups are brought into the mixture before crosslinking to gels. This enables the modification materials to link to the monomers and get strongly embedded after the scaffold is formed. Surface modifications can be carried out by easy drop-on or engulfing the already crosslinked material into a solution of the coating material. Functional groups can be delivered by RGD-peptides or collagen which can interact with the integrins at the cell surface, thus enabling attachment, migration and even cell survival. The RGD-peptides are an amino acid sequence containing arginine, glycine and aspartic acid and can be found as a binding motif on the fibronectin as shown in Chapter 3.4.2. This small peptide fragment is able to bind with the integrin receptors found on the cell surface (Boontheekul et al. 2008; Humphries et al. 2006). Humphries et al. describes the RGD-binding integrins as one of the most “promiscuous” binding receptors in the integrin family (Humphries et al. 2006) underlining the importance of the RGD sequence as a mean to improve cell attachment on biomaterials. From the previous section we know that collagen is one of the main ECM constituents to promote structural stability and with the help of GPs like Laminin and Fibronectin and their functional regions a link can be established from cells to the ECM. Fibronectin itself has both collagen as well as RGD binding sites, thus modifications with these two components are a common choice in scaffold design. (Temenoff & Mikos 2008; van Blitterswijk, Clemens Thomsen et al. 2008)

3.4 Cells

3.4.1 Choosing the right cell line – C2C12 cell line

The choice of the right cell line for the respective study is one of the main components necessary to start a project. Therefore, this decision is of great importance with respect to scope and goals of the project as well as the specific research questions.

Figure 7 shows a detailed illustration of the cellular neighbourhood of a skeletal muscle. The cells can be seen residing in their respective niches of the muscle. For regenerative purposes or cultured meat production, two cells shown here are of particular interest, the satellite cells embedded below the basal lamina of the myofibres and the mesenchymal progenitors between the fibres (Pannérec et al. 2012). Different sources report about a recruiting process of the satellite cells to bring other stem cells (SC) to the damaged area (Pannérec et al. 2012) and that other cells can enter a satellite-state in the tissue coming from the bone marrow (Péault et al. 2007). Thus physiologically a tissue (re)generation can depend on other cell sources outside of the skeletal muscle as well. With this other cell types are considered in the production of tissue engineered constructs such as embryonic stem cells (Willenberg et al. 2006) and induced pluripotent stem cells (iPS cells) (Goldthwaite 2006) as they both possess pluripotent properties. Therefore are able to form the three germ layers and eventually form every tissue found in the human body (Binder et al. 2009). Together with their universality for generating all sorts of cellular cultures these cells are unequivocally harder to guide into differentiated cells than progenitor cells. The progenitors are determined to a specific cell lineage (totipotent) (Burattini et al. 2004) and the protocols for triggering specialisation are more reliable to perform (Blau et al. 1983).

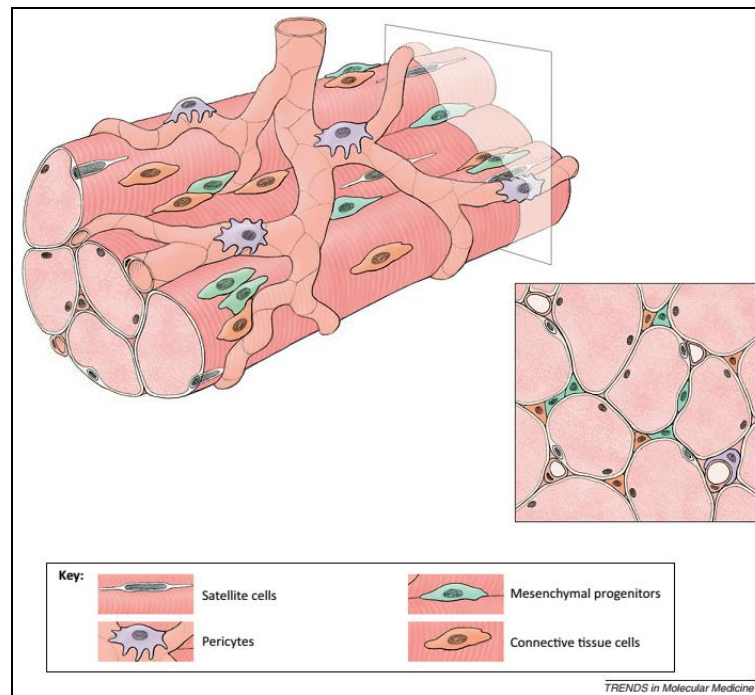


Figure 7: Cellular composition of the skeletal muscle tissue; showing the long striated myofibres tightly packed together and a vessel stem sitting on top and interspersing the bundle with the respective cells sitting on the tissue (Pannérec et al. 2012)

All the aforementioned cells have the opportunity to generate new muscle cells. Thus either produce newly specialised cells to compensate functional losses of the tissue or produce larger quantities by division to compensate for the loss of cell population. Different forms of division have been identified to occur with cells in a stem cell or progenitor state. These forms are asymmetric and symmetric cell division, effecting maintenance and differentiation of the cells in different ways. As shown in Figure 8 the two main forms of division can be divided clearly, but the symmetric division allows for multiplication of the multipotent parent generation or can generate two cells of the new specialized daughter generation. The asymmetric division on the other hand will self-renew the parent generation while forming a new cell of the daughter generation hence only increase the number of daughter cells whilst maintaining the progenitor numbers. (Blanpain & Fuchs 2009)

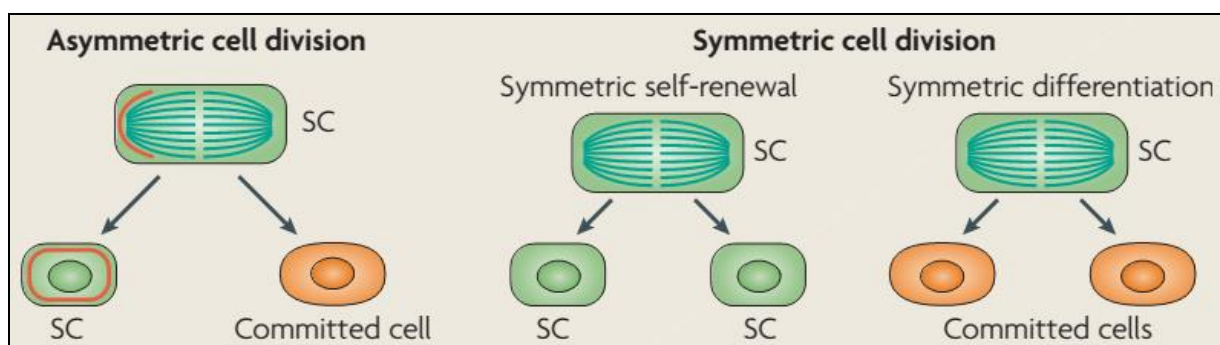


Figure 8: Different forms of stem cell division (Blanpain & Fuchs 2009)

Controlling these processes in cell cultures is at the core of guiding cellular fate processes towards the specific goals, e.g. generation of high cell numbers, invoke different cell lineages or the creation of a functional tissue. Those are the challenges to be taken on when creating tissue constructs for tissue engineering purposes.

The C2C12 mouse muscle progenitor cell line has been established by Yaffe and Saxel (YAFFE & SAXEL 1977) and has been used as a model cell line for skeletal muscle development in numerous studies (Kislinger et al. 2005; Grossi et al. 2011; Burattini et al. 2004). As a progenitor cell line the handling and manipulation of the cell culture is straight-forward as demonstrated by Blau et al. (Blau et al. 1983).

3.4.2 Cell-Environment Interactions

As discussed in the previous Chapter, guiding the cells down and towards the specific lineages of the cells to generate tailor made cell cultures is a main goal in tissue engineering. In the natural environment the cells will be exposed to different cues provided by the ECM materials, mechanical forces or the flowing fluids containing different soluble compounds e.g. oxygen, GFs. These main processes have the ability to act on the single cell in culture over different ways, where the specific cell receptors make up the link between effector and reaction in the cell. (van Blitterswijk, Clemens Thomsen et al. 2008)

In Figure 9 examples for the different effectors on the stem cells and their fates are shown. Within the main effector categories there are many different factors that can act on the cell. Here we have a schematic of two cells in close proximity to each other. These kind of close interactions between cells can keep cells in a quiescent state as a niche cell (Discher et al. 2009). As observed by Pannérec et al. for the satellite cells that are kept on top of the myofibres below the basal lamina (Pannérec et al. 2012). The illustration only shows a few examples of the different fates a cell can be determined to and it exemplifies the vast majority of ways to influence the cell. Inside of a single cell a lot of different signals come together where the results can work together or may even be contradicting to each other. For example, a cell can get signals for proliferation and differentiation at the same time (left cell in Figure 9). Other might be triggered towards differentiation and even get the initial cues for apoptosis (right cell in Figure 9). This superposition of different signals can be assumed to happen inside of the cell at all times given the sheer amount of effectors on the cell in a complex culture. Finally, the most prominent signal or cross inhibition will determine what pathway the cell will go down.

On the very basic level we can observe the nutrients and the oxygen supporting the cell survival. A lack of those factors can lead to the secretion of other GFs such as vascular endothelial growth factor (VEGF) to stimulate the vessel growth around the cell (Forsythe et al. 1996; De Coppi et al. 2005). Going more into detail on the illustration we can observe the chemical signalling between the cells (paracrine) and the signalling of cells to themselves (autocrine) with the help of GFs. The paracrine signalling allows cell communication in close proximity or in larger cultures to allow for culture wide maturation processes (DeHart et al. 2006). Besides the signalling with GFs direct cell to cell binding can trigger culture development. In many culture protocols aiming for proliferation a dense cell culture (confluency) needs to be avoided to suppress the triggering of differentiation. Another common way of triggering maturation processes is by either actively reducing the media content of GFs or create gradients as seen in the Figure 9 as well (Blau et al. 1983). On the left cell all the cell receptors for the growth factors provided by the cell culture are occupied contrary to the slow depletion on the right cell due to the growth factor gradient. This results into proliferative signals for the left and triggers differentiation in the right cell (Blau et al. 1983).

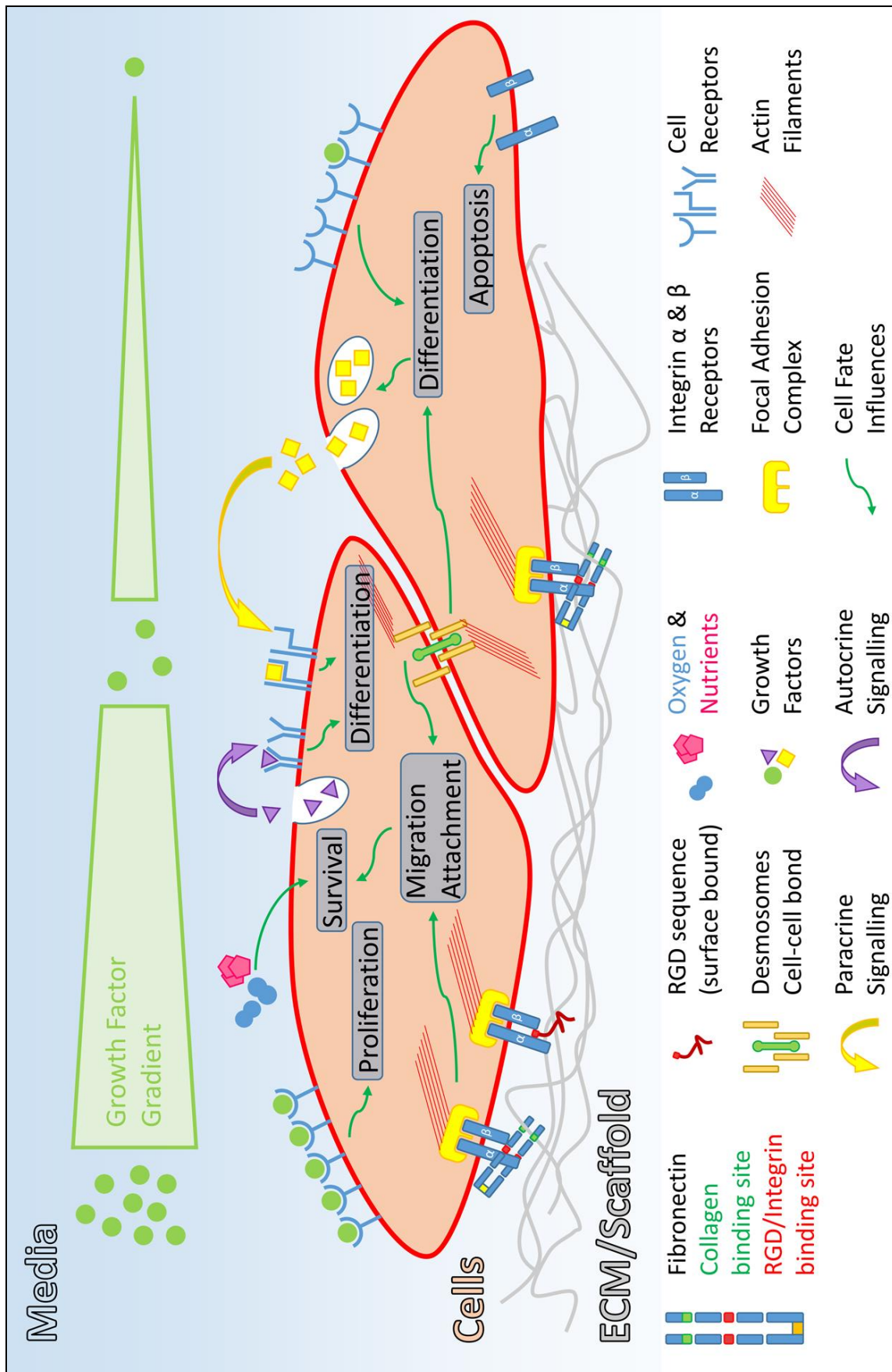


Figure 9: Schematic of two cells in culture showing the different effectors and respective reactions of the cells; based on the illustration by Discher et al. (Discher et al. 2009)

Besides the triggering through media and cells among each other, the scaffold or the ECM in a physiological environment provides another group of effectors on the cell culture. The main example in Figure 9 is the binding of the integrin receptors to the RGD sequence of the fibronectin or artificially brought down to the matrix (Puleo & Bizios 2009). When establishing that link between RGD domain and integrin receptors the presence of cations, especially calcium is of great importance. On the cellular side the calcium can invoke structural changes in the integrin receptors to improve the binding efficacy (Lawler 1988). The binding is established by embedding the R residue of the RGD molecule into a cleft of the α integrin and with the help of the calcium cation the D residue can attach into the β subunit of the integrin receptor (Humphries et al. 2006). When forming the connection, the receptors are drawn together and form the focal adhesion complex (FAC). This complex allows for the stable attachment of actin filaments or referred to as the development of stress fibres in cells (Chaudhuri et al. 2015). With the help of those complexes reaching from the surrounding material deep into the cell via filaments a migration and attachment to the surface is ensured which in turn promotes survival of the cell. With the help of these complexes the cells are also able to sense the mechanical properties of the scaffolding material and mechanical stimulations can be successfully communicated to the cell. As Chaudhuri et al. or Genes et al. show those mechanical stimulations are important beyond spatial fixation (Chaudhuri et al. 2015; Genes et al. 2004). Ensuring the stimulation of the cell allows for all other downstream processes like proliferation and differentiation. On the right cell it is illustrated that a lack of attachment inhibits the formation of FACs.

Figure 9 only shows a few of the many pathways possible acting on the cellular fate. The cross talk between the different effectors and pathways is much more complex in the native cell. This gives researchers a lot of different possibilities to stimulate their cultures. The key is to find the effectors that efficiently achieve the goals for the specific research question or application.

3.5 Sterility

Sterility is a crucial topic when it comes to culturing cells in vitro. The conditions we want to achieve in the bioreactor for the benefit of the cell culture are also beneficial for bacteria, fungi or other impurities of the culture. Achieving a successful outcome for cell experiments does not just lie with a well-designed project and a feasible concept, furthermore one should always keep the sterility in focus. All materials used, all processing methods applied should be tailored to work with aseptic techniques and withstand at least one sterilization method without altering the substantial properties (Gatenholm 2014). Common techniques of sterilization are autoclaving, ethanol treatment, UV light or Gamma radiation (Ratner et al. 2012). During the work with the cell culture procedural measures, like clothing and working in a laminar flow hood are compulsory to maintain a sterile state.

Millet et al. proposed the autoclave sterilization of PDMS to be beneficial even beyond achieving a sterile material (Millet et al. 2007). By autoclaving the PDMS the crosslinking process is driven further, thus increase the average culture viability by reducing the PDMS monomer leaching into the well. The next main material used is ABS the printing material of the 3D printer. With this autoclaving is not possible, but due it being resistant to ethanol a sufficient sterilization with ethanol treatment is possible (Dynamalab Corp 2014).

The alginate gel itself is more challenging to keep sterile. An autoclaving of the solution should be possible before forming the capillary gels. In previous experiments this applied to gelatin:alginate, but Schuster et al. succeeded at autoclaving the alginate 1.5% weight to weight (w/w) solution beforehand and still forming capillary gels (Schuster et al. 2014). A possible change in viscosity caused by the autoclaving process should be accounted for. Stoppel et al. immersed the alginate cuts into ethanol

for 20 minutes to achieve a sterility even after crosslinking (Stoppel et al. 2014). When successfully sterilizing the hydrogel before the cell culture no problems with viscosity change or gelation under strict sterile conditions arise. All the other materials like culture media, single-use tools and other additives should be kept strictly sterile as well (Gatenholm 2014).

3.6 Measurement Techniques

3.6.1 Light Microscopy

Light or optical microscopy can help to investigate specimens that are not resolvable with the human eye. Those microscopes are based around the spectrum of the visible light, hence their naming. Simply put, the purpose of a microscope is to magnify the image of a smaller sample. This encompasses an important property of a microscope, which states that “we are looking at an IMAGE of a specimen rather than at the specimen itself” (Oldfield 1994). Building on that statement as we are working with images of specimens only, which should allow for changes in the formation of the image (Oldfield 1994) and enables the manipulation of the image representation of the specimen in such a way that we can extract the necessary information for our application. With this we have to accept that the image itself will never be a “perfect, enlarged copy of the specimen” (Oldfield 1994). Therefore, one has to understand and be aware of the limitations connected to light microscopy to be able to enhance the application opportunities.

From a singular point in the object the light rays will emanate in a wave-like fashion equally in all directions thus create a spherical wave front around the object. The condenser (optical lenses) in the microscope are gathering that light to form the real image in the microscope. In Figure 10 A we can see how only a small portion of the wave fronts can be caught by the lens. From that the numerical aperture (NA) results as a limiting factor of the lens itself. As expressed in equation 1 where n is the refractive index as relation of the media the light is travelling through and the lens. α denotes half of the intake angle of the lens (Oldfield 1994). The NA results in different sizes of the airy disk as seen in Figure 10 B (Wegerhoff et al. 2006).

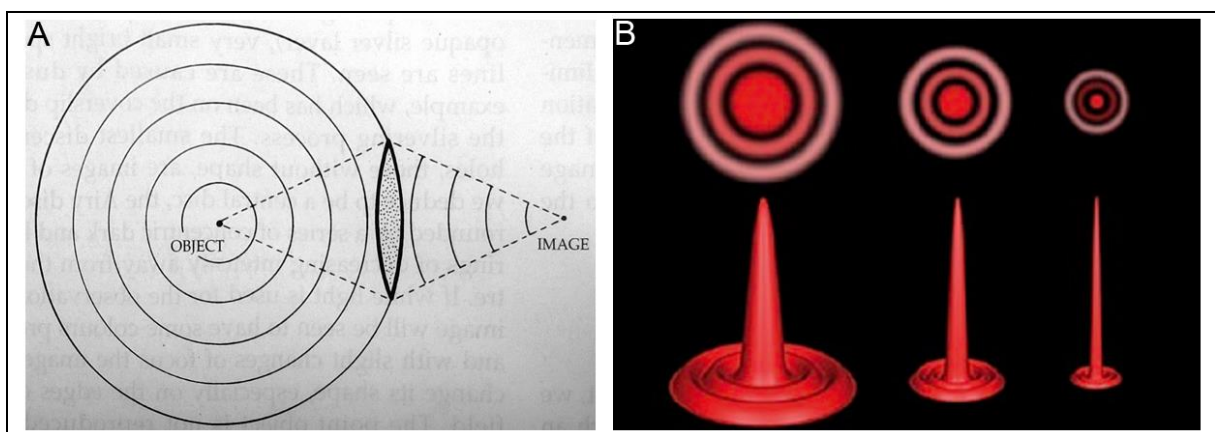


Figure 10: A) Lens (bold framed object) Acceptance of a spherical wave front (Oldfield 1994); B) Airy disk patterns of different size depending on the NA of the lens, low NA (left) to high NA (right) (Wegerhoff et al. 2006)

$$NA = n \cdot \sin \alpha \quad (1)$$

More importantly what we can use the NA for is to calculate the ability of a lens system to distinguish between two points in the sample. This is expressed through the minimal recognizable distance between the two points. Thus it determines if the system is able to represent the two points as two points in the image plan as well and the distance is the quality measure of the optical system. This is referred to resolving power or resolution of the system and gives one of the most important measures of an optical microscope. (Oldfield 1994)

Additionally, to the NA we have to take the wavelength λ into consideration for determining the resolving power of a lens which has been calculated by Abbe to determine R the minimum distance that can be resolved by the setup. This introduces a new limitation as the wavelength size should not exceed the dimensions of the object to be observed (Oldfield 1994). More importantly is to have another look at the resolving power with respect to the magnification looking at the Abbe Equation 2 one can see that the minimum resolvable distance (MRD) is independent from the magnification of the object (Oldfield 1994). Thus it can be concluded that by increasing the magnification alone the detail richness or texture resolution does not have to be increased. All we achieve is an “Empty Magnification” (Oldfield 1994) as the purpose of the microscope is to enlarge the image to a size that is resolvable by the human eye. If we are able to magnify the MRD of the microscope to the MRD of the human eye (0.2 mm (Oldfield 1994)) every magnification above that will be rendered useless, as the “eye can already perceive the smallest [...] detail [...] in the image” (Oldfield 1994). Furthermore, artefacts could be introduced by choosing the magnification too high.

$$R = 0.5 \frac{\lambda}{NA} \tag{2}$$

$$MRD = 0.5 \frac{\lambda}{NA_{max}}$$

Figure 11 shows a simple optical microscope with a bottom illumination and top-down observation. The light is focused on the object where the sample is placed and allows for the illumination of the specimen thus the condenser (here objective lens) can gather the emitted light. It shows how a real image is formed in the microscope allowing for the aforementioned manipulations of the image itself and eventually the eye is able to form a virtual image for the observer to perceive.

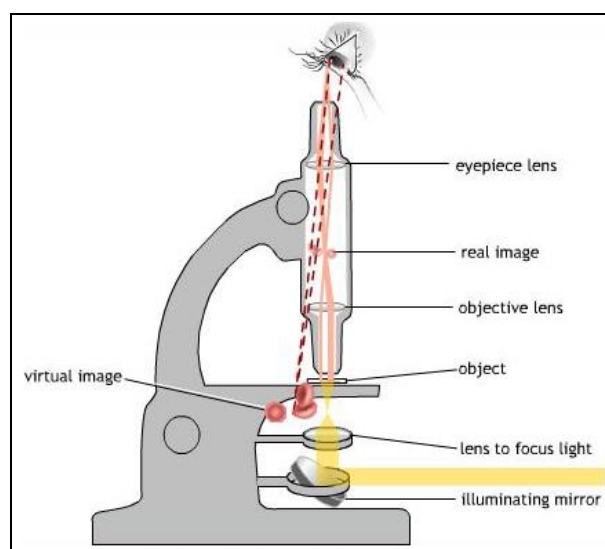


Figure 11: Schematic of a simple light microscope (Imaging Technology Group 2015)

Today the most optical microscopes are equipped with a digital camera containing a CCD (charged coupled device) chip for transforming the optical image into a digital image. The image has to be quantized into pixels to allow for the composition of a digital image. To not introduce an additional loss of information or detail the digital spatial resolution has to be at least equal or higher than the optical spatial resolution (Wegerhoff et al. 2006). This is expressed in the Nyquist theorem with “the sampling interval (i.e. number of pixels) must be equal to twice the highest spatial frequency present in the optical image” (Wegerhoff et al. 2006). This introduces another part that has to be dimensioned correctly to allow for a well enough representation of the details in the image.

In this Chapter, the basics of optical microscopy have been introduced and some of the many limitations or challenges have been presented. Most of which are linked to the direct setup or dimensions of the microscope. Additionally to that there are challenges lying within achieving a sufficient contrast in the images as well as the thickness of the specimens investigated (Oldfield 1994). With this techniques have been developed based on the simple light microscope presented here like phase contrast microscopy to pronounce less contrasted areas (Imaging Technology Group 2015) or additional hardware to reduce out of focus blur like the pinhole in the confocal microscopy (Wegerhoff et al. 2006) as discussed in Chapter 3.6.4.

3.6.2 Immunostaining

At the basis of immunocytochemistry lies the specific interaction between a probe and a target which can be utilized for selective immobilization of particles on a surface, the antibodies on specimens or to build different forms of aggregates. Additionally, to this initial binding process a signal transducer has to be used to allow for the binding information to be converted to an easily detectable signal, e.g. dyes or radioactive markers. In the case of immunostaining a fluorescent dye is brought into the sample to allow for imaging or intensity measurements. This information can be used for either qualitative or quantitative measurements on the samples depending on the specific application. (Wild 2013)

As introduced above the antibodies are used for their unique properties (Wild 2013):

- **Flexibility**, ability to bind to a wide range of chemicals, molecules and biological specimens
- **Specificity**, only binding (strongly) to objects presenting the counterpart to the antibody
- **Sensitivity**, strong binding strength between antibody and target allowing for even small amounts to be detected

The antigen marked and identified by the assays is not necessarily of main interest of the investigation, more over it is used as an identifier for different processes or structures in the sample. Either we want to be able to stain specific parts of a cell or it allows for the investigation of the developmental status of a whole cell culture by coupling to the antigens specific to the proteins expressed during differentiation.

Figure 12 shows the most commonly used methods to label a sample fluorescently for use in immunoassays. The first method involves a singular antibody with the fluorescent dye directly tethered to it, thus it can directly be bound to the antigen and after rinsing one can perform the measurements on the sample. The indirect coupling shown in the middle of Figure 12 includes a primary and secondary antibody to which the fluorescent markers are coupled to. Resulting in a two-step process in which first the primary antibody has to be bound to the antigen and to this the secondary antibody can be bound later. There are certain perks of performing an indirect coupling for example economic reasons so that the secondary antibody can be produced sensitive to a wider range of primary antibodies. In applications like ELISA it allows for measuring particles free in solution. Thus we present an antigen immobilized on the surface, and bring in the secondary antibody into the sample solution. The antibody

to be measured will be trapped in between and due to immobilization on the surface as well as fluorescent labelling the sample content can be estimated. The last method presented here is a direct coupling without a readily fluorescent marker thus it will only emit fluorescent light after being bound to the antigen and after undergoing the conformational change following the binding event. (Wallin 2009; Wild 2013)

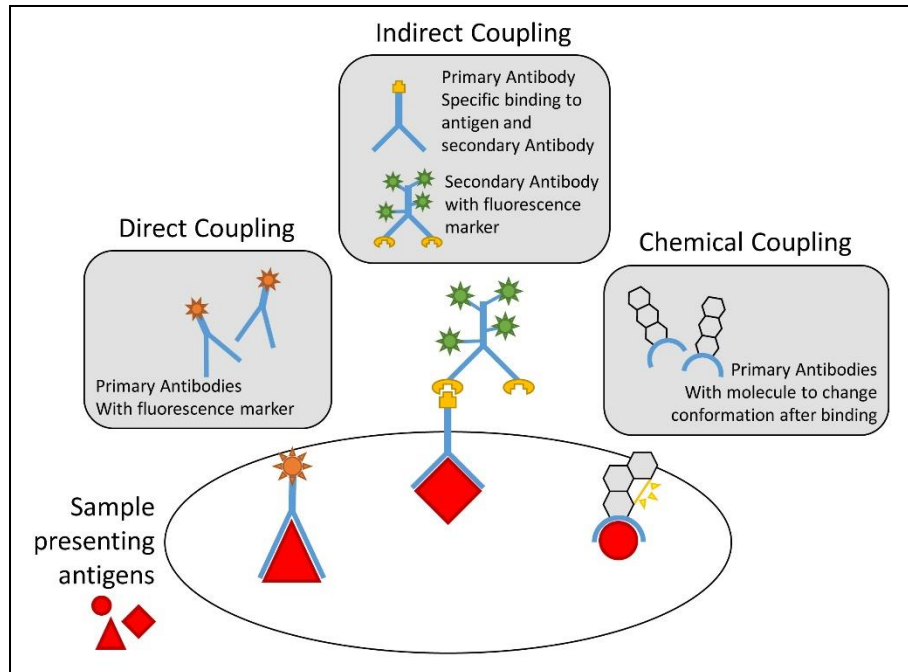


Figure 12: Different techniques used in immunostaining for fluorescently marking the expressed antigens (Wallin 2009)

3.6.3 Fluorescence Microscopy

The previous Chapter discussed the topic of immunostaining and the most common techniques performed with fluorescent dyes. It was introduced how this allows to selectively stain for specific antigens and materials in the sample. To extract the information highlighted in the immunostaining a fluorescent microscope is used to selectively extract images of the different fluorophores.

A fluorophore has the opportunity to emit light of a characteristic wavelength when excited with light of a specific wavelength. The basic process of fluorescence is explained by incident photons of the light source that excite the molecules into higher energetic but unstable states. The energy of the photons is absorbed by the fluorochrome, a fraction of that energy is translated into vibrational energy resulting in heat development in the sample. The remaining energy is emitted in the form of an emission photon when the molecule jumps back to its normal energetic state. Thus the energy of the emitted photon is lower than the energy of the exciting photon. A lower energy leads to lower frequencies and a higher wavelength of the emitting photons. (John Innes Centre 2015)

The wavelength shift can be seen in Figure 13 for the two fluorochromes DAPI and AlexaFluor 488. With the help of those curves the relation between absorbance and emission is displayed. This can be used to configure the fluorescence microscope for the specific fluorophores.

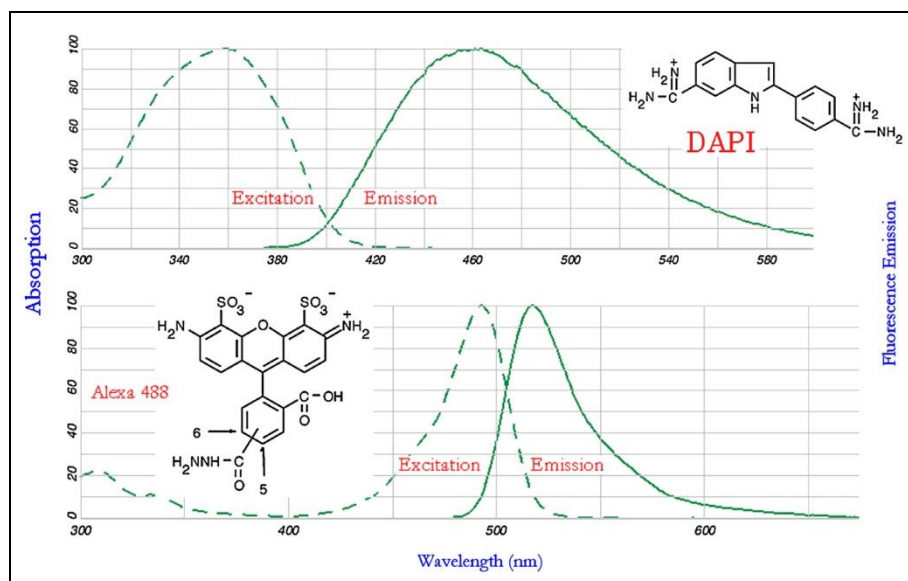


Figure 13: Excitation and Emission curves of the fluorophores DAPI (top) and AlexaFluor 488 (bottom) (Mondal & Diaspro 2014)

In Figure 14 we have the opportunity to look at the basic principle behind a fluorescence microscope. A light source of choice containing the wavelengths that are necessary for sufficient excitation of the used fluorophores. Following the path of the light emitting from the light source we can see the multispectral light hitting on the excitation filter where it is narrowed down to the necessary excitation wavelength (shown with the blue ray) which is reflected on the dichroic mirror down to the sample where it excites the fluorochromes to emit lights of smaller frequency as explained above. The excited light rays are allowed to pass vertically through the dichroic mirror and hit the emission filter eventually. This emission filter is chosen to permit the passage of the wavelengths to be expected from the used excitation frequency and fluorescent label.

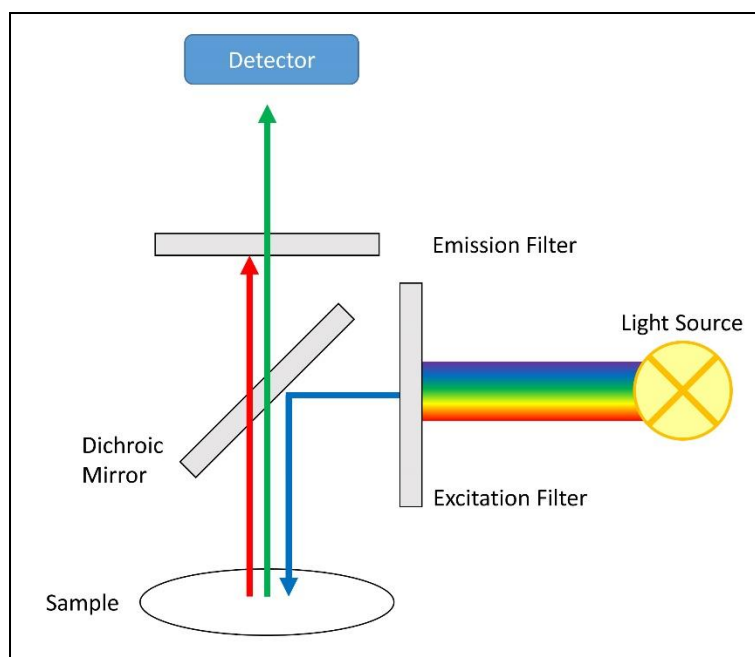


Figure 14: Schematic showing the basic setup of a fluorescence microscope (Mondal & Diaspro 2014; John Innes Centre 2015)

After the reduction of the light to one fairly narrow band of wavelengths the detector can record an intensity image. Thanks to that a fluorescent specific image can be taken as a grey value representation. This allows for easy handling and processing of the multiple images as different channels. These images are easier to manipulate and require less computing power, hence simplify image analysis (Chodorowski 2014). The filters and mirror are commercially available as filter cubes allowing for easy switching between the channels. With this a step-wise exposure of every individual channel is achieved resulting in an image exemplified in Figure 15.

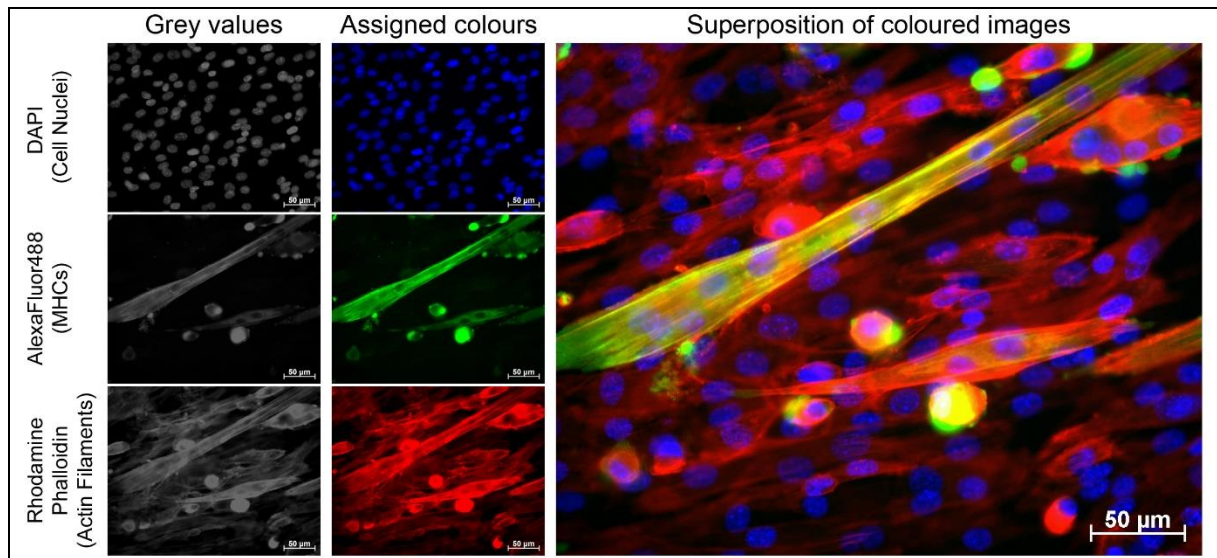


Figure 15: Example of the image construction after fluorescence microscopy

Every single channel of wavelength gets assigned 256 grey values and the channels can be analysed separately. In the example the grey value images directly recorded can be seen on the left. For the individual image the different cell organelles of interest were labelled with another fluorophore. Thus we retrieve an image of the cell nuclei, the myosin heavy chains (MHCs) as well as the actin found in the exposure frame. After that colours can be assigned to the different channels with the help of the used recording software as seen in the middle row and eventually a superposition of all the channels gives the final resulting microscopic image.

When working with fluorescence microscopy different drawbacks have to be mentioned, as indicated beforehand portions of the incident light energy are converted into heat energy and emitted into the surroundings of the fluorophore. This heat energy can lead to damage like photobleaching or photodamage of the sample (Mondal & Diaspro 2014). The photobleaching itself is the destruction of the fluorophore due to the energy exposure of the exciting light which will limit the cumulative exposure time of the sample and demand for working in a darkened environment. The photodamage will have effects on the sample itself especially when it is a heat sensitive sample or imaging of live cell cultures is performed. The additional energy brought into the culture will lead to denaturation of the proteins and often result in bursting of the cells. (Magidson & Khodjakov 2013)

3.6.4 Confocal Microscopy

After introducing the basics of light microscopy and fluorescence microscopy we can build on further by adding the confocal microscopy into the background knowledge for the project. In Figure 16 we can already see the principle setup of a confocal microscope. Here we have an illumination source attached to the side of the optical pathway through the filter cube similar to the principal setup of a fluorescence microscope. Furthermore, we can see that the microscope used here works in inverted mode as it illuminates and records images from below. What sets the confocal microscope apart from the microscopes introduced before is illustrated on the right hand side of Figure 16. There we can see the optical elements together with a pinhole right before the detector. Two main optical paths shown by a blue and a red set of rays, where the blue originates from an off-focal plane and the red directly from the focal plane. These rays are now traversing to the objective lens and only the light originating from the focal plane will be traversing parallel through the optical system. Right before the pinhole the light is focused for a sharp image represented on the detector. At that stage the function of the pinhole can be observed as it discriminates between the light that originates from the focal plan and the light outside of the focal depth. The light originating from the rest of the volume is blocked by the pinhole and does not contribute to the final image. (Mondal & Diaspro 2014)

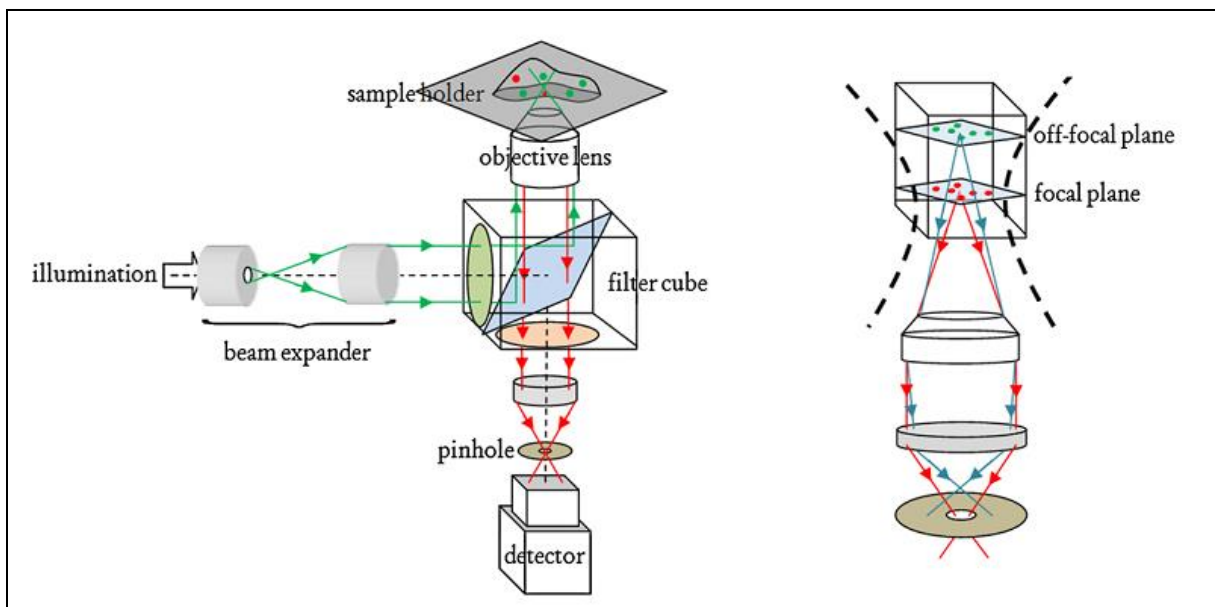


Figure 16: Schematic setup of a confocal microscope (left); function of the pinhole (right) (Mondal & Diaspro 2014)

With this technique a scanning process is necessary to achieve a whole image of the sample as only one point of the focus area will be represented sharply in the image (Wegerhoff et al. 2006). Furthermore, it enables to perform 3D mapping of the specimen as we can also scan through the axial plane of the sample. The final image will not be blurred by the light emanating from outside of the focus. Besides the increased axial resolution an additional effect of the pinhole will be the improvement of the spatial resolution (Scientific Volume Imaging B.V. 2015). Additionally, to the specific properties of a confocal microscope it can be specifically expanded to accommodate for fluorescence measurements by dimensioning the filter cube, light source and detector accordingly. (Mondal & Diaspro 2014)

Materials & Methods

4.1 Approach

The basis of the project was the idea of differentiating C2C12 cells in a three-dimensional environment provided by the capillary alginate into functional skeletal muscle cells. The third component in addition to cell culture and alginate scaffold would be the design of the bioreactor. In Figure 17 we can see a sketch of the basic concept on which this project was based. The three main components of the experimental setup are shown. On the left we have the alginate scaffold in a schematic showing the unidirectional capillaries, on the right we have the cells precultured and on the middle bottom the bioreactor shown as a rectangular casing. The concept was to develop a bioreactor where the capillary alginate can be placed in (Step 1), the precultured cells can be seeded into (Step 2) and that would allow the culture media to flow through the bioreactor and through the capillary respectively to bring the nutrients and oxygen down to the cell culture (Step 3).

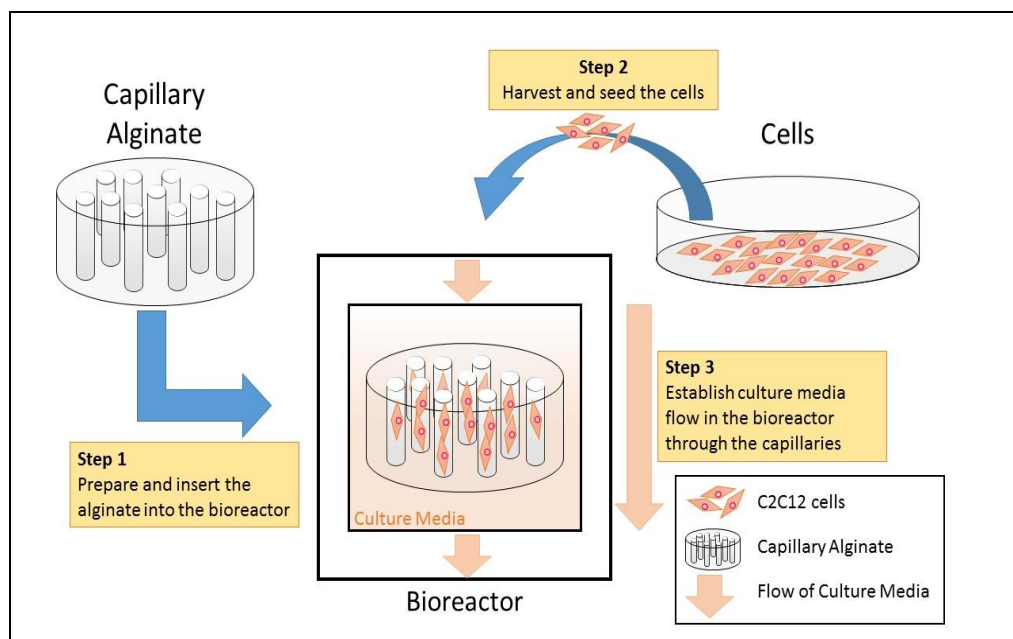


Figure 17: Sketch of the basic idea of the experimental setup and cell culture procedure

This here presented project is the continuation of a student project started during the tissue engineering courses (KPO065/FTF225) at Chalmers which had a similar goal in building a bioreactor system, with the capillary alginate to achieve skeletal muscle differentiation of C2C12 cells. Therefore, the findings and results of that student project build a good starting ground for progression and allow for improvement of the previously used systems.

In a first step computer simulations were performed to compare the bioreactor design of the previous project with an improved version of the system. Here flow and oxygen distribution inside the culture chamber and through the capillary alginate were of main interest. With these simulations the inner geometry of the bioreactor was to be evaluated and improved. On top of these inner parameters for the bioreactor the outside of the bioreactor was improved to address leakage problems.

When starting to work with the alginate scaffolds it was known that the alginate bulk modification with gelatin and alginate that was pre-coupled with RGD sequences yielded the best attachment of the cell cultures in the previous project. Therefore, those were chosen to be in the main focus of the scaffold development process with the inclusion of new surface modifications. The sterilization process of the alginate scaffolds has been known to be problematic from the previous project to address this a new sterilization method was employed.

Cell culture experiments on the surface of the alginate gels had proven to be a feasible manner. This allowed for easy cell culture handling as well as simple fixation, staining and imaging to assess the culture status with respect to the capillaries and different modifications.

A detailed list of materials can be found in Appendix 1.

4.2 Bioreactor

4.2.1 Simulations

The simulations in this project were performed with the help of “Comsol Multiphysics 4.2” (Comsol Inc. 2015) in the designing phase. Over the course of the project the simulations were picked up later again to see if the system could be developed further and additional more refined simulation steps could be run. The new modelling was performed with a re-build version of the conical bioreactor in “Comsol Multiphysics 5.0” (Comsol Inc. 2015). One of the main goals was to update the simulation to a newer version for easier updating in the future and to implement the Glucose consumption into the overall model. In the following Chapter the design of the simulation is introduced and the used parameters are presented as well as moderated.

Two different designs of the culture chamber were tested in the computer simulations during the designing phase of the project. Figure 18 shows the two different models used for simulating the conditions in the proposed Bioreactor. On the left side we have a representation of the old bioreactor design according to the previous project and on the right we can see the new design used in this project. The physical models applied were “Turbulent Flow” and the “Transport of Diluted Species” for the oxygen distribution.

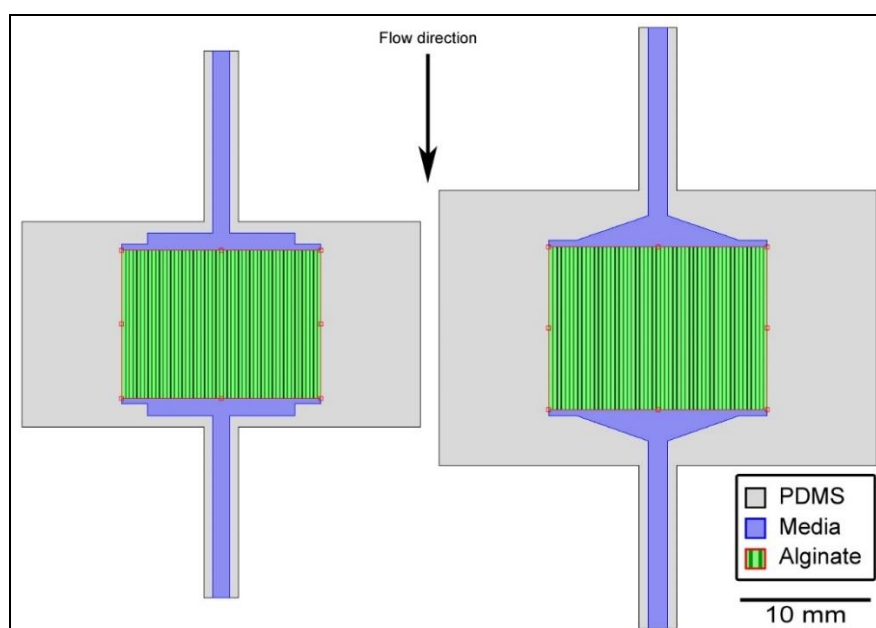


Figure 18: Old rectangular Bioreactor format (left) and new conical channel design (right)

In the previous project alginate gels with varying modifications and concentrations of the crosslinking agent were imaged and analysed to assess pore diameter and pore density in the scaffolds. Based on these results Table 1 gives the modelling parameters for the average alginate used in this project (see Chapter 4.3.2) and the maximum cell number used in the previous project for estimating the oxygen consumption of the cell culture. (Peng et al. 2014)

Table 1: Alginate properties in the simulation

Parameter	Dimensions
Pore density	30 Pores/mm ²
Pore diameter	78 μ m
Alginate diameter	17.5 mm
Cell number	500,000 cells

For modelling the oxygen diffusion through the materials the corresponding coefficients had to be defined. Table 2 shows the parameters for the three main components media (approximated as water), PDMS and alginate with their respective literature sources and coefficient values. In the publication by Kim et al. a mathematical model was created to estimate the oxygen transfer through microfluidic devices made from PDMS and Mehmetoglu et al. investigated the oxygen transfer through calcium alginate beads by the moment analysis method (Kim et al. 2013; Mehmetoglu et al. 1996).

Table 2: Diffusion coefficients for the oxygen transport

Material	Diffusion Coefficients (m ² /s)
Media (Water) (Kim et al. 2013)	2.80e-5
PDMS (Kim et al. 2013)	7.88e-5
Alginate (Mehmetoglu et al. 1996)	2.50e-5

To further model the oxygen diffusion through the system a constant inflow was realized by setting the outer boundaries to a concentration of 0.2 mol/m³ corresponding to the 20% oxygen in the air. For the current simulation cells are solely modelled as oxygen consumers therefore sinks for the diluted O₂ got placed inside of the capillaries. Table 3 shows the values for oxygen consumption converted into SI base units for usage in Comsol and the respective literature sources. Both Nicholls et al. and Li et al. were interested in the metabolic behaviour of the C2C12 cells under changed environmental circumstances. Nicholls et al. measured the cells with the Seahorse XF 96 analyser (Seahorse Bioscience 2015) from here the basal oxygen consumption of the two different measurement series was used. In the publication by Li et al. the main interest was on determining the effects of different levels of glucose and oxygen on the metabolic activity of the C2C12 cells. The data was measured with the Becton and Dickinson (BD) Biosensor system (BD Biosciences 2015) from here the normoxic and high glucose (in accordance to the used culture media) oxygen consumption rate was taken. (Nicholls et al. 2010; Li et al. 2013)

Table 3: Oxygen Consumption of C2C12 cells

O ₂ Consumption (mol/(m ² *s))	Source
4.115e-9	Nicholls et al. 2010
9.969e-9	Nicholls et al. 2010
2.288e-5	Li et al. 2013

The whole setup was assumed to be fully saturated with oxygen at the beginning of the simulation and the media is assumed saturated as well thus allows for additional inflow of dissolved oxygen from the reservoir. The flow velocities through the bioreactor was swept over several extrema as displayed in Table 4. The first two parameters are the minimum and maximum pump speeds used in the 3D cell cultures during the previous project (Peng et al. 2014). Dennis et al. compiled a general guide for bioreactors to culture muscle tissue (Dennis et al. 2009) and the parameters given in Table 4 and Table 5 are the boundaries in which a perfusion bioreactor should operate to increase the number of cells deep in the tissue (Dennis et al. 2009).

Table 4: Simulated flow rates

Inflow (m/s)	Inflow (pump dim)	Source
1.415e-6	0.6 µl/min	Min
1.415e-7	6.0 µl/min	Max flow rates used in (Peng et al. 2014)
1.415e-3	0.6 ml/min	Min
7.074e-3	3.0 ml/min	Max flow rates used in (Dennis et al. 2009)

In the updated model in “Comsol Multiphysics 5.0” the flow rates were chosen according to the range given by Dennis et al. as they were planned to be used in the 3D cell cultures as well. Additionally to the boundary parameters two intermediate speeds were chosen to allow for better approximation of the ideal flow speed as shown in Table 5 (Dennis et al. 2009).

Table 5: Simulated flow rates for Comsol Multiphysics 5.0 (Dennis et al. 2009)

Inflow (m/s)	Inflow (pump dim)
1.415e-3	0.6 ml/min
2.830e-7	1.2 ml/min
5.660e-3	2.4 ml/min
7.074e-3	3.0 ml/min

The oxygen consumption was now modelled as a reaction at the position of the cells in the capillaries and it was focused on the maximum oxygen consumption according to Nicholls et al. Incidentally, Table 6 shows the oxygen consumption converted for usage in the new model based on the value from Table 3. (Nicholls et al. 2010)

Table 6: Oxygen Consumption as reaction in the Comsol Multiphysics 5.0 model

O ₂ Consumption (mol/(m ³ *s))	O ₂ Consumption (mol/(m ² *s))	O ₂ Consumption (pMol/min)
6.6468e-4	9.969e-9	550

The Glucose usage was estimated stoichiometrically as shown in equation 3. It got implemented in a similar fashion as the oxygen consumption (“Transport of Diluted Species” and the consumption as a reaction) but limited to the culture media only. The glucose content of the used DMEM (Sigma Aldrich 2015) was 24,98 mol/m³ (4.5 g/l).

$$\begin{aligned}
 & C_6H_{12}O_6 + 6 \cdot O_2 \rightleftharpoons 6 \cdot CO_2 + 6 \cdot H_2O \\
 & G_{\text{glucose}} C_{\text{consumption}} \left(\frac{\text{mol}}{\text{m}^3 \cdot \text{s}} \right) = \frac{O_2 \text{ Consumption}}{6} \quad (3) \\
 & \underline{\underline{GC = 1.1078 \cdot 10^{-4} \frac{\text{mol}}{\text{m}^3 \cdot \text{s}}}}
 \end{aligned}$$

4.2.2 Design and Manufacturing

In concert with the results of the simulation the design of the bioreactor was determined. AutoCAD 2012 (Autodesk Inc. 2014) was used to draft the models and handed over to MakerWare for 3D printing with the MakerBot Replicator 2X (Makerbot Industries 2014). The PDMS was moulded in 3D printed casts according to the attached protocol (see Appendix 2). Furthermore, the retainer pressing the PDMS halves together and the culture stands have been printed for usage during the experiments in this project. Figure 19 shows a schematic of the PDMS channel to illustrate the interlocking of the top with the bottom half of the PDMS channel. This was achieved by creating a general mould for the vertical borders and allow for different horizontal inlays. The printing roughness of the 3D printer was compensated by smoothing the inlays inner face to achieve soft meeting faces of the PDMS halves. This in concert with the interlocking mechanism allowed for better tightness and leakage prevention of the bioreactor.

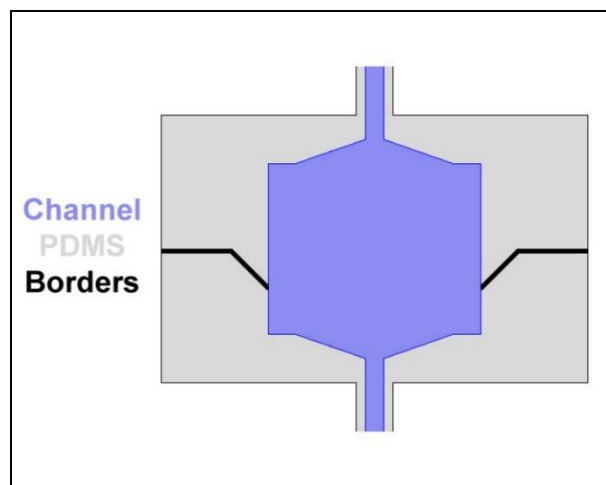


Figure 19: Schematic of the PDMS interlocking with each other

Figure 20 shows the printed moulds on the left side (A-C) in C the smoother surface can be seen on the sides compared to the roughness from the filament extrusion at the other surfaces. The two halves shown in Figure 20 D need to be tightly pressed together to achieve stable culture conditions inside of the bioreactor. For this a holder system was designed as depicted in Figure 21.

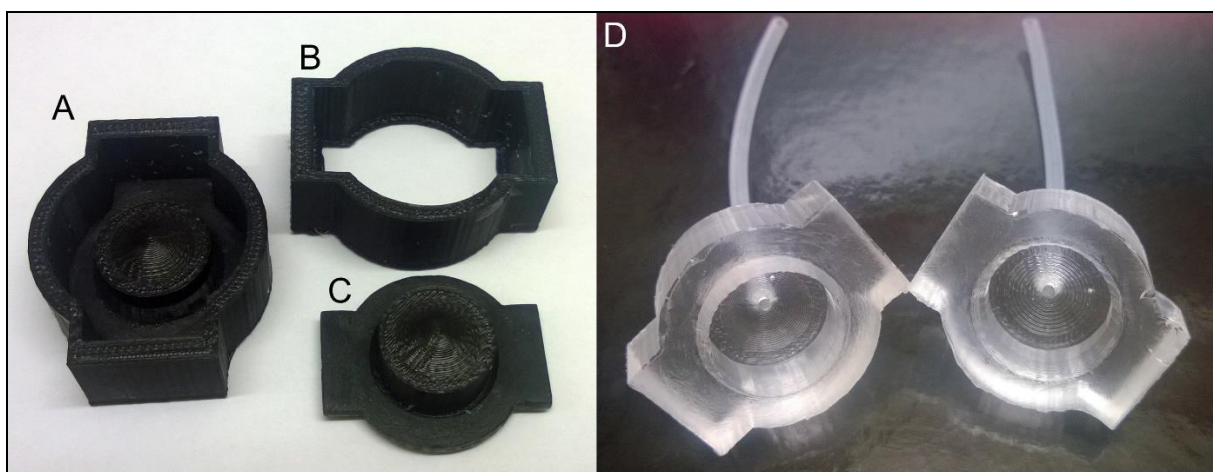


Figure 20: Printed ABS moulds (left) and PDMS moulding result (right); A) Outer cast with positive inlay B) Outer cast C) Negative Inlay D) PDMS half with positive lip (left) and with wider opening (right)

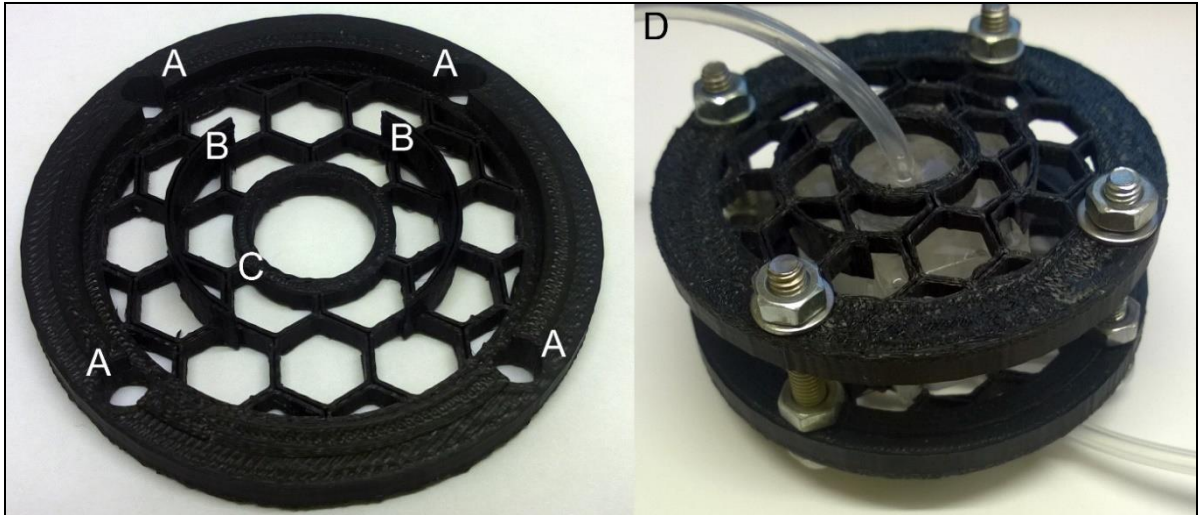


Figure 21: ABS Retainer for assembling the PDMS with screw holes (A), lateral retainers (B) and inner ring (C); (D) shows the PDMS channel and retainer fully assembled

The screws allow for a very tight pressure application on the PDMS channel and fine tuneable re-screwing in case of later leakages due to pressure spikes. With the lateral retainers (Figure 21 (B)) a sliding of the PDMS channels is inhibited. The inner ring (Figure 21 (C)) together with the honeycomb mesh structure allow for a good distribution of the force over the whole PDMS whilst letting air into the culture chamber. Additionally, the inner ring takes prevents direct pressure to be applied on the culture chamber.

In Figure 22 the bioreactor is placed in the culturing stand, a 3D printed stand made from ABS together with a 250 ml container below. The culturing stand allows for better handling during the cell culture as well as more stable conditions with respect to positioning of the culture channel.

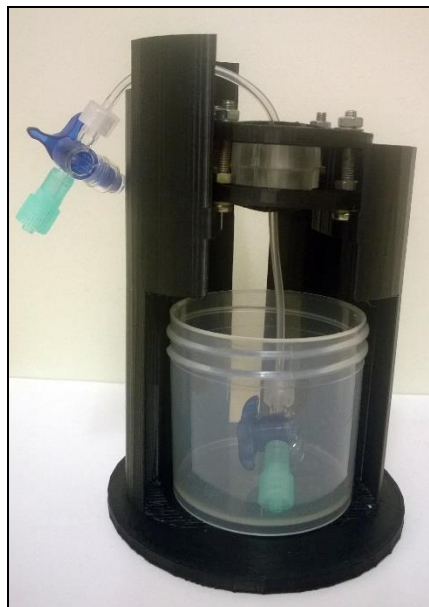


Figure 22: Full assembly of the bioreactor together with the culturing stand

4.2.3 Leakage Experiments and Flow Through

For the leakage experiments the retainer together with the conic PDMS channel was assembled completely (Figure 23) and filled with water while pushing the remaining air out. The potential risk of bubble formation was given great attention to achieve a good representation of the desired culturing conditions and assess the feasibility of the new PDMS channel.

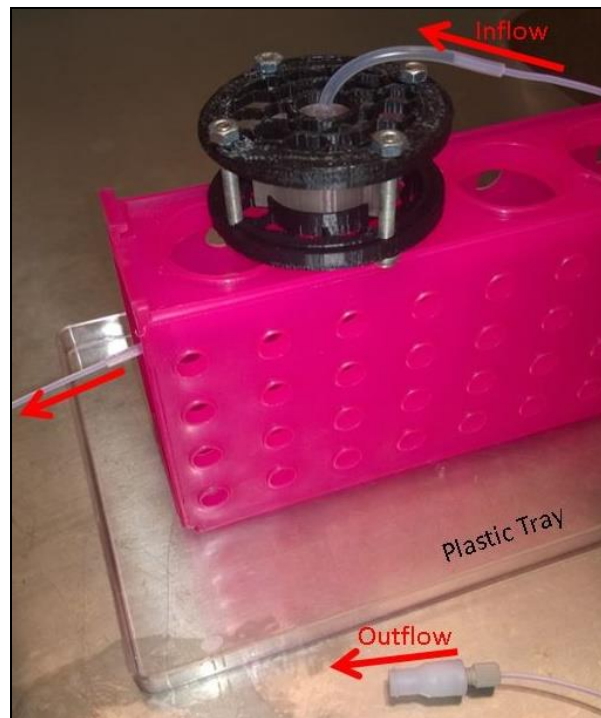


Figure 23: Setup for the leakage experiments with the pump system

During the flow through experiments a gelatin:alginate (1:1) sample was inserted into the flow chamber. MilliQ water dyed with blue food colouring was used as a flushing media to assess the flow distribution after opening the bioreactor again. Areas of higher colour intensities were assumed to have higher throughput. Flow was performed for 30 minutes at 10 $\mu\text{l/s}$ adapted from Dennis et al. (Dennis et al. 2009).

4.3 Scaffolds

4.3.1 Alginate Gel Formation

The non-porous gels were prepared in 100 ml beakers by filling 30 ml of alginate (1.5% w/w) solution into them. The next step was to spray the surface with CaCl_2 (1M) amounting to roughly 5-6 ml. After letting the gels settle for 20 mins the beakers are filled up with additional 25 ml of CaCl_2 -solution (1M). The last step was to cover the beakers with Parafilm and the whole formation process will take 12-24 h.

4.3.2 Formation of Capillary Alginate Gels

The capillary alginate gels need additional steps prior to crosslinking the alginate. The inner walls of the beakers (100 ml) are covered with a thin layer of alginate (1.5% w/w) solution, the excess was let

dripped off and then they are baked in the oven for 1 h at 140 °C. After cooling off they can be used for gel formation or stored for later use by covering with Parafilm.

The further processing steps are similar to the formation of the non-porous gels. After spraying the alginate solution with CaCl₂ (1M) and waiting for 20 mins a meniscus has to form on top of the gels. The filling up with the last 25 ml of CaCl₂-solution (1M) has to be performed carefully to not destroy the meniscus, otherwise the capillary structure cannot form. To allow for clean growing of the capillaries the beaker should not be moved after filling up and left unattended for up to 48 h.

A detailed protocol used as basis can be found in the Appendix 4.

4.3.3 Modification of Alginate Gels

(a) Bulk Modifications

Bulk modifications used during this project have been gelatin or pre-coupled GRGDSP alginate. Both were mixed with the pure alginate at the desired weight-to-weight ratios and further handled like the alginate solution for crosslinking to capillary or non-capillary alginate gels as described in the previous Chapters 4.3.1 & 4.3.2.

(b) Surface Modifications

Surface modifications were performed with collagen or GRGDSP sequence obtained by BACHEM (BACHEM 2015). The peptide sequence arrived in a freeze-dried powder state and was dissolved to a stock solution of 0.1 mg/ml GRGDSP:MilliQ water and kept at – 18 °C for later usage (according to the BACHEM customer service (BACHEM 2015)). The alginate gel used for the surface coupling protocols was pre-formed 1.5% alginate without capillaries and stored in MilliQ and fridge prior to usage.

The first RGD couplings (see Table 7) were adapted from Rowley et al. (Rowley et al. 1999) in which the preformed alginate gels are suspended in an aqueous solution of ddH₂O (40 ml), Sulfo-NHS and EDC in a ratio of 1 to 2. Eventually followed by the addition of the GRGDY peptide and a reaction time of 20 h. In this project it was refrained from using such a high solution of the reagents, and MES buffer was added to reduce the risk of hydrolyzation of the EDC.

Table 7: RGD surface coupling on alginate discs; protocol adapted from Rowley et al. (Rowley et al. 1999)

Experiment	Alginate discs	Quantities and Procedure
1 st RGD surface coupling	14 (7/7)	NHS & EDC dissolved in MES (0.1 M) stock MES buffer (0.1 M) freshly dissolved GRGDSP 0.1 mg/ml <ol style="list-style-type: none"> 1. discs suspended in 2.5 ml MES buffer 2. 3 µl EDC and 6 µl NHS added 3. 100 µl RGD solution 4. 20 h incubation
2 nd RGD surface coupling	14 (7/7)	sNHS & EDC prepared as new stock solutions 0.1M MES buffer (0.1 M) freshly dissolved GRGDSP 0.1 mg/ml <ol style="list-style-type: none"> 1. discs placed in 15 ml centrifuge tube 2. 20 µl EDC, 40 µl sNHS and 100 µl RGD stock added 3. Filled up to 1 ml with MES buffer 4. 70 h incubation
3 rd RGD surface coupling	18 (9/9)	sNHS & EDC prepared as new stock solutions 0.1M MES buffer (0.1 M) freshly dissolved GRGDSP 0.1 mg/ml <ol style="list-style-type: none"> 1. discs placed in MilliQ (total of 2.5 ml) 2. 500 µl of MES Buffer added 3. 4 mg sNHS freshly dissolved around discs 4. 2 mg EDC freshly dissolved around discs 5. 17 h incubation

In the coupling process for RGD experiments 4-5 (see Table 8) a new protocol by Life Technologies (Thermo Fischer Scientific & Life Technologies 2015) for “Two-step Coupling of Proteins Using EDC and NHS or Sulfo-NHS” (see Appendix 5) was altered to fit the necessary conditions. Activation and coupling buffer have been prepared as described in the protocol.

Table 8: RGD surface coupling of alginate discs, protocol adapted from Life Technologies (Thermo Fischer Scientific & Life Technologies 2015)

Experiment	Alginate discs	Quantities and Procedure
4 th RGD surface coupling PBS	10 (5/5)	<p>Activation and coupling buffer freshly prepared</p> <ol style="list-style-type: none"> 1. discs placed in 2 ml activation buffer 2. 6.74 mg EDC + 2.35 mg sNHS dissolved in 2 ml activation buffer Added 1 ml to each disc batch 3. Incubate for 15 mins at RT 4. Quenched with 4.22 µl 2-mercaptoethanol 5. 200 µl RGD stock solution mixed with 800 µl coupling buffer Added to one batch 6. 800 µl of coupling buffer to the other batch 7. Incubated for 2 h at RT 8. Aspirated solution from the vials 9. Wash with PBS 10. Placed in MilliQ
4 th RGD surface coupling HEPES	10 (5/5)	<p>Activation buffer NaOH adjusted to pH 6.04 Prepared new Coupling buffer substituting PBS with HEPES and NaOH adjustment to pH 7.02</p> <ol style="list-style-type: none"> 1. discs placed in 2 ml activation buffer 2. 6.64 mg EDC + 2.49 mg sNHS dissolved in 2 ml activation buffer Added 1 ml to each disc batch 3. Incubate for 15 mins at RT 4. Quenched with 4.22 µl 2-mercaptoethanol 5. 200 µl RGD stock solution mixed with 800 µl coupling buffer Added to one batch 6. 800 µl of coupling buffer to the other batch 7. Incubated for 2 h at RT 8. Aspirated solution from the vials 9. Wash with MilliQ; two times for 5 mins 10. Placed in MilliQ
5 th RGD surface coupling	6 (3/3)	<p>Same protocol and chemicals as in previous coupling, Sterilization of the alginate discs before coupling according to Stoppel et al. (Stoppel et al. 2014) sNHS 6.71 mg/EDC 2.42 mg in 2ml activation buffer</p>

The collagen surface coating was performed with a surface coverage of $5 \mu\text{g}/\text{cm}^2$ and dropped on the prepared slides (see 4.4.1). After incubation in the LAF bench for 1 h the excess collagen was aspirated and the sample washed with serum free medium (DMEM). The coating was always performed directly prior to the seeding. The detailed protocol can be seen in the Appendix 6.

4.3.4 Sterilization

In preparation to cell cultures the alginate scaffolds have to be sterilized to allow for long standing cultures and reduce the risk of infections. In this study a protocol proposed by Stoppel et al. was used to achieve sterile scaffolds (Stoppel et al. 2014). This includes placing the alginate in 70 % Ethanol for 20 mins and washing the slides 3 times in MilliQ water for 2x5 mins and 10 mins successively. In between the steps thorough aspiration and rinsing has to be performed to ensure the sterility and simultaneously prevent residing Ethanol to not negatively influence the culture. Sterile working methods apply during the whole procedure.

Detailed protocol in Appendix 3.

4.4 Cells

4.4.1 Flat Gel Experiments

The cells have been cultured in T-flasks prior to the usage in the culture experiments. For these culture conditions the seeding and counting protocols are attached in the Appendices (8-10). The media that has been used during the culture in the T-Flasks and in the proliferative phase was the Growth Media (GM) and when initializing the differentiation in the culture experiments the Differentiation Media (DM) was used. Culture media compositions are shown below:

Growth Media: DMEM
 10 % Fetal Bovine Serum (FBS)
 1 % Penicillin Streptomycin

Differentiation Media: DMEM
 2 % Horse Serum (HS)
 1 % Penicillin Streptomycin

For the Flat Gel Experiments, small rectangular (w*b*h: 18*15*2 mm) slides have been cut from the alginate gel and were transferred to multi-well culture dishes for cell experiments. The cell solution with desired cell concentration was dropped onto the gel slides, trying to get as much cells as possible on the gels. After an initial attachment time of 30 mins, the excess media was aspirated and growth media (GM) was filled in around the gel slides.

Table 9 shows an overview about the experiments performed on the flat gels prepared as described previously. The first column gives a rough description and the used work title for the respective experiment. Under specifications the motivation, newly implemented techniques and method changes between the experiments are listed to give an overview of the development process. As the goal was to analyse the attachment efficiency of various scaffolds, a list of the materials used for each experiments is given under scaffolds. Besides the seeding amounts and the theoretical cell densities on the surface the durations of the cell cultures are given. These time points are also the time points at which the samples were imaged. Noteworthy is that after the introduction of the live-staining the cultures could be checked more often and the same cultures could be followed up for prolonged periods without terminating the experiment through fixation and staining.

For Flat Gel Experiment 3 and 4 the cell solution was diluted to be up to 3 ml of GM and later contain a lot of cells in comparison to the gel size. With this the whole culture well was filled up allowing the cells to settle anywhere and to increase the chances of the cells landing on the culture slides.

Table 9: Experiments in cell culture dishes

Experiment	Specifications	Scaffolds	Samples	Duration	Seeding Amount/ Density (cells/mm ²)
Cell culture on various Scaffolds	Tested new sterilization method acc. to <i>Stoppeler et al.</i>	Alginate	1	1 d	150,000
		Cap. Alginate	1		2,300
		Gelatin:Alginate 1:1	1		
		RGDA:Alginate 1:100	1		
FlatGelExp 1					
Cell culture on various Scaffolds	New gel cutting method	Alginate	2	1 d; 7 d	51,000
		Cap. Alginate	2		196
		Gelatin:Alginate 1:1	2		
		RGDA:Alginate 1:100	2		
		Alginate Collagen coat.	2		
FlatGelExp 2					
Cell culture on various Scaffolds	Live staining	Control	1	30 mins;	50,000
		Alginate	1	1 d; 2 d;	192
		Cap. Alginate	1	3 d; 4 d;	
		Gelatin:Alginate 1:1	1	7 d; 8d	
		RGDA:Alginate 1:100	1		
FlatGelExp 3					
Cell culture on various Scaffolds	Addition of transmission imaging	Control	2	3 d; 7 d	500,000
		Alginate	2		1,900
		Cap. Alginate	2		
		Gelatin:Alginate 1:1	2		
		RGDA:Alginate 1:100	2		
		Collagen Coating	2		
FlatGelExp 4					
Cell culture on various Scaffolds	Live staining and fixation + staining comparison	Collagen Coating	2		
		Collagen Coating	2		

4.4.2 PDMS dish Cell Cultures

A refinement of the gel cultures on flat gels has been proposed during the project. The PDMS dishes were created by filling in PDMS (mixed according to the PDMS protocol Appendix 2) letting it sit in for crosslinking at room temperature for 24–48 hours. After that a small piece of the PDMS was punched out with the help of a hole punch (diameter 7 mm). These dishes were sterilized with ethanol and rinsed with sterile MilliQ prior to the culture. The culture ready alginate was cut with the help of a hole punch to small gel discs (diameter 7 mm; ~2 mm thick). The discs were stored in GM either after or before cutting, due to swelling in the GM a re-cutting was performed before placing it in the middle of the PDMS. A small drop of the cell solution of desired density was placed directly on top of the alginate gel by utilizing the PDMS's hydrophobicity. After initial incubation and attachment of the cells, the excess media was aspirated and the whole dish filled with culture medium.

The schematic in Figure 24 shows a cross section of a PDMS dish during the cell seeding process. It displays how the punched whole in the middle of the PDMS is filled with the alginate disc prior to cell culture. In red we can see how the cell media is placed as a droplet over the scaffold with the help of the hydrophobicity of the PDMS.

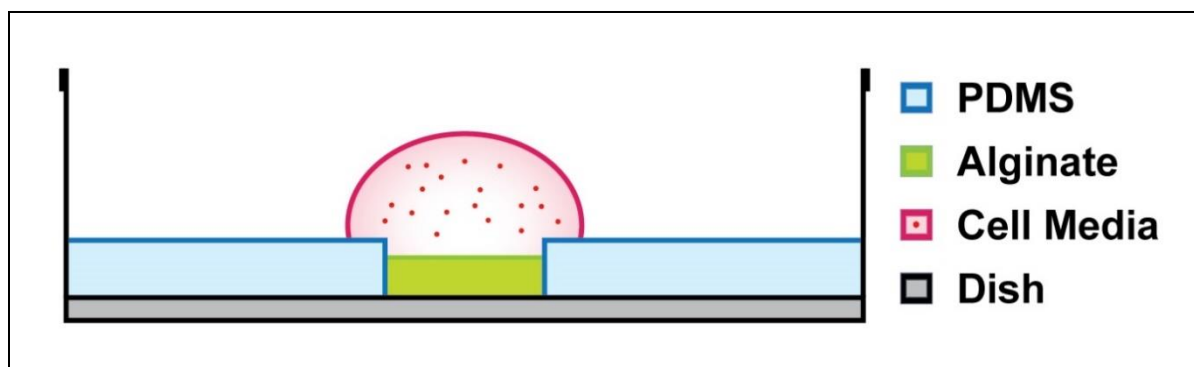


Figure 24: Schematic of the PDMS dish during cell seeding

Table 10 shows the different culture experiments performed in the PDMS dishes to compare the bulk modified alginate gels with respect to their influences on cell attachment. For this many different alginate modification combinations were screened as shown in the columns scaffold. From experiment “PDMSFlatGelExp–3+7d” onwards the GM was exchanged after a few days by DM to test the different effects of both culture medias. The respective culture times for the GM and DM are shown in the specifications column.

The PDMS dishes were also used during the testing of the RGD surface coupling efficacy shown in Table 11. In addition to the experiment parameters given in the previous tables, the alterations of the surface coupling protocols together with a reference to the basic surface coupling protocol is given. This couplings have been performed based on the one published by Rowley et al. (Rowley & Mooney 2002) or Life Technologies (Thermo Fischer Scientific & Life Technologies 2015) as described in Chapter 4.3.3.

Table 10: Experiments in cell culture dishes with PDMS retainer

Experiment	Specifications	Scaffolds	Samples	Duration	Seeding Amount/ Density (cells/mm ²)	
Cell Culture in PDMS dishes	New Culture Dish	Control (no gel)	1	3 d	300,000	
	Smaller Alginate size	Gelatin coat. Dish	2		7,792	
		Alginate	1			
		Cap. Alginate	2			
PDMSFlatGelExp – 3 d	Live-stained before seeding	RGDA:Alginate 1:100	1			
		Gelatin:Alginate	1			
	RGDA:Alg. variations	Control (no gel)	1	30 mins;	80,000	
		Gelatin 3% (w/o Alginate)	1	1 d; 4 d;	2,078	
		RGDA:Alginate 1:1	1	10 d		
		RGDA:Alginate 1:10	1			
		RGDA:Alginate 1:25	1			
		RGDA:Alginate 1:50	1			
RGDA:Alginate 1:100	1					
PDMSFlatGelExp – RGD	Live-stained before seeding	Control (no gel)	1	30 mins;	10,000	
		Cap. RGDA:Alginate 1:1	1	3 d; 7 d	260	
	Differentiation Experiments	Cap. RGDA:Alginate 1:2	1			
		Cap. RGDA:Alginate 1:5	1			
	Lower cell numbers seeded	Cap. RGDA:Alginate 1:10	1			
		Cap. RGDA:Alginate 1:100	1			
	Proliferation and too dense	Cap. RGD-Alginate 1.5%	1			
		Cap. Alginate 1.5%	1			
	PDMSFlatGelExp – 3+7 d	Live-stained before seeding				

Experiment	Specifications	Scaffolds	Samples	Duration	Seeding Amount/ Density (cells/mm ²)
Cell Culture in PDMS dishes	Differentiation Experiments 1 d in GM 7 d in DM	Control (no gel)	1	30 mins;	50,000
		RGDA:Alginate 1:1	1	1; 7 d	1,299
		Cap. RGDA:Alginate 1:1	1		
		RGDA:Alginate 1:2	1		
		Cap. RGDA:Alginate 1:2	1		
		RGDA:Alginate 1:5	1		
		Cap. RGDA:Alginate 1:5	1		
		RGDA:Alginate 1:100	1		
		Cap. RGDA:Alginate 1:100	1		
		Alginate 1.5 %	1		
		Cap. Alginate 1.5%	1		
		Control (no gel)	1	30 mins;	10,000
		live-stained	2	Daily	260
RGDA:Alginate 1:5 – 4d	2	imaging			
live-stained					
RGDA:Alginate 1:5 – 4d	2				
no staining					
Control (no gel)	1	– 1+3d		50,000	
live-stained				1,299	
RGDA:Alginate 1:5 – 1+3d	1				
live-stained					
RGDA:Alginate 1:5 – 1+3d	1				
no staining					
ControlFlatGelCulture GM/DM					

Table 10 continued

Table 11: RGD surface coupling cell experiments

Experiment	Specifications	Scaffolds	Samples	Duration	Seeding Amount/ Density (cells/mm ²)
RGD surface coupling with Cell Culture <i>Rowley et al.</i>	EDC and NHS pre-dissolved from kit in MES-Buffer	Alg. 1.5 % MilliQ Alg. 1.5 % EDC/NHS Alg. 1.5 % EDC/NHS/RGD	1 1 1	30 mins; 1 d	30,000 779
First RGD surface coupling	Live-stained/PDMS dish				
RGD surface coupling with Cell Culture	New sNHS used EDC and sNHS freshly dissolved 0.1 M in MES Buffer	Control (no gel) Alg. 1.5 % EDC/NHS/RGD Alg. 1.5 % EDC/NHS/RGD sterile Alg. 1.5 % EDC/sNHS Alg. 1.5 % EDC/sNHS sterile	1 1 2 1 2	30 mins; 2 d	6,000 156
<i>Rowley et al.</i>					
Second RGD surface coupling	Live-stained/PDMS dish				
RGD surface coupling with Cell Culture	Dissolved EDC and sNHS on top of the immersed gels directly	Control (no gel) Alg. 1.5 % EDC/NHS/RGD Alg. 1.5 % EDC/NHS/RGD sterile Alg. 1.5 % EDC/sNHS Alg. 1.5 % EDC/sNHS sterile	1 1 2 1 2	30 mins; 3 d	10,000 260
<i>Rowley et al.</i>					
Third RGD surface coupling	Live-stained/PDMS dish				

Table 11 continued

Experiment	Specifications	Scaffolds	Samples	Duration	Seeding Amount/ Density (cells/mm ²)
RGD surface coupling with Cell Culture	First trial of new protocol from life-technologies	Control (no gel)	1	30 mins;	10,000
		PBS Alg. 1.5 % EDC/NHS/RGD	1	3 d	260
<i>Life Technologies</i> Fourth RGD surface coupling	PBS and HEPES used as Buffer	PBS Alg. 1.5 % EDC/NHS/RGD sterile	2		
		PBS Alg. 1.5 % EDC/sNHS	1		
		PBS Alg. 1.5 % EDC/sNHS sterile	2		
		HEPES Alg. 1.5 % EDC/NHS/RGD	1		
		HEPES Alg. 1.5 % EDC/NHS/RGD sterile	2		
		HEPES Alg. 1.5 % EDC/sNHS	1		
RGD surface coupling with Cell Culture	Live-stained/PDMS dish Sterilized gels before surface coupling Used fourth coupling protocol with HEPES Live-stained/PDMS dish	HEPES Alg. 1.5 % EDC/sNHS sterile	2		
		Control (no gel)	1	30 mins;	10,000
		HEPES Alg. 1.5 % EDC/NHS/RGD sterile	3	2 d; 5 d	260
<i>Life Technologies</i> Fifth RGD surface coupling	Used fourth coupling protocol with HEPES Live-stained/PDMS dish	HEPES Alg. 1.5 % EDC/sNHS sterile	3		

4.4.3 3D Cell Cultures

A protocol was put together to guide through the seeding process of the 3D cultures. See Appendix 14.

The cell cultures in the bioreactor (as well as the previously discussed 4.2.3 Leakage Experiments and Flow Through) have been performed with gels cut from the capillary alginate gel. Gels with a height of 10-15 mm were cut out in a barrel shape with the capillaries aligned parallel to the longitudinal axis. The diameter was chosen a bit larger than the diameter of the culture chamber resulting in gels around 20 mm in diameter. The gels were sterilized according to the standard procedure (4.3.4), emerged in culture media and placed in the incubator over night for swelling and letting the media diffuse in the matrix. It is important to cut the alginate from the central part. If we remember the spindle like structures from the capillary alginate formation (Figure 6 in Chapter 3.3.1), we can imagine that the border of the beaker and the height will influence the capillary distribution in the gel. Therefore, the central part of the gel will yield the most parallel aligned capillaries.

Figure 25 shows the different pump and valve configurations used during the project. Where the schematic key displays the individual components of the system. As one can see all the setups relied on one pump and four stop-cocks. The three way stop-cocks allowed for conveniently accessing the system with syringes at specific spots for either insertion or extraction of media. In the two configurations on the bottom an additional component was added to the setup, the bubble trap. This was chosen to be done for the longer cell cultures to avoid air accumulation in the system, to have a reservoir for more culture media and it allowed for refreshing the culture with new media during the culture.

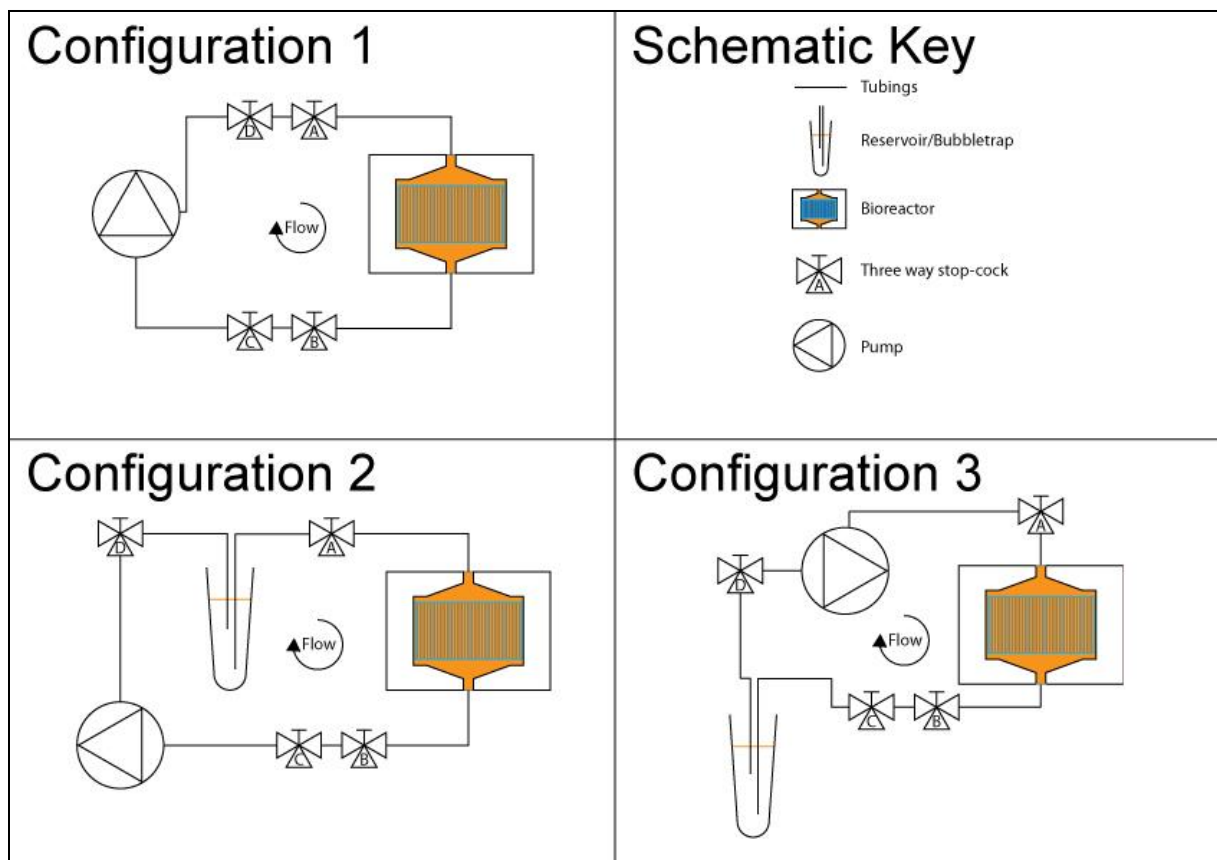


Figure 25: Schematic of the different system configurations used during 3D cell culture

To ensure a healthy cell culture the preparation process had to be optimized to reduce the amount of enclosed air in the system as much as possible. Especially when working with serum containing culture media a bubble formation can lead to immense foaming. The first step was to connect the alginate loaded bioreactor to the connectors A and B. Then GM filled syringes (10 ml) were connected to those connectors and the media was pressed through while holding the syringes in an upright position as shown in Figure 26. This allowed the air to enter into the syringes but not back into the culture chamber. A turning of the bioreactor was beneficial to allow the air to traverse into the syringes more easily. After the bioreactor was prepared it would be stored in the incubator at 37 °C; 5 % CO₂ until the culture was started.

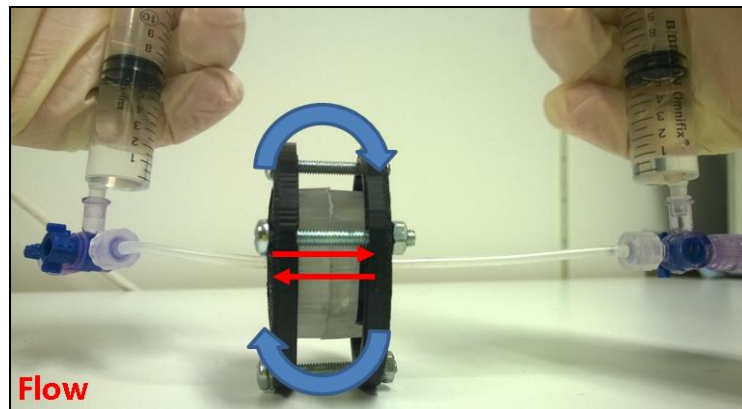


Figure 26: Flushing of the Bioreactor with media (here MilliQ)

The rest of the system was filled with media in a similar fashion by attaching two syringes step wise over the different connectors (e.g. B to C, D to A or over the pump) followed by the cell harvesting and preparing the desired cell concentrations in the seeding solution.

The cell seeding was performed either by hand or with the help of the pumps. The respective seedings have been performed for several minutes perfusing the alginate gels while trying to maintain a stable flow regime inside of the bioreactor. When using the hands two 2 ml syringes were connected at the stop-cocks A and B. One syringe was empty and the other one was filled with cell solution. By pressing the media back and forth for several minutes the cells were given the opportunity to settle into the capillaries. The speed was tried to remain equal over the course of the seeding and a similar seeding time was used as for the seeding with the pump.

The other way was performing the seeding process with the help of the pumps. This was only performed in configuration 1. For this the cell solution filled syringe was placed right before the bioreactor (connector A) and the empty syringe after the pump (connector D). The pump was set to a speed of 5 or 10 $\mu\text{l/s}$ and the cell solution was sucked in automatically into the system. After all the media was out of the seeding syringe, the perfusion was immediately set to closed-loop and the cell solution was circulated in the bioreactor system for an equal amount of time as the injection time (time until the syringe at A was empty). More detailed information about the seeding and other parameters are displayed in Table 12.

For the seeding experiments no waiting time afterwards was used, as direct imaging was supposed to assess the efficacy of the seeding. For the culture experiments however, multiple waiting steps were incorporated to allow for better distribution and attachment. An initial attachment time in the incubator of 30 mins followed up the seeding process immediately, after that the pumps would be turned on for 5 mins at 5 $\mu\text{l/s}$ and the bioreactor turned by 90° as depicted in Figure 27. This was followed by another hour of waiting. The whole process of 5 mins pumping and turning the bioreactor

is repeated four times with a total of 3-4 hours of waiting times in between. After that the bioreactor is transferred into the culture stand, the setup modified to configuration 2 or 3 by attaching the bubble trap to the respective connectors. Eventually the culture is started at the chosen pump speed at either 5 or 10 $\mu\text{l/s}$ (minimum flow speed according to Dennis et al. (Dennis et al. 2009)). For further details, refer to Table 12. In Table 12 an overview of the 3D cell cultures is given it is structured in the same way as tables 9-11 thus the specific parameters of the respective experiments can be taken from there.

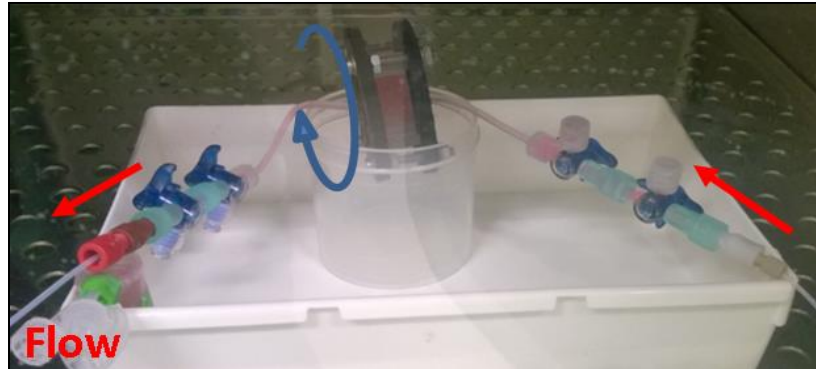


Figure 27: The bioreactor in the Incubator during the seeding process; red arrows depicting the flow direction through the culture chamber; blue arrow showing the vertical rotation of the bioreactor

Figure 28 shows an overview of the whole 3D culture setup fully placed in the bioreactor in configuration 2 with the bubble trap being positioned between valve D and A. The red arrows give the flow directions and show how the media is coming from the pump directly into the bubble trap. From there the pump draws the media through the bioreactor back into the pump.

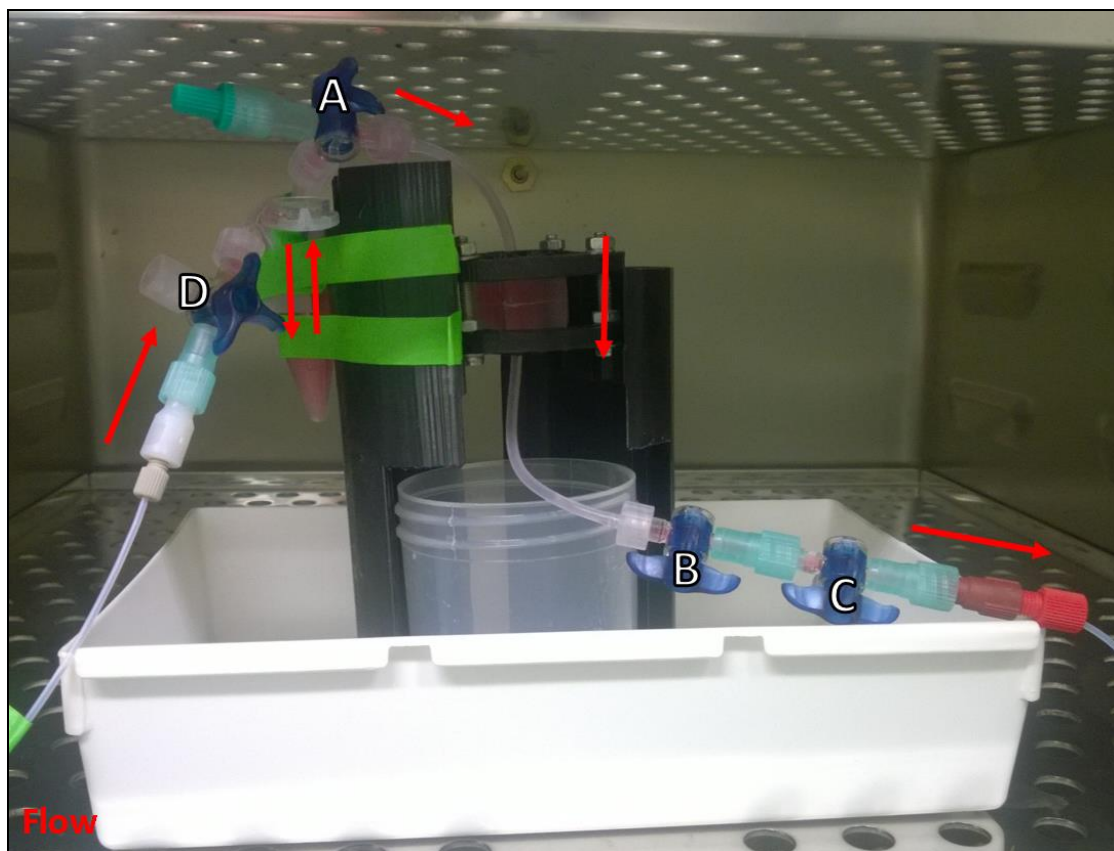


Figure 28: Bioreactor setup right before starting the culture during “First 3D cell culture”; showing configuration 2 and the flow directions of the media (red arrows)

Table 12: Cell experiments on the 3D gels

Experiment	Specifications	Scaffolds	Samples	Duration	Seeding Amount Cells in # Cells in ml
3D cell seeding	Sterilization and culture preparation performed with gel placed in Bioreactor Performed by pump system Live-stained before seeding	Capillary Alginate 1.5% Full-sized gel	1	Imaged right after seeding	2,950,000 2
First 3D-cell seeding					
3D cell seeding	Preparation of gels outside of the Bioreactor Comparison of Hand and Pump seeding	Capillary Alginate 1.5% Full-sized gel	2	Imaged right after seeding	2,960,000 (Hand) 2,980,000 (Pump) 2
Second 3D-cell seeding					
3D cell culture	Live-stained before seeding Preparation of gels outside bioreactor Seeding by the pumps Introduction of Bubble trap (closed loop)	Cap. RGDA:Alginate 1:5 Full-sized gel	1	3 d;	4,506,250 2
First 3D-cell culture					
3D cell culture		Cap. RGDA:Alginate 1:5	2	1 d; 7 d	3,893,750 2.5
Second 3D-cell culture					

4.4.4 Staining & Fixation

Different staining techniques have been performed throughout the course of the project. Such as live-staining, cell staining with DAPI and Rhodamine Phalloidin (RP) as well as MHC staining. The later ones have been performed after fixation of the cell culture.

The live-staining was most commonly performed before seeding the cells. The staining agent was NucBlue and it would allow for a follow-up of the cell cultures during the experiments. A detailed protocol can be found in the Appendix 7.

The gels were fixed with either ethanol (70%) or by using cold formaldehyde (4%, cold) as a fixative agent. After that the cell staining would be performed according to the protocols listed in the Appendices 11-13. The used fluorescent stains have been DAPI for the DNA content of the cell nuclei, Rhodamine-phalloidin for the actin filaments in the cytosol and Alexa Fluor 488 for staining the expression of MHCs.

5 Results

5.1 Bioreactor

5.1.1 Simulations

For simplification reasons the system was modelled as a two dimensional representation as the culture channel was radial symmetric and the reduction of the computational load was staggering compared to the first trials with 3D models. With this multiple experiments and parameter sweeps were possible to easily test different conditions in the bioreactor.

One of the first question that was addressed by the simulation was the flow field inside the culture chamber. More specifically two designs were compared (rectangular and conical design) as shown in Figure 29.

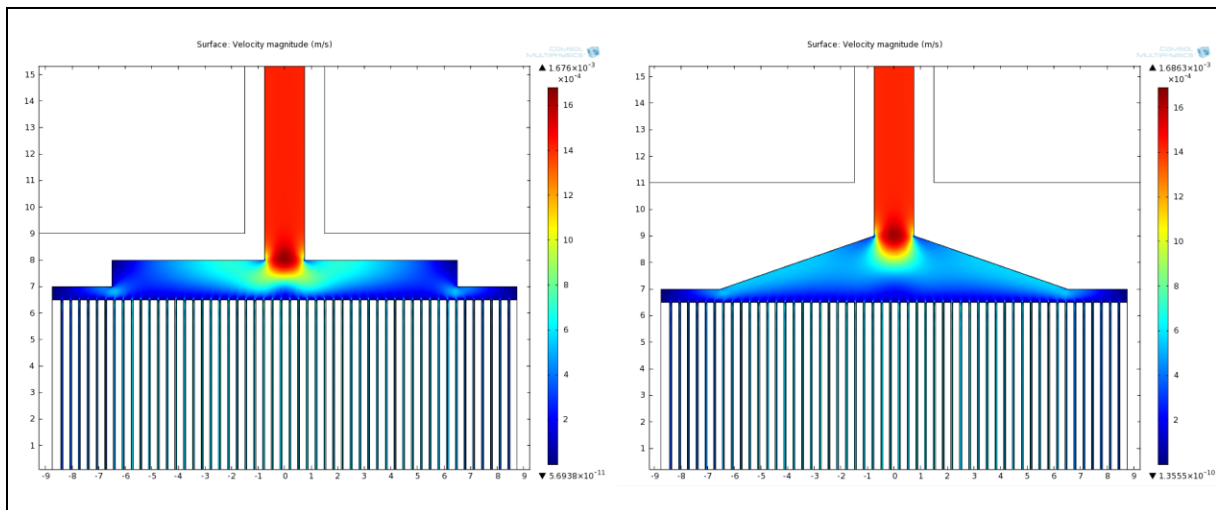


Figure 29: Flow velocity simulation, rectangular design (left) and conic design (right); Inflow 0.6 ml/min; colour scheme depicts the velocity magnitude

When investigating the rectangular design of the PDMS channel it got clear that there was a great disturbance of the flow by the edges found in the channel layout so the idea was to reduce the amount of edges by introducing a more funnel shaped in/outlet. The initial entry point is still causing disturbances so increasing the volume of the pre-chamber and moving it away from the gel was another way to reduce the strains on alginate and cells alike.

In the current modelling the oxygen transport can be influenced by the different flow speeds as the diffusion into the chamber is only reacting according to the gradients build up. When the oxygen consumption is assumed in the range according to Nicholls et al. (Nicholls et al. 2010) and with sufficient flow, smaller local deficiencies can be compensated by the diffusion through the PDMS shown in Figure 30 (left). Here the minimum is 0.1999 mol/m^3 and the model is completely red estimating a full saturation of oxygen throughout the whole system. When the oxygen consumption is assumed according to Li et al. (Li et al. 2013) not enough oxygen reaches the centre of the alginate Figure 30 (right).

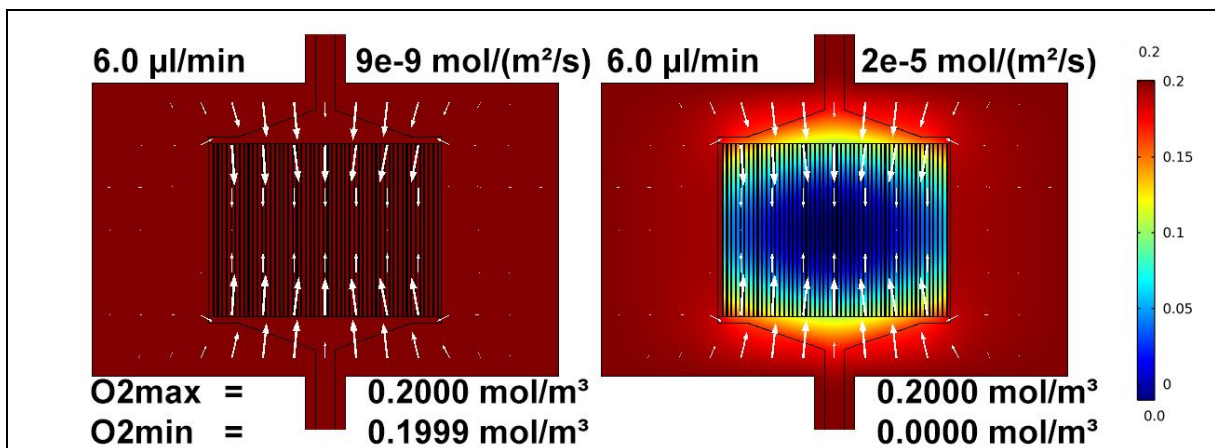


Figure 30: Comparison of preferred and unwanted oxygen distribution showing the maximum and minimum values; flow= $6.0 \mu\text{l/min}$; oxygen consumption $9 \times 10^{-9} \text{ mol/(m}^2/\text{s)}$ (left) and $2 \times 10^{-5} \text{ mol/(m}^2/\text{s)}$ (right); white arrows showing diffusive flux and the colour scheme resembles the spatial concentration of oxygen

In the new modelling with Comsol Multiphysics 5.0 (Comsol Inc. 2015) the parameters according to Nicholls et al were used as those seemed to be closer to the actual oxygen consumption of the cells. See Chapter 6.1.1 for further discussions. Incidentally the oxygen results of the new model did not differ much from the results of the first modelling. The implementation of the glucose consumption was not successful.

In the next step the time dependence of the system was investigated. The simulations were calculated for a total of one hundred seconds ($t=100\text{s}$) and the oxygen concentration plotted for different time points. The systems usually reached steady conditions between 5-10 seconds as no significant changes can be observed when comparing $t=10\text{s}$ and $t=100\text{s}$.

In Figure 31 the different time points are illustrated and the oxygen concentration is displayed by the coloured background (see scale to the right). The arrows show the direction and magnitude (size) of the diffusion into the system. With this the main paths of influx into the system are shown. Most of it originates from the top and bottom of the PDMS channel. The consumption here is estimated according to Li et al. which caused the oxygen insufficiencies in the middle of the bioreactor (Li et al. 2013).

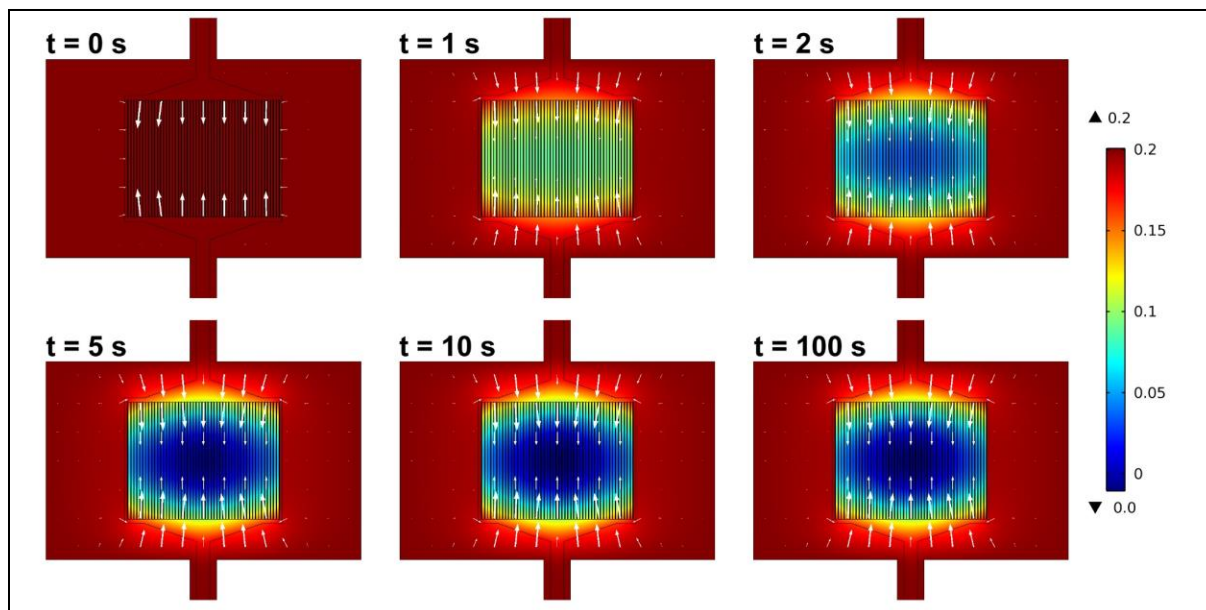


Figure 31: Oxygen diffusion according to Li et al. at different time points; $t=0-100\text{ s}$; $c=0.0-0.2\text{ mol/m}^3$; $v=0.6\text{ ml/min}$; oxygen consumption= $2.28\text{e-}5\text{ mol}/(\text{m}^2\cdot\text{s})$; colour scheme resembling the concentration of oxygen and the white arrows depicting the diffusive flux

In Figure 32 the case of oxygen consumption according to Nicholls et al. (Nicholls et al. 2010) is presented. This results in a different colour distribution as the need for oxygen diffusion inwards is not as large as in the previous example. The steady-state conditions are reached in the same time scale as in Figure 31.

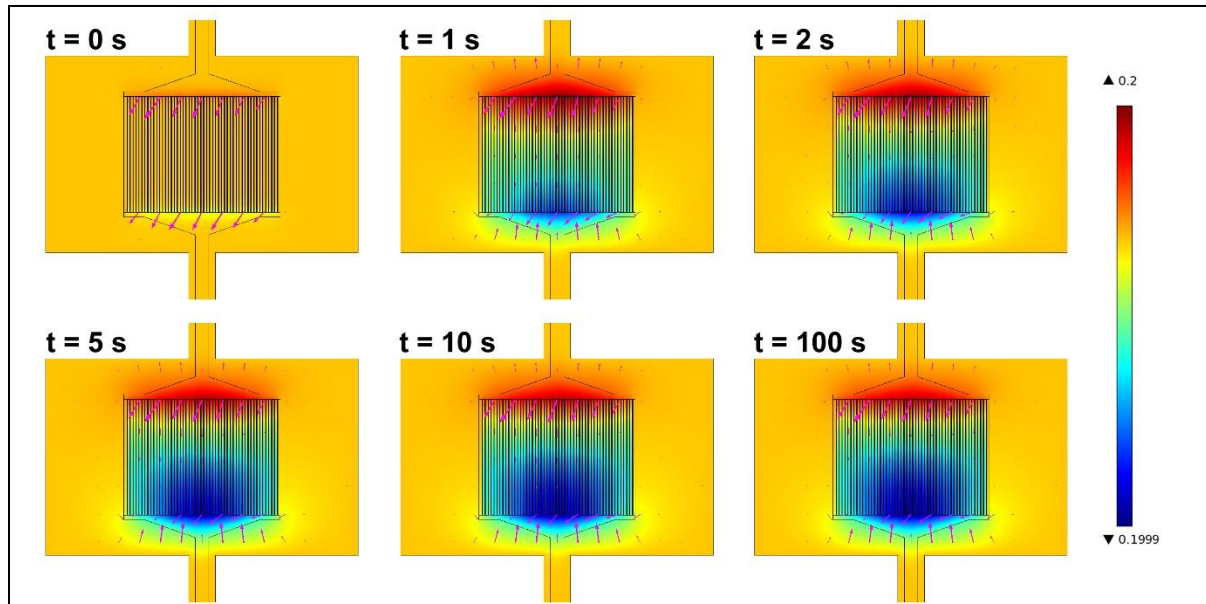


Figure 32: Oxygen diffusion according to Nicholls et al. at different time points; $t=0-100\text{ s}$; $c=0.19-0.20\text{ mol/m}^3$; $v=0.6\text{ ml/min}$; oxygen consumption= $4.12\text{e-}9\text{ mol}/(\text{m}^2\cdot\text{s})$; colour scheme resembling the concentration of oxygen and the magenta arrows depicting the diffusive flux

The interaction of the different models was of interest to evaluate the importance of diffusion and flow especially with respect to the oxygen concentration. Therefore, another way of illustrating the diffusion of the oxygen in the system was chosen for Figure 33. Here the red lines display the main paths of the oxygen diffusion into the system alongside the blue arrows of the diffusive flux. The flow

speeds in the two cases are different to make an assumption about the model interaction. At the low flow speed, the diffusive influx is quite equally displayed and symmetrical between inflow and outflow. Here the diffusion seems to take over most of the oxygen transport as the flow speeds are too low to compensate for the usage of the cells. When looking at the higher flow speed on the right side we get a different picture as the diffusive flux is reversed compared to the case on the left at least on the inflow. At the outflow diffusion through the PDMS still is necessary to support the culture.

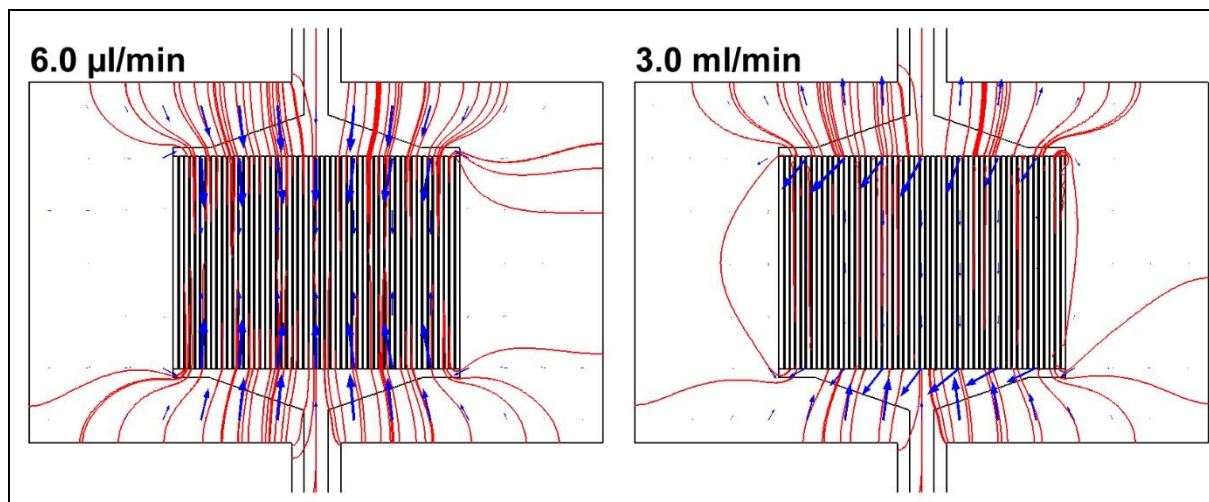


Figure 33: Diffusive flux and diffusion pathways of oxygen through the bioreactor; Blue arrows display the flux and the red lines depict the pathways; oxygen consumption= $9.97e-9 \text{ mol}/(\text{m}^2 \cdot \text{s})$; oxygen saturation= $\sim 0.2 \text{ mol}/\text{m}^3$ throughout the whole bioreactor

These findings indicate that the diffusion is still the main process of oxygen transport into the cell culture and the flow only supports the culture additionally.

5.1.2 Leakage and Operability of the Bioreactor

The leakage and operability has been assessed either through dedicated experiments or by observations made during the project. The experiments have been presented in Chapter 4.2.3 and the other observations have been gathered during the 3D cell seeding as well as 3D cell cultures presented in Table 12.

Other characterizations and how to operate the system in a feasible manner have been performed before the first 3D seeding experiment. During this experiment the amount of media that can flow through the system has been estimated. The system could store between 4-5 ml without the alginate gel, with the alginate gel this amount reduced to 1-2 ml. The addition of the bubble trap increased the total volume to 6-7 ml.

The Table below illustrates the testing of the tightness of the bioreactor. It shows that a full closure of the culture channel is possible to achieve thus it can be safely used for culture experiments.

Table 13: Leakage experiments performed with the pump system

	Experiment 1		Experiment 2
Flow speed (ml/min)	0.6	3.0	6.0
Duration (h)	16	1	1
Volume pumped (ml)	417	130	264
Volume lost (ml)	3	55	0
Volume lost (%)	0.7	42	No loss

As a follow-up experiment about the media distribution in the culture chamber flow through tests have been performed (results shown in Figure 34). Which showed a good distribution of the dyed media throughout the gel, it was assumed that areas of higher flow-through would stain darker and areas with less flow would appear paler. The diffusion was not taken into consideration during this experiment, but the flow through times were tried to be limited to reduce the influence of other processes besides flow through.



Figure 34: Alginate after flow through tests; Rectangular design (left) and conical design (right)

Here a rectangular design used during the tissue engineering project (Peng et al. 2014) has been compared to the gel in the newly designed conical bioreactor used for this project. The distribution in of the blue dye seemed more equal and spatial differences were not as prominent as in the rectangular design.

As aforementioned the leakage also has been assessed during the course of the cell experiments. The observations show that although a good sealing of the bioreactor is possible, when using the pump system for perfusion, it is possible to provoke leakage when using syringes to manually pump in media. In concert to that also the used alginate gel in the flow chamber can have adverse effects to the sealing of the bioreactor. If it sits too loose or to high pressure is exerted on the gel it can slide down and block the exit thus increasing the chamber pressure beyond the sealing capacity. An illustration of that process can also be seen in Figure 35.

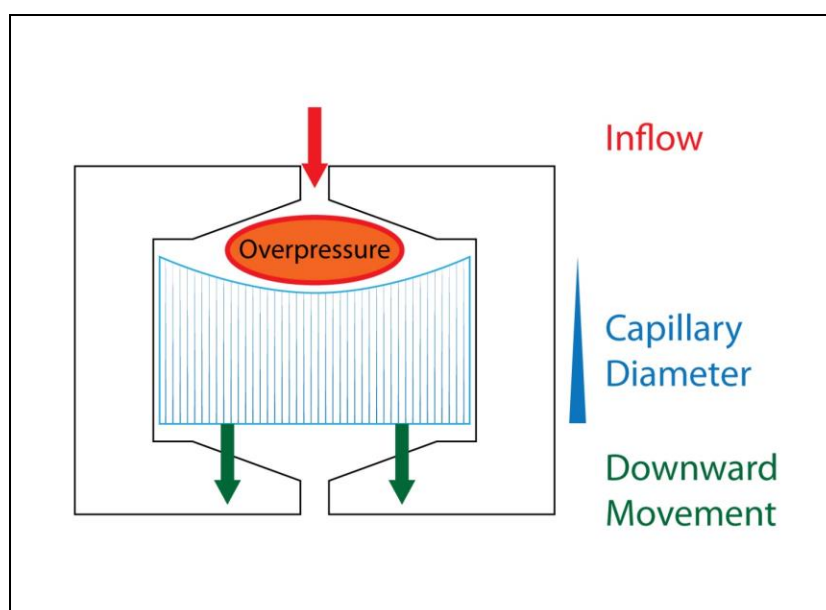


Figure 35: Schematic to show the overpressure results during flow through the bioreactor

In the second 3D culture experiment different configurations of the pump system had been utilized (see Figure 25). Configuration 2 has proven to be the best choice for the cell experiments performed in this project. It took the old media from the bottom part of the bioreactor thus the inflow coming from the bubble was driven by the under pressure in the culture chamber. This culture has been stable without leakage or bubble build up in flow system for 6 days. Alongside that experiment another culture was performed with the configuration 3 but probably resulted in the situation described in Figure 35. Resulting in a leakage of the bioreactor and the stop-cocks drawing in air as well as finally depleting the bubble trap. Eventually inhibiting the usability of the configuration 3 in the current setup.

5.2 Scaffold

5.2.1 Alginate

The alginate has been crosslinked by the method presented in Chapter 4.3.1 and the corresponding parameters, thus the achieved gels have been fairly uniform throughout the whole project. Only exerting differences due to the beakers used or the typical variations of a self-assembly process.

In Figure 36 we can observe the first result after crosslinking the alginate in the 100 ml beaker from which the alginate gel for later characterization and cell experiments are cut. Red food colouring has been used as a contrast agent to verify the formation of capillaries in the alginate gels. It can be observed that the dye is not taken up in the non-capillary alginate (Figure 36 B) contrary to the flow through the capillary alginate gel (Figure 36 C).

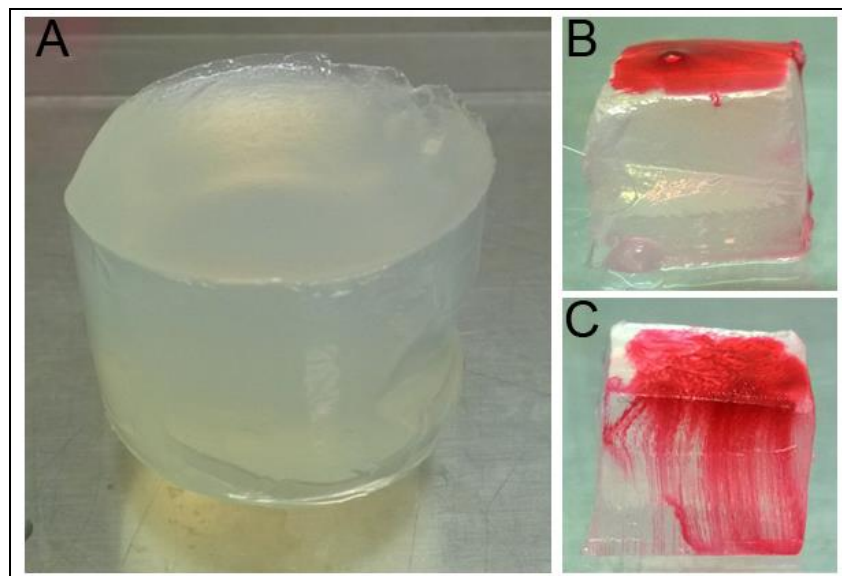


Figure 36: Gelling result of 1.5 % pure alginate gel; A) Capillary alginate gel directly from the beaker \varnothing 40 mm height 30 mm; on the right alginate blocks (ca. 10x10x10 mm) from non-capillary (B) and capillary (C) alginate with 5 ml red food colouring dropped on top

After the initial investigation of the alginate gels the gel was cut into slices and investigated under the microscope. The gel was cut along and perpendicular to the capillaries resulting in slices of 1-2 mm thickness. The capillary alginate gel in Figure 37 (left) shows the capillaries opened towards the observer thus exerts smoother valleys and more pronounced ridges that makes up the material between the individual capillaries in the gel. For the gel on the right (Figure 37 (right)) the round shapes are the capillaries shown from a top down view and the material between the capillaries can be seen more clearly than on the left side. Furthermore, it displays the typical variation in diameter between the assembled capillaries.

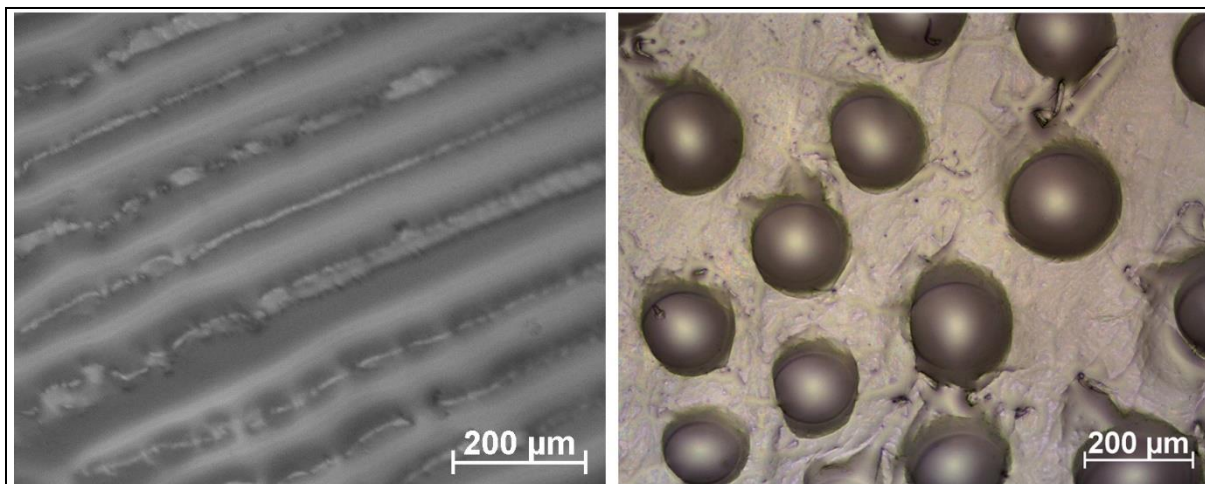


Figure 37: Capillary alginate gel cut along the capillaries (left) and perpendicular to the capillary direction (right)

In the gels formed variations have been observed regarding the capillary density (amount per mm^2) and capillary diameter when observing the gels cut like in Figure 37. Those factors are also affected by the origin of the cut sample with regard to the crosslinked gel. As introduced in Chapter 3.3.1 with Figure 6 where spindle like capillary bundles formed thus giving vertical variations as well as interacting with the beaker wall resulting in differences along the horizontal plane. This has been observed when investigating the alginate gel and also later been confirmed by imaging the gelatin:alginate.

Differences in mechanical properties were discovered while handling and cutting the alginate gels. This seemingly depending on the amount of capillaries interspersing the hydrogel. The non-capillary alginate gels seem to behave more elastically contrary to a more plastic deformation behavior of the capillary alginate. No further mechanical testing has been performed in this project, as opposed to the previous work of my collaborators on capillary alginates (Schuster et al. 2014).

5.2.2 Gelatin:Alginate

The confocal microscopy imaging has revealed that the gelatin has been distributed equally throughout the gel. In Figure 38 one can observe the reflective as well as the auto-fluorescence of the gelatin in the gels. The top row shows the reflective channel of the confocal microscopy, thus showing an image of the alginate gel as a whole. In the bottom row only the auto-fluorescence of the gelatin is visible, thus the spatial distribution of the gelatin in the hydrogel can be assessed.

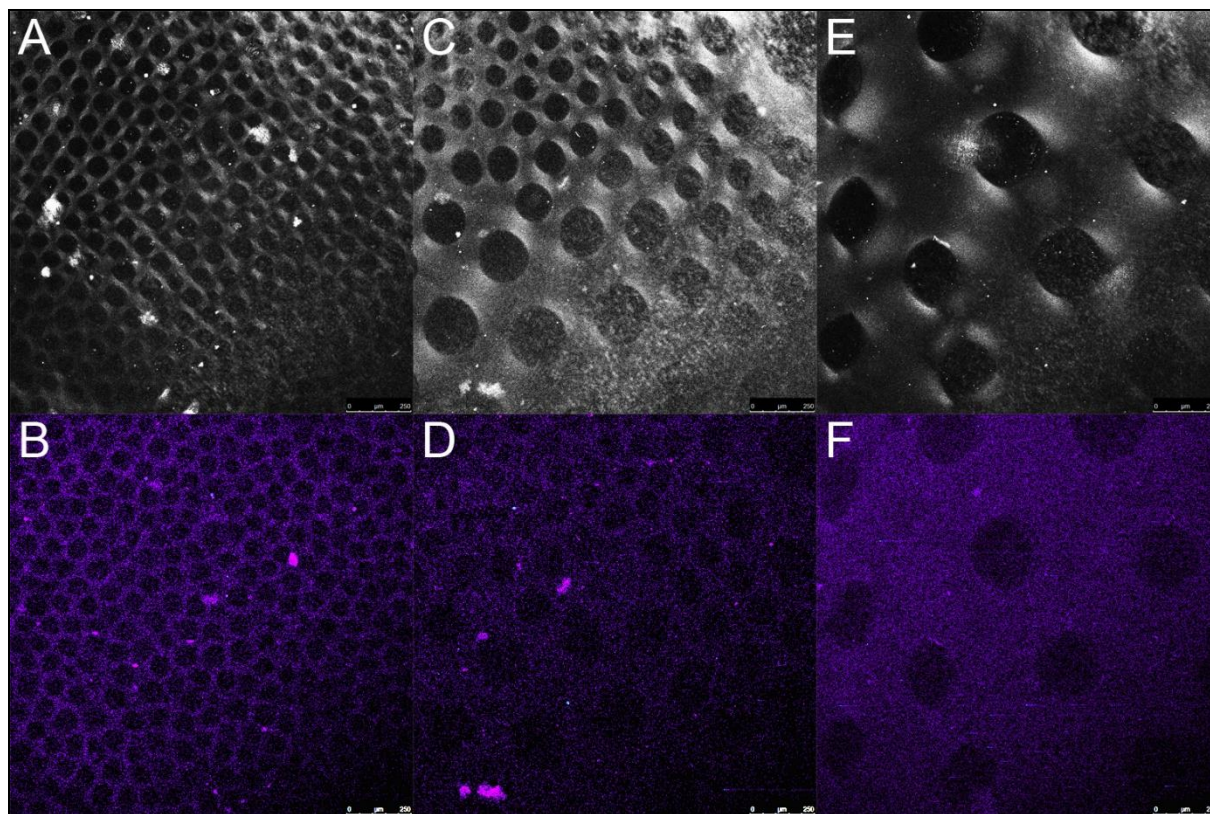


Figure 38: Result of the confocal microscopy done on gelatin:alginate 1:1 (A; B), gelatin:alginate 1:1 (C; D) stored in MilliQ for several months and gelatin:alginate 1:10 (E; F), A-C displaying the reflective channel, D-F displaying the autofluorescence of the gelatin in the wavelength interval from 500-650 nm

One additional question was if the storage of the gelatin:alginate in MilliQ water over prolonged times would affect the gelatin concentration inside of the alginate gels. This could not be observed in the confocal microscopy, because there were no significant differences found between the newly crosslinked (Figure 38 A; B) and the stored ones (Figure 38 C; D).

Furthermore, SAXS measurements have been performed on the gelatin:alginate gels in comparison to pure alginate gels (see Appendix 15). Similar results have been retrieved for both cases indicating an equal distribution of the gelatin throughout the alginate matrix.

The confocal microscopy and SAXS measurements have been performed and subsequently been evaluated by my collaborators Anna Ström (Chemistry and Chemical Engineering, Chalmers) and Erich Schuster (SIK, SP Sverige).

5.2.3 RGD Modified Alginate

The bulk modification of the alginate with the GRGDSP peptide-coupled alginate worked well and formed capillaries in most of the cases. It was observed that the RGD-coupled alginate shows a lower viscosity at 1.5 % w/w solutions as Protanal RF6650 at the same ratios. This might impair the ability of the formation of capillaries in the gel. Also performing the capillary formation in beakers below the usual volumes (50–100 ml) like performed in PDMSFlatGelExp – 3+ 7d and 1+7d (see Table 10) did not form capillaries reliably. Those gels were formed in small 4 ml beakers with a consequently smaller diameter. In these cases, capillaries could not be found throughout the whole gel. Especially for gels with higher amounts of the RGD-coupled alginate, e.g. RGDA:alginate 1:1 and 1:2. Figure 39 compares RGDA:alginate 1:5 (left) and RGDA:alginate 1:2 (right) formed in the 4 ml beakers. On the right side the striated structure in the background is missing indicating the lack of capillaries. Albeit being an interesting observation the capillaries were formed reliably in any other case .

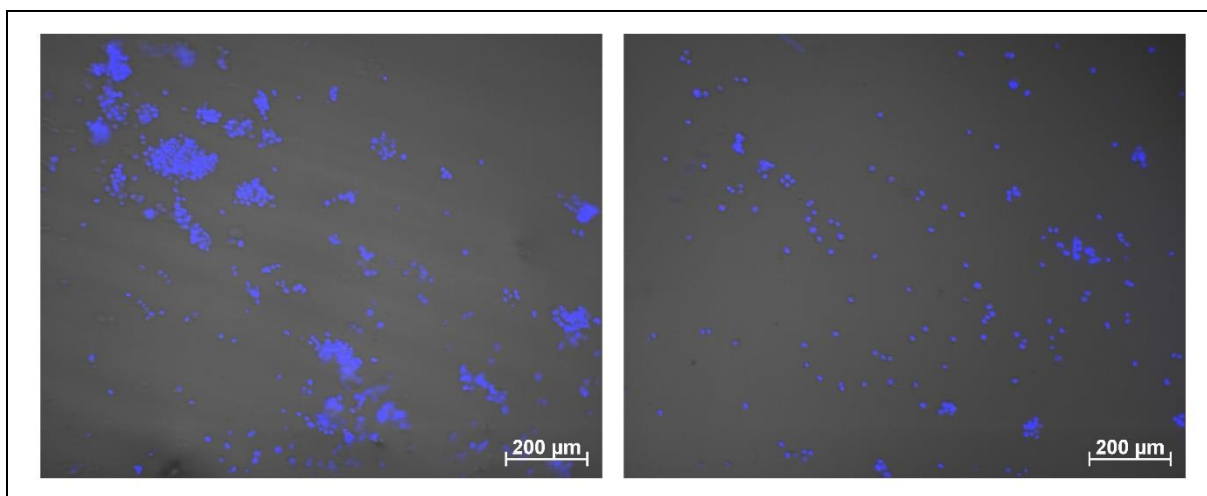


Figure 39: PDMSFlatGelExp 3+7d right after seeding the cells, cells live-stained with NucBlue (blue) and the brightfield channel; capillary RGDA:alginate 1:5 on the left and capillary RGDA:alginate 1:2 on the right

After performing the last RGD surface coupling experiment the other gels from RGD coupling 1-4 have been inspected as they had been stored in MilliQ water in the fridge for several weeks. When doing so it was discovered that the gels had lost a lot of stability and even started to break apart under mechanical pressure. In contrast to bulk modified alginate gels were such a behaviour has not been observed during the project.

Additional to the stiffness changes of the RGD surface coupled gels a drastic loss in gel stiffness has been observed when cells were cultured on top of the flat gels or inside of the capillary gels. When storing weakened gels in GM and in the Incubator for longer periods of time a stiffening has been observed. As soon as cells were added to the gels a decrease in matrix stiffness started over the period of culture time. The gel used in the second 3D cell culture and cultured for 7 days softened up and it broke apart easily even with minimal mechanical force applied to it.

5.2.4 Sterilization

The sterilization process used in this project was a method proposed by Stoppel et al. in which emulsion in ethanol with subsequent washing steps in MilliQ water was applied (Stoppel et al. 2014). Several observations were already made during the sterilization process of the alginate gels. When the ethanol treatment was over and the samples were transferred into the MilliQ they would start floating. After all the washing steps thus longer exposure to the MilliQ these phenomena would cease and the alginate slides would start sinking again. As shown in Figure 40 a shrinkage of the gel after exposure to ethanol has been observed in some cases, such as the fixation with ethanol or when sterilizing after surface coupling according to the protocol used in the 4th RGD surface coupling HEPES/PBS.



Figure 40: Alginate without capillaries from FlatGelExp4 after fixation with ethanol

The gels relaxed again by washing with PBS or when placed in MilliQ water. The changes in MilliQ have been rather drastic as it expanded beyond the original size of the gel sample. This led to chipping of, breakage at the outer rim and a softening that made handling without breaking the gels impossible. In the case of the surface modification an addition of GM helped to cure the gels from that deformation again.

The change of sterilization and surface coupling order in the 5th RGD surface coupling experiment helped to prevent those drastic alterations of the gels.

5.3 Cells

5.3.1 Flat Gel Experiments

The flat gel experiments have been performed, as described in Chapter 4.4.1, thus the slides were placed in multi well culture dishes and the cell media was dropped on. The different experiments could only provide qualitative estimations of the influences of the different scaffold modifications or other properties.

Figure 41 shows an overview of the results from the FlatGelExp3 that should illustrate the individual progression of the cultures from the seeding up to the fixation and staining of the culture on day 8. The images show only one dish over the course of the whole culture time, as the live-staining with NucBlue allowed to observe the progression of each single culture on a daily basis. This series of images was included to exemplify the broad screening process that has been done for every culture experiment on the flat gels. Many images were taken in every step together with noting down the observations to assess the trends in the culture without quantitative data. The control in this experiment was a plain cell culture dish without any gel placed inside.

In the Figure 41 green and red was used to mark positive or unwanted effects respectively. The red marks the areas of clustering of the cells over the alginate. These clusters are cells attaching to each other rather than the substrate and will eventually lift off from the gel. Especially observed on the alginate without capillaries where the live-staining highlights (blue) the clustering of the cells. On the bottom right image for the RGD modified alginate the clustering (shown by the red rectangles) is probably additionally induced due to the washing steps during fixation and staining. In this process the cells can easily detach from their original anchoring points.

The last three rows show images of capillary alginate gels, which can be observed by the striated background and by the ridges or grooves shown at the fixed gels without culture media on top of the gels. On those gels the organisation of the cells in the cut open capillaries could be observed, see the green highlighted images. The blue labelled cells align inside the capillaries and build chains in the same direction as the substrate striation shows in the background. Furthermore, the loss of the cells on the gels often induced by clustering does not have such a great impact on the capillary gels in general. Overall the cell numbers seemed to be retained better on the gelatin and RGD modified alginate gels.

After fixation and staining further wash off of cells was observed and when imaging the gels without media the cells were also located on the ridges between the capillaries. Indicating that also positive topographical cues improve the attachment of the cells.

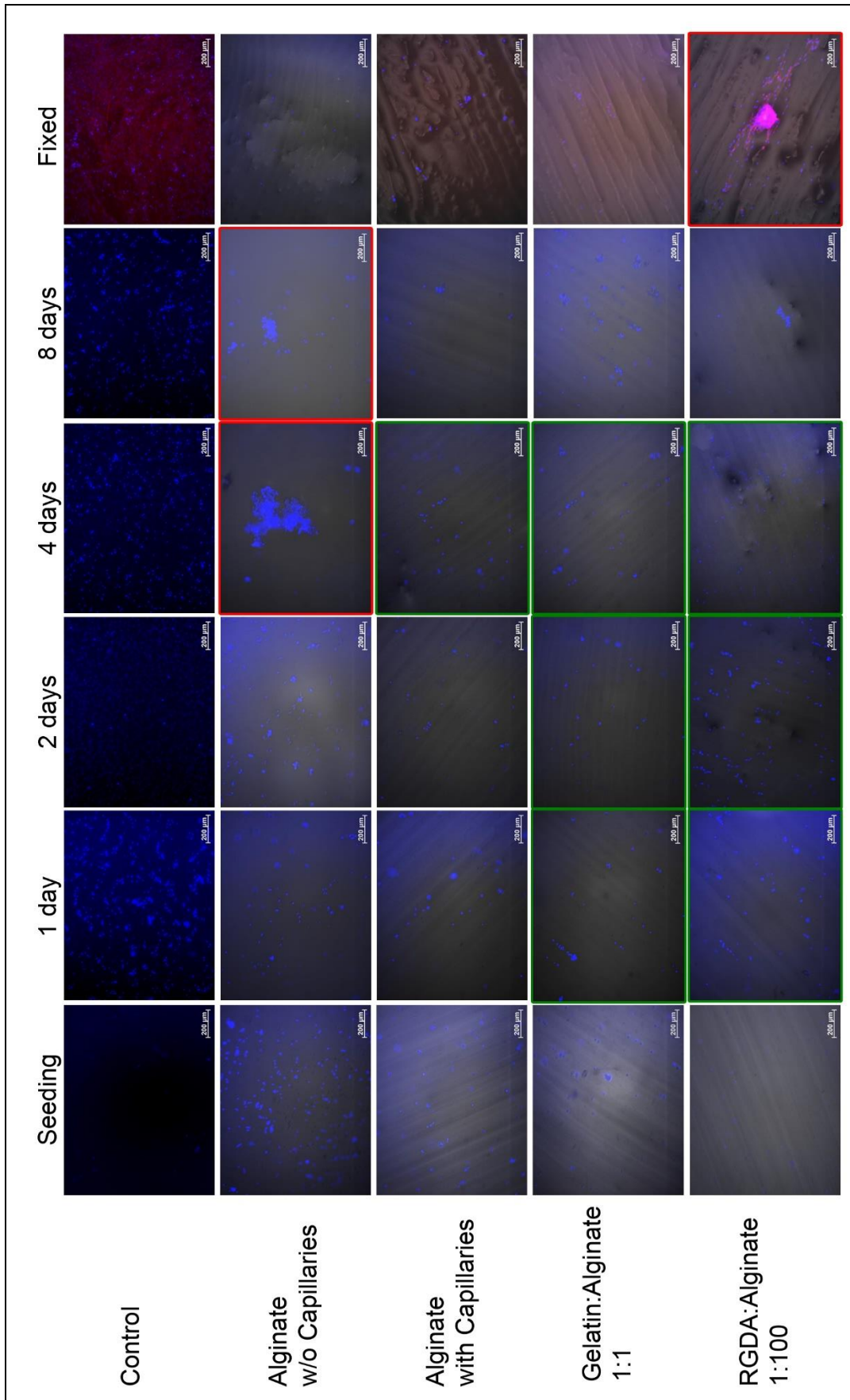


Figure 41: Overview of the FlatGelExp3; Stained with NucBlue (blue) until day 8; afterwards fixed with DAPI (blue) and RP (red); merged with brightfield image (not for control); magnification 10x

After the fixation and staining process some cells have been found still attached and elongated on the substrate gel. When looking at the other samples the most cells found have been ball shaped or have been attached to each other in bundles but are detaching from the substrate. Different examples can be seen in Figure 42 showcasing the different morphologies found on the alginate gels. In Figure 42 A we can see multiple cells in parallel to each other and aligning with the ridges and grooves of the capillary RGDA:alginate. The cell bodies shown in red build small fibre like structures and group together very tightly. Interesting to note in Figure 42 B is that even without any modification the cells were able to find attachment points which can be seen by the long elongation of the cell bodies (in red) but contrary to the capillary gel in Figure 42 A the lateral spreading is wider. In Figure 42 C what seems to be partially detached cells can be seen. Here the cells start to clump together but slowly lose integration with the matrix. For the last gel shown here without modification but with capillaries no interaction with the topographical properties of the scaffold can be observed. These cells only form balls loosely “swimming” on top of the sample.

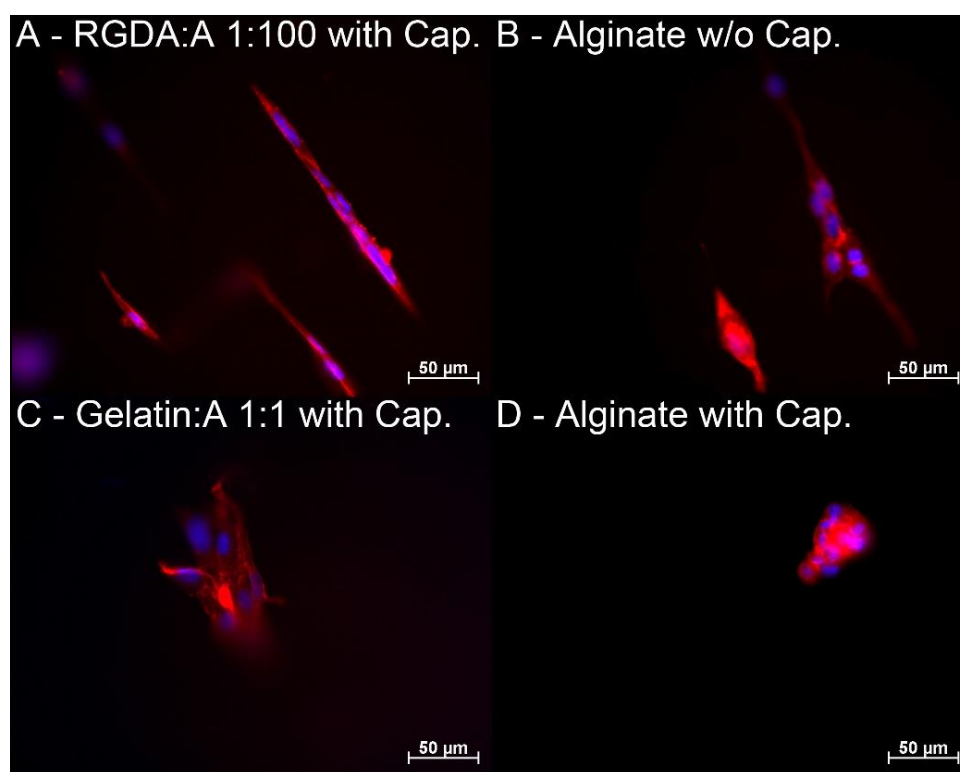


Figure 42: Images from the FlatGelExp3; fixed and stained with DAPI (blue) and RP (red), imaged at 40x magnification with immersive lens

One exceptional finding during this experiment has been an elongated fibre on the RGDA:alginate 1:100 presented in Figure 43 as a stitched image. The length was calculated to be a total of 643 μm with a total amount of 9 nuclei. One can observe the cell nuclei (blue) to stretch out which indicates the fibre like structure of the cell cluster. When compared to the one found in Figure 42 A where clear grain borders can be seen between the cytosols (red) of the neighbouring cells those seem to be vanished for the fibre in Figure 43 indicating the beginning of fusion processes. This even without the introduction of DM potentially triggered by the surface structure due to the capillaries bringing the cells together very tight.

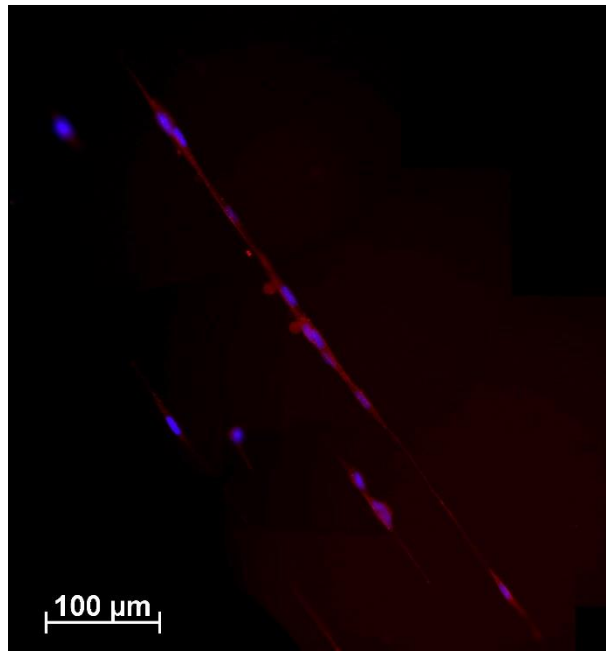


Figure 43: Stitched image of an elongated fibre; on RGDA:alginate 1:100 during FlatGelExp3; fixed and stained with DAPI (blue) and RP (red); imaged at 40x magnification with immersive lens

5.3.2 PDMS Dish Experiments

The PDMS experiments have been introduced to allow for more comparability of the different materials, mainly to optimize the seeding process. Thus decrease the systematic variations of cell numbers on the alginate gels.

The first experiments in the newly made dishes proved that the drop of seeding solution could be easily balanced on top of the alginate gel, thus decreasing the chance of flow-off from the sample. Hence it was observed that the seeding densities used previously were too high for the optimized seeding process. Every blue dot in Figure 44 is one live-stained cell nucleus and the orange circle marks a particular dense area.

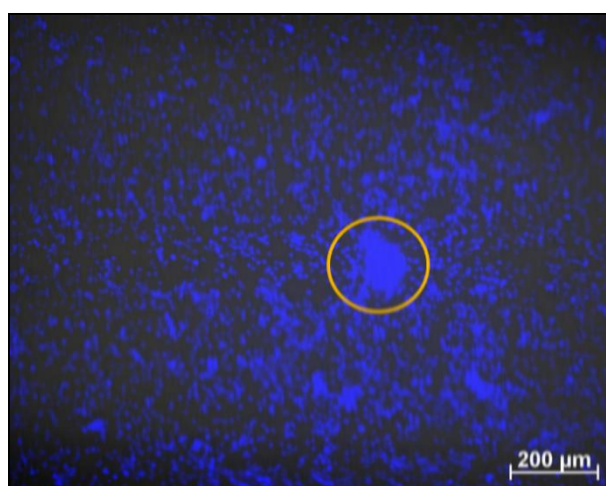


Figure 44: Live-stained (NucBlue) image from PDMSFlatGelExp2 showing the RGDA:alginate 1:100 30 mins after seeding (10x)

These clusters were only loosely attached to the substrate and they were observed moving around the anchor point in a cloud-like fashion. Similar observations have been made on other gels, for example

the RGDA:alginate 1:50 during the FlatGelExp2. The progression of cluster formation over time is shown in Figure 45. Right after the seeding the distribution of the cells is quite equal over the whole substrate, after 24 h clumps start to form in which the singular nuclei are not distinguishable anymore, this process increases towards the fourth day and a loss in cell numbers can be observed. It seems to be more favourable for the cells to attach to each other instead of the alginate substrate. With this only a few cells of the cluster keep the whole bulk down on the scaffold and eventually they will start to float away. Resulting in lack of environmental cues and cell death.

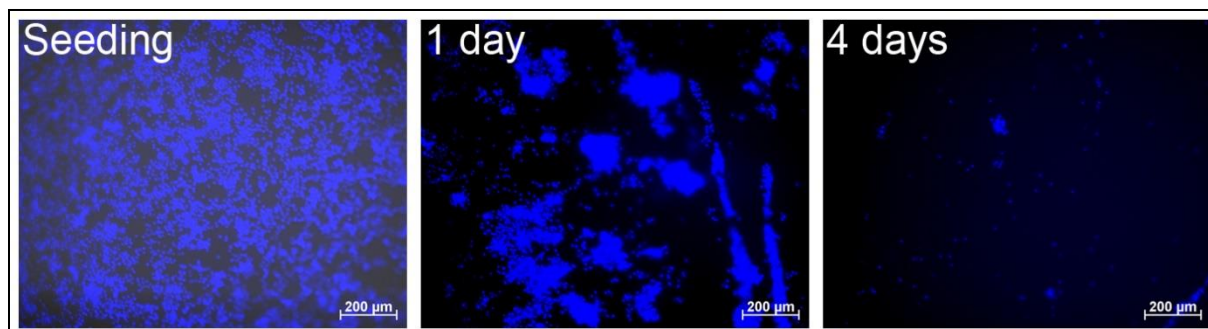


Figure 45: Live-stained (NucBlue) image from PDMSFlatGelExp2 showing the RGDA:alginate 1:50 30 mins after seeding, 1 day of culture and after 4 days of culture (10x)

After those first findings the cell seeding concentrations were reduced further to prevent the clustering and give the cells room for proliferation. Additionally, the culture time with GM was restricted and an additional few days of culture with DM was applied. In none of the slides a well spread culture could be found even after 3 days only some clusters remained on the gels. See Figure 46 where the cell nuclei are live-stained and only dim remnants can be observed at day 10 of the cell culture.

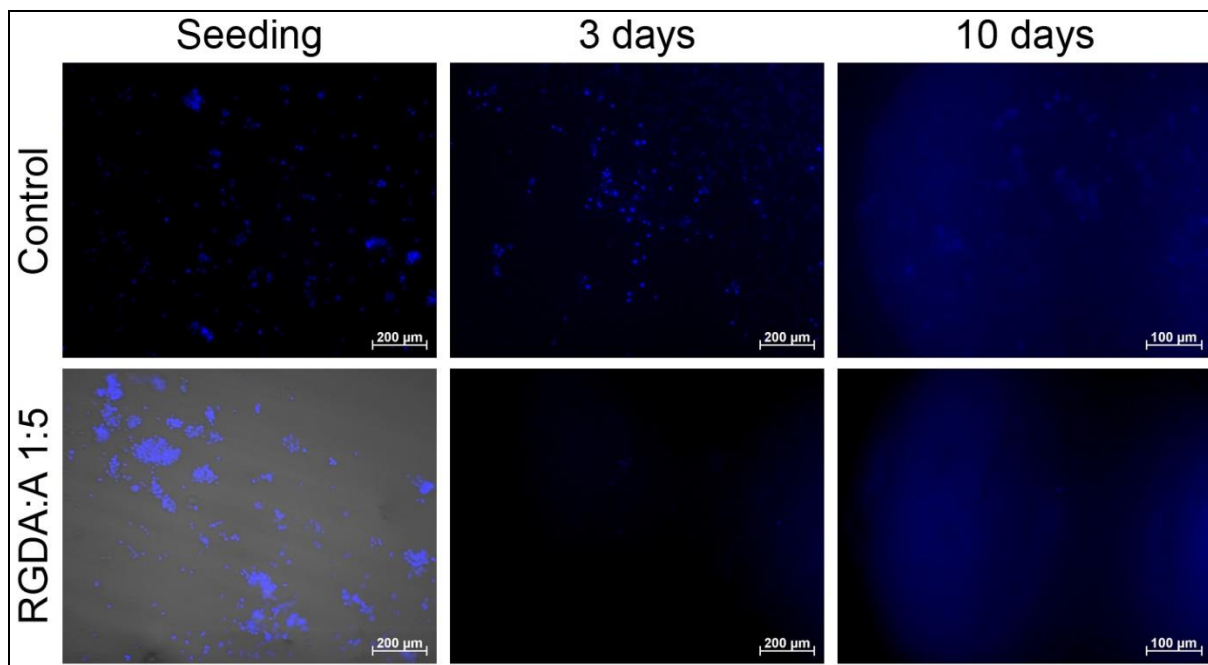


Figure 46: Live-stained (NucBlue) image from PDMSFlatGelExp2 showing the RGDA:alginate 1:5 in the first row and control dish without gel in the second row; 30 mins after seeding (10x), 1 day of culture (10x) and after 4 days of culture (20x)

To further investigate the theory of clustering and cell ablation the switch to DM was performed even earlier in the culturing process. This should reduce the proliferation time of the cells on the gels and

was hoped to “freeze” the state on the gels in a way to see whether they can live on the substrate or not. This experiment called the PDMSFlatGelExp – 1+7 d proved to be quite successful in terms of maintaining a healthy cell culture, as shown in Figure 47.

In the control dish (no alginate scaffold; Figure 47 A) we can see a dense coverage of the dish, comparable to the RGDA:alginate 1:2 in Figure 47 B. The highest densities are usually observed at the out rim of the gel. In C and D, the cells are a bit sparser distributed over the alginate gel not reaching that sheet like structure as in A and B.

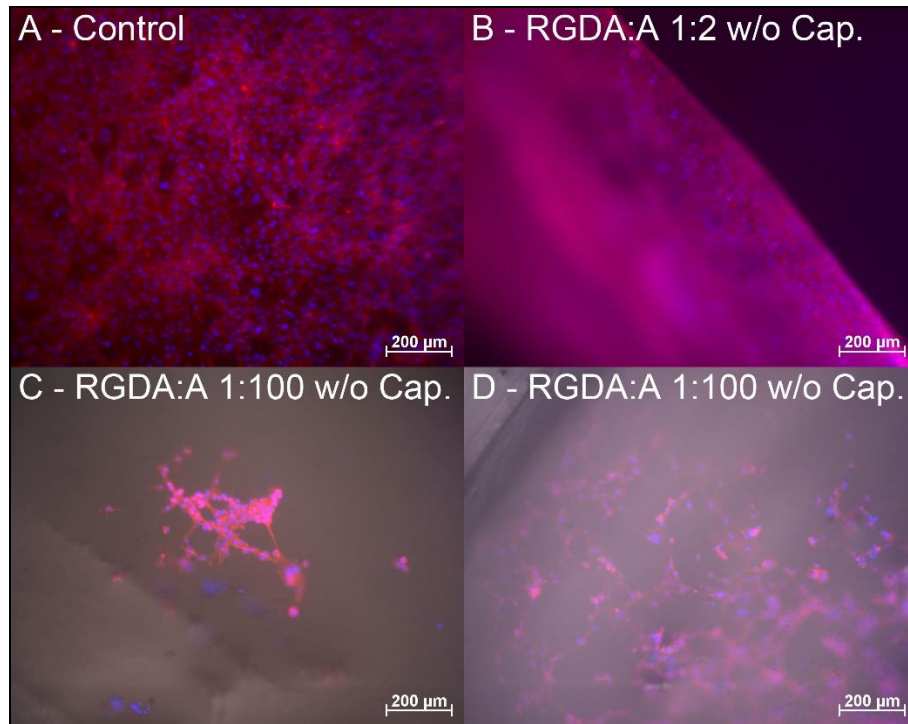


Figure 47: Images of the PDMSFlatGelExp 1+7d after fixation and myosin heavy chain staining; showing staining with DAPI in blue, RP (A-D), and brightfield (C, D); magnification 10x

Regarding the myosin heavy chain staining no differentiation has been observed during the whole culture experiment, even in the control dish no evidence for myosin heavy chains has been confirmed. Only some unspecific signals as few green dots throughout the dish (see Figure 48) have been observed.

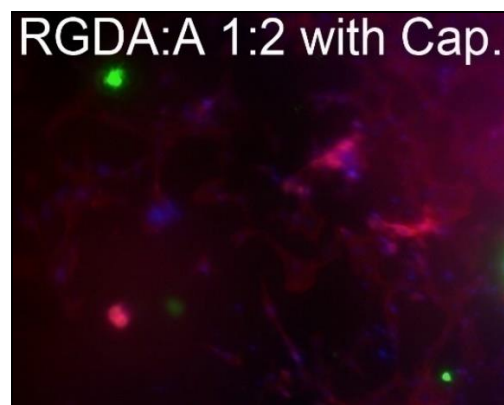


Figure 48: RGDA:alginate 1:2 stained with DAPI (blue), AlexaFluor488 (green) and RP (red) magnification 10x

In Figure 49 a very dense coverage of the alginate surface has been observed and a good distinction of the capillaries was possible. Figure 49 A shows two parallel aligned lines in the gel that are easily contrasted towards the background. These are capillaries that are cut open to the top and the cells had the opportunity to form multiple cell layers inside. That got apparent when increasing the magnification in Figure 49 B. While further panning along the z-axis of the gel it was observed that the cells were not only covering the surface but grew into the alginate from the borders as well.

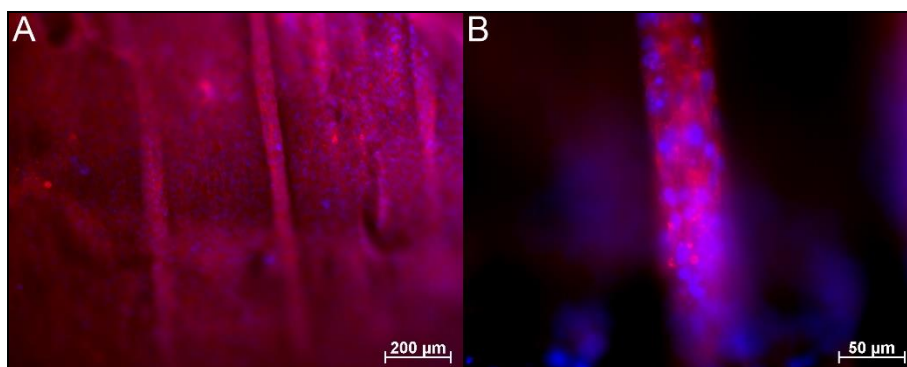


Figure 49: RGDA:alginate 1:5 with capillaries fixed and stained with DAPI (blue) and RP (red); magnification A – 10x, B – 40x immersed

The analysis of the flat gel cultures has been impaired by the wash off of cells. In very dense cultures sheets of cells have been seen lying aside from the sample on the PDMS or being half attached (Figure 50). The folded sheets as seen here make the assessment very challenging as the cell well-being cannot be related to the spatial surroundings of the cell anymore. When the cells are washed off completely the approximation of the cell numbers over the course of the culture time is impossible.

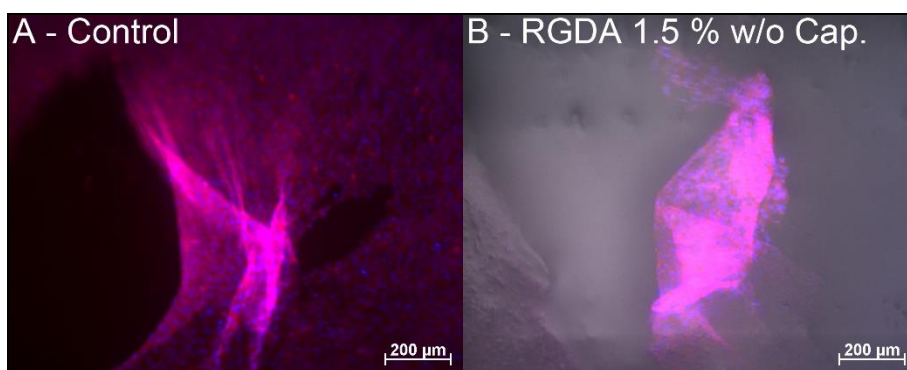


Figure 50: Wash off of cell sheets during the PDMSFlatGelExp1+7d, fixed and stained with DAPI (blue), RP (red) in A and B, + brightfield channel in B; magnification 10x

The last experiment performed on the alginate gel in the PDMS dish have been the control cultures alongside the second 3D cell culture. Here the gel was seeded for either proliferation or differentiation experiments comparable to the aforementioned experiments in the PDMS dishes (the exact modalities of the experiment can be seen in Table 10 in Chapter 4.4.2). Although the material of choice has been the RGDA:alginate 1:5 with capillaries the results of the previous experiment could not be reproduced. During this experiment even the controls have not produced satisfying results, after the fixation and staining process almost no actin expression has been found in the samples. The images of the control cultures are showing almost no fluorescence signals, neither nuclei nor actin staining. Only one patch of actin expressing cells has been found in the GM control (Figure 51 middle of top row).

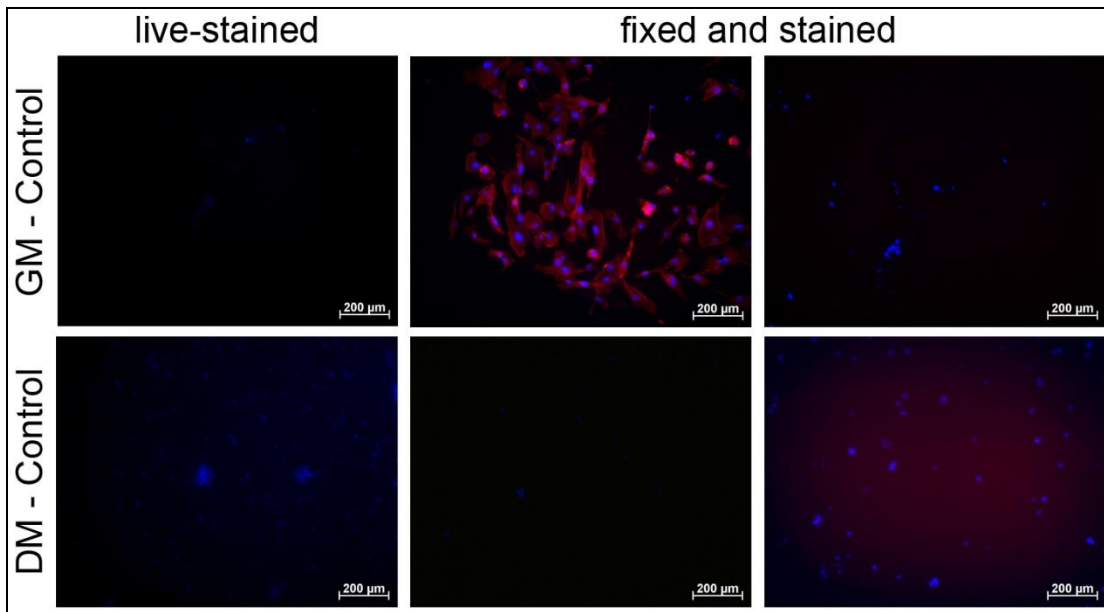


Figure 51: Control dishes of the PDMSFlatGel cultures seeded in parallel to the second 3D cell culture; Fixed with 4 % formaldehyde and stained with NucBlue (blue), DAPI (blue) and RP (red); magnification 10x

Figure 52 shows the cells that remained attached on the gel after culture, fixation and staining process. Some cell clusters are stretched out on the substrate and seem to be provided with the necessary cues to maintain their position. Some cells formed clusters (Figure 52 left row) and what could be tube like structures (Figure 52 down right), but a fusing of the cells or the expression of MHCs has not been proven.

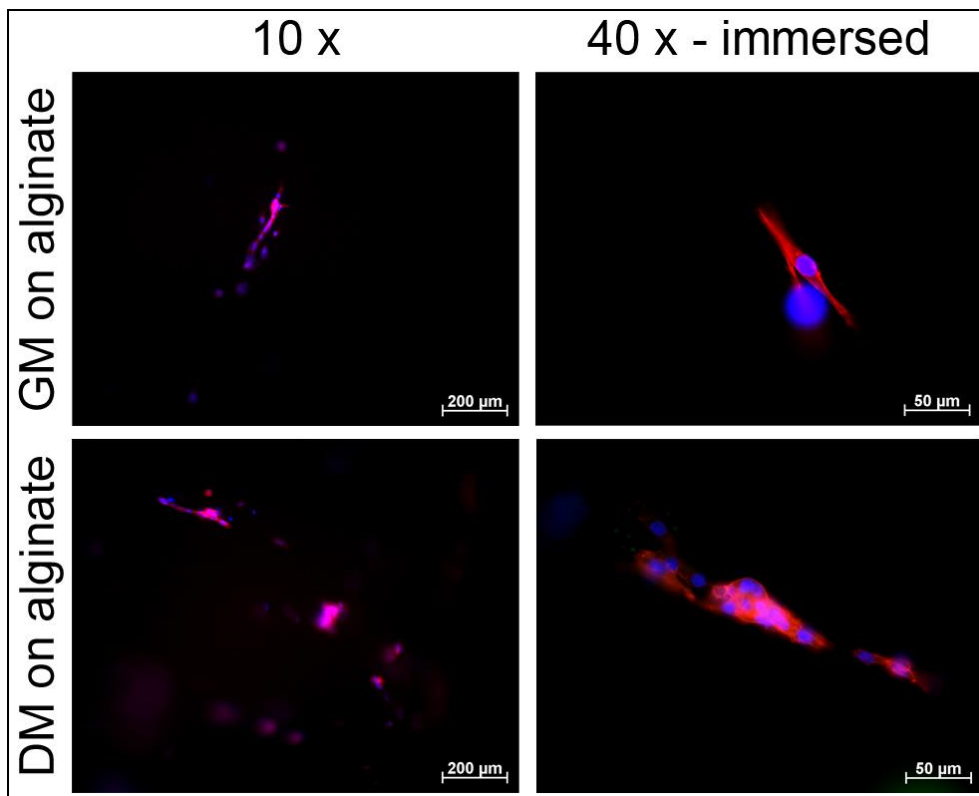


Figure 52: Images from cell cultures on the RGDA:alginate 1:5 with the GM or DM protocol; fixed with 4% formaldehyde and stained with DAPI (blue), RP (red) and AlexaFluor488 (green); varying magnifications

5.3.3 3D Cell Seeding

The refinement of the seeding and culture preparation protocols had to be assessed before starting the cell cultures in the bioreactor. As explained in Chapter 4.4.3 two main approaches were utilized for the cell seeding. After the performance of the different seeding techniques (here by hand and pump system) the gels were cut into 4 slices and imaged with the help of the fluorescent microscope. The cutting technique can be seen in Figure 53 displaying a schematic of the alginate gel in the background. The three black lines overlaid show the cutting lines at their respective depths in the gel dividing the alginate into four slices (S1-4). These have been imaged directly after cutting from the inward out shown by the red arrows. The so retrieved images were stitched together to the position where they were taken on the gel slice resulting in the images of Figure 54 and Figure 55. The cells were live-stained with NucBlue and we achieve a grey value representation of the alginate in the background and the cells are shown as white spots throughout the matrix. During the assessment of the seeded gels it was observed that the cells were easily distinguishable in larger clusters even with the bare eye. Therefore, pictures were taken with an external camera as displayed in Figure 56. The setup schematic shows how the alginate slide was illuminated by the microscope from the top and with that a volume of the gel could be observed showing small fluorescing clusters even throughout the slice thickness of the alginate gel.

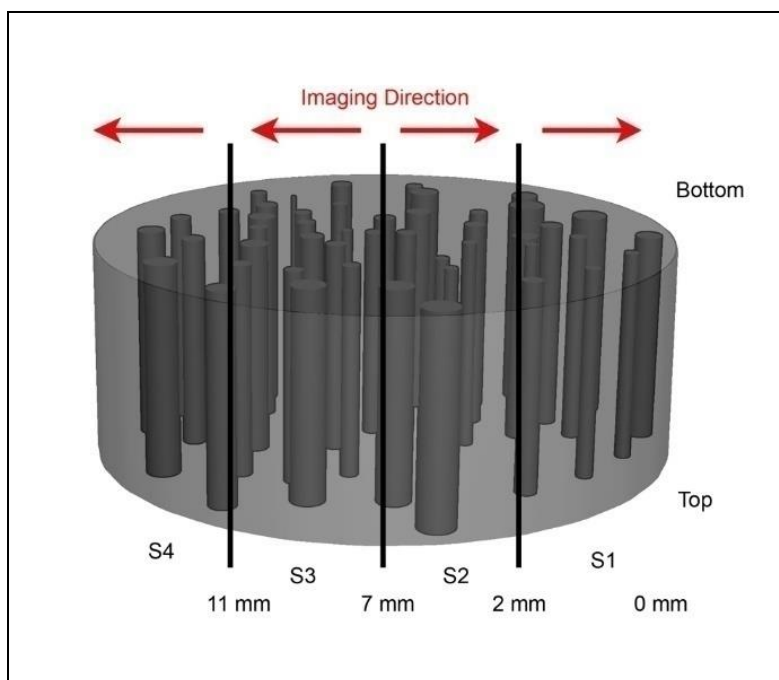


Figure 53: Schematic of the gel cutting process to assess the cell seeding

At first glance both cases resulted in cells being distributed throughout the gel but some differences between the two techniques should be noted. When looking at slice 3 of the hand seeded alginate (Figure 54) a large cluster of cells that accumulated directly at the inflow of the culture chamber can be easily spotted. This is once more illustrated in Figure 56 here the same cluster can be seen from the front. This indicates that a lot of the seeded cells got stuck already at the inflow without even reaching further into the alginate gel.

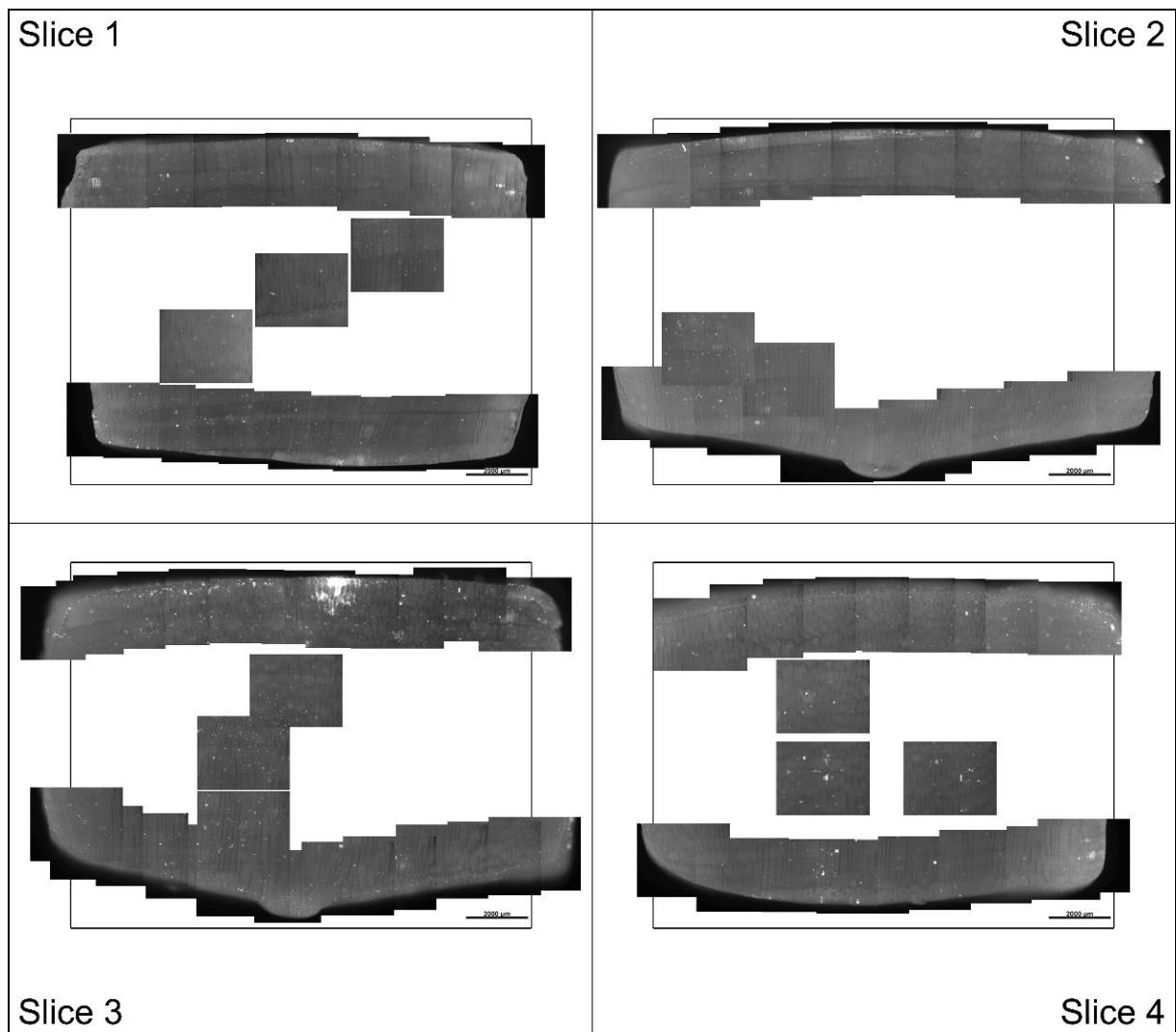


Figure 54: Seeding by hand

Further comparing the two seeding methods the pump seeding seemed to have resulted in a better distribution of the cells along the capillary direction of the alginate gels thus higher densities of cells were achieved further down into the gel towards the outflow. Cells lying on top (at the inflow side) of the alginate gels can be observed for both seeding methods. In addition to the evaluation by imaging the further observations with the hand seeding should be recognized. When seeding with the hand it is challenging to remain a constant flow of media through the bioreactor, the alginate can be easily moved around the culture chamber and the danger to break the sealing density of the bioreactor due to overpressure is higher.

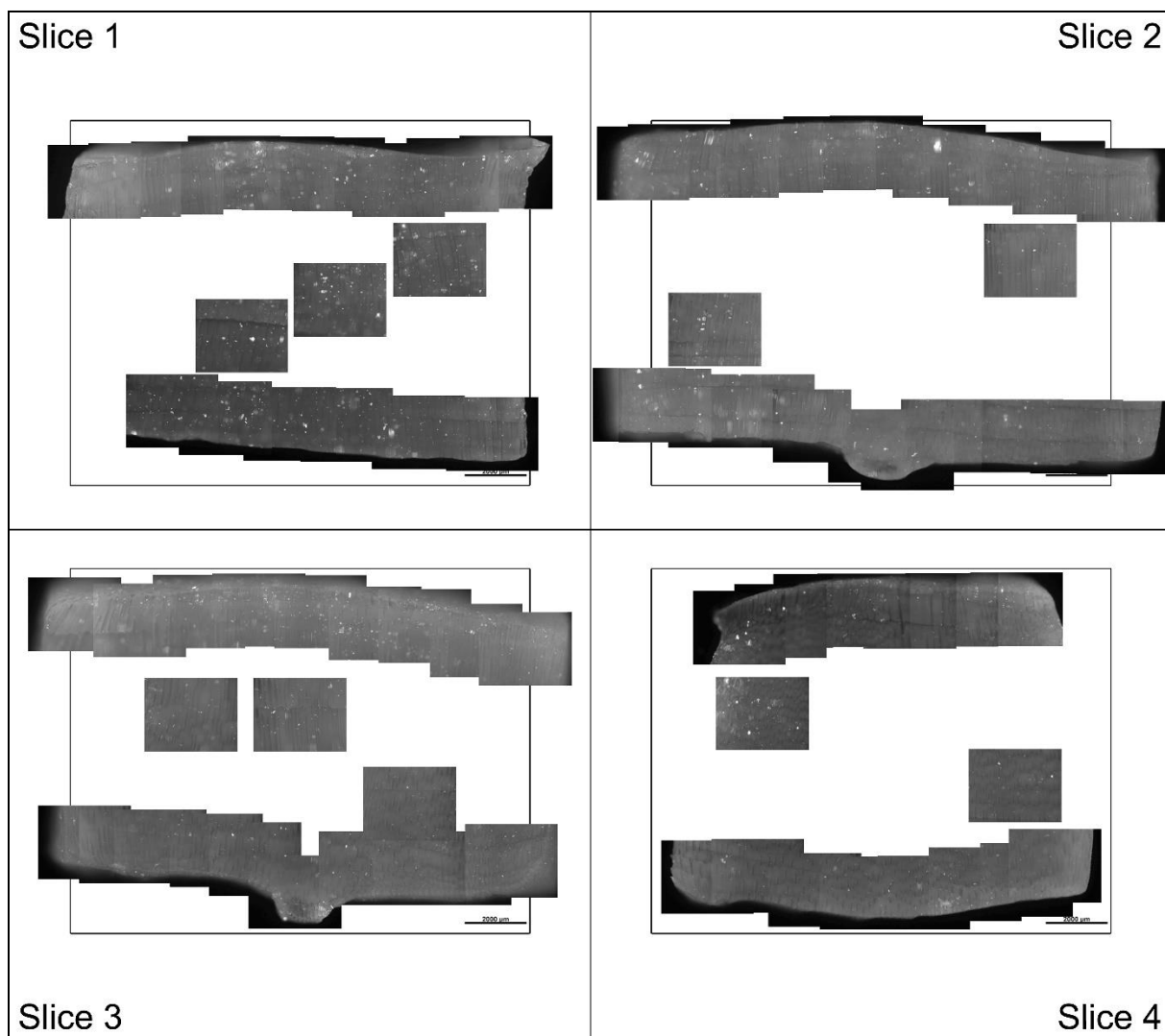


Figure 55: Seeding by pump

The images presented in Figure 56 show that the cells seemed to be better distributed also through the thickness of the slide for the pump seeded gel as small dots light up throughout the whole bulk. This way of imaging allowed for quite good estimation of the cellular distribution even for thicker gels without being limited by the focal depth of the microscope.

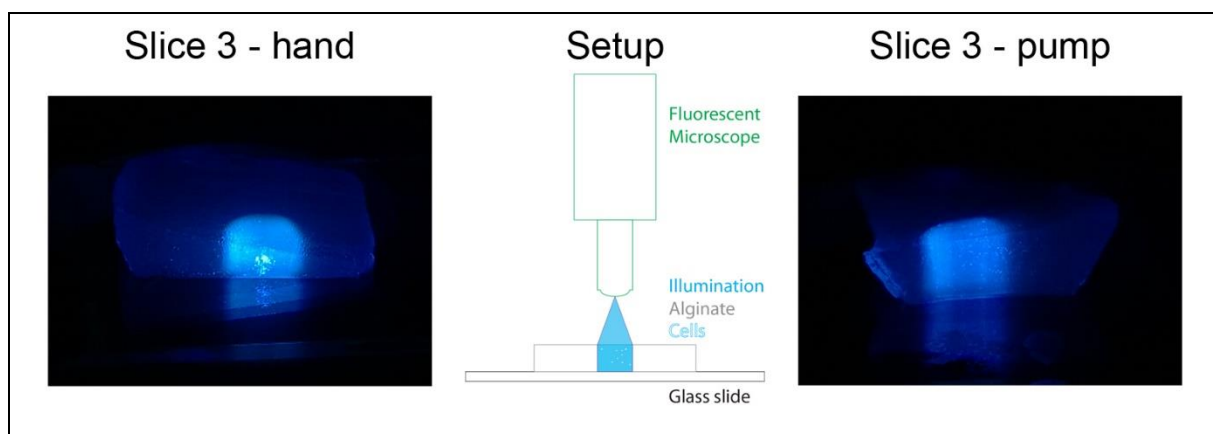


Figure 56: Frontal images taken with additional camera utilizing the DAPI illumination of the fluorescent microscope

5.3.4 3D Cell Cultures

The first 3D cell culture ran for a total of 3 days but was stopped because of too much air leaking in the system. The pump was running completely on air leaking in at the stop-cocks below the bioreactor see Figure 57 A. This air was released into bubble trap so no culture media was transported to the alginate. Figure 57 B shows the air on top of the alginate gel the culture chamber is only filled up to 50 % with media and the gel started to dry out. After that first assessment the bioreactor was disassembled and the gel investigated.

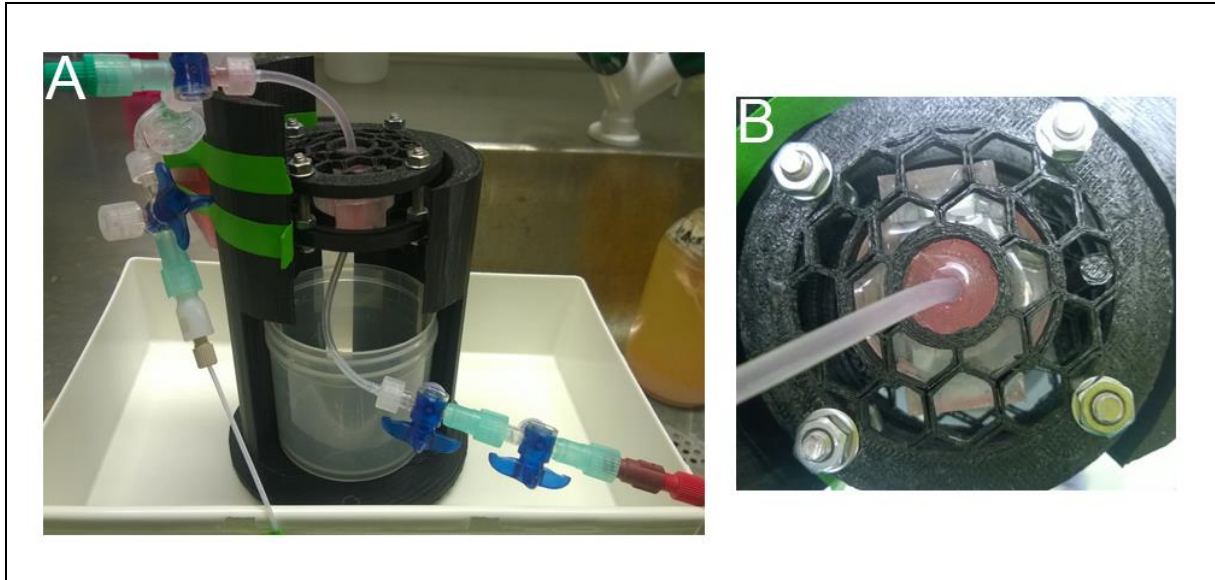


Figure 57: First 3D cell culture after 3 days of cell culture; A) bioreactor system outside of the incubator with air filled tubings on the pump side (connector B to D), B) top of the bioreactor upper part large air bubble visible

In the Figure below one can see the deformations of the gel in A and B and the accumulation of some black remnants in the bubble trap C. Some culture media was standing on top of the alginate gel but no flow was performed anymore. When looking at Figure 58 B the PDMS channel is clearly imprinting into the alginate gel. The small protrusion is where it was pressed into the exit of the culture chamber.

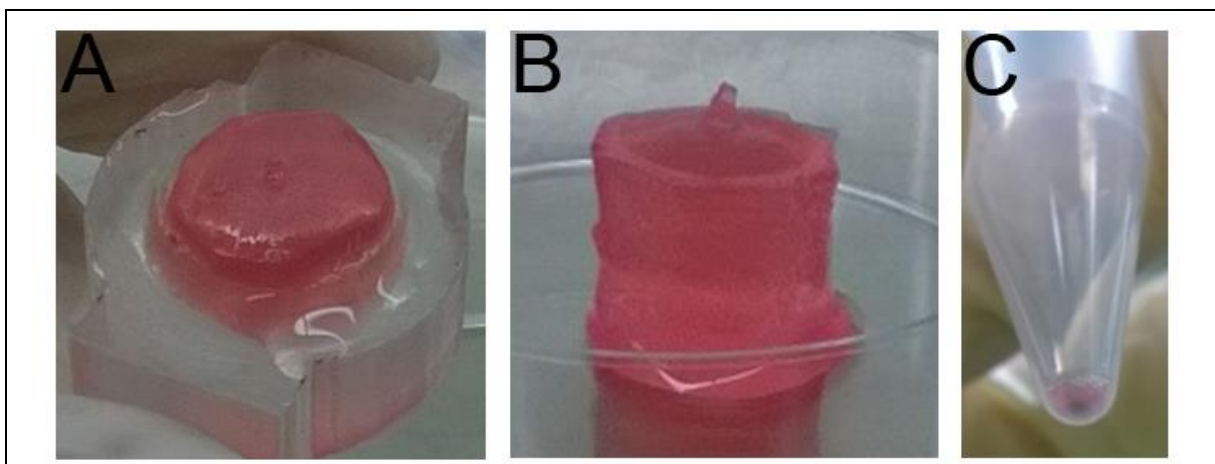


Figure 58: A) alginate gel after disassembly from the top/inflow site B) gel turned around with the bottom side pointing upwards C) remnants at the bubble trap

The gel was cut and stained as shown in the 3D cell seeding experiments but no viable cell culture could be found inside of the alginate gel.

In the second 3D cell culture experiment 2 different systems for flow through were utilized. The first culture, with the pump right before the bioreactor (configuration 3), had to be stopped after 1 day as it could not assure leakage free operability and the culture medium started to foam up around the bioreactor. Afterwards the gel was investigated in terms of cell survival and distribution.

In Figure 59 we can observe that after 1 day of cell culture in the capillary alginate gel we are still able to find some cells residing in the gel. Especially on the images B, D and E we can see them placed (the blue dots) along the capillaries indicating that they not only float on top of the gel after cutting but are distributed throughout the gel thickness. In A and F the signals from the NucBlue cannot be related to the topographical properties so easily, the fluorescent signal of the cells might originate from deeper in the scaffold. C shows the protrusion tip seen in Figure 58 B it is challenging to image but there seems to be a lot of cells accumulating at the exit of the culture chamber and a similar phenomenon has been observed in the first 3D cell culture.

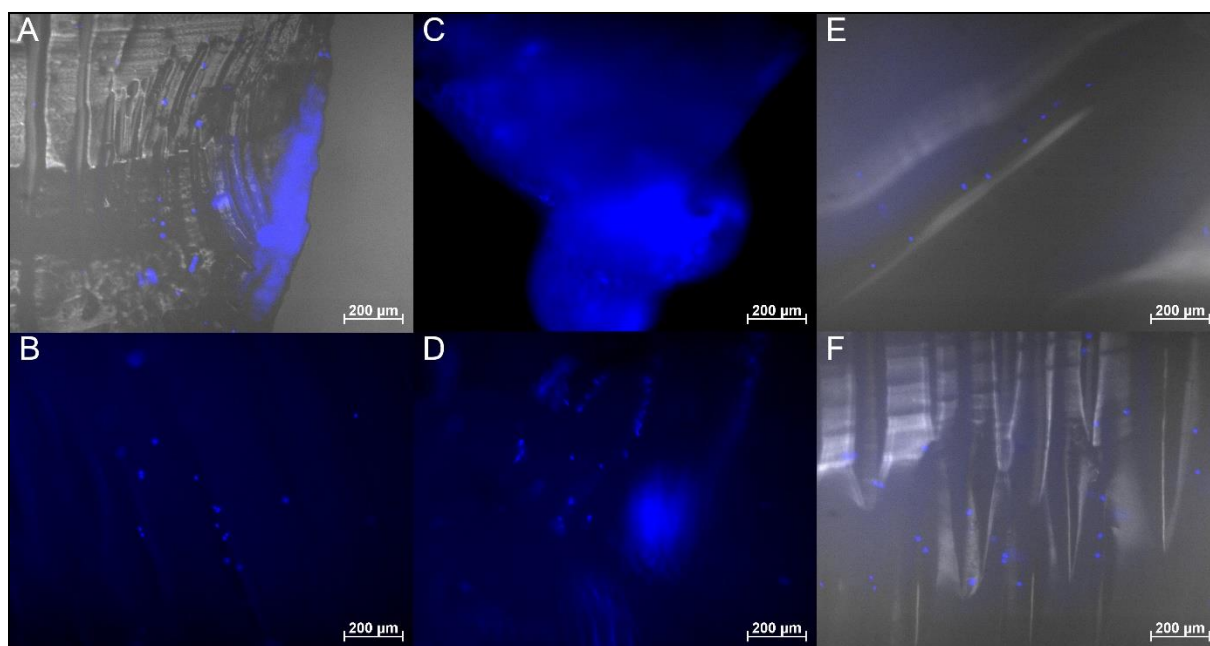


Figure 59: Images showing the live-stained (blue) cells of the second 3D cell culture experiment after 1 day of culture, A/E/F Brightfield channel and DAPI channel; B/C/D only DAPI channel; Slice 1 in A & B; Slice 2 in C & D; Slice 3 in E & F

Over the course of the first 24 hours some air leaked into the other bioreactor and small bubbles were showing up on top of the alginate gel. They had been gently removed after pausing the flow through and the culture was started again. After that no bubble formation has been observed on the bioreactor side of the culture system over the course of 6 days. Although no drastic colour change of the culture media was observed, 3 ml of the GM (at the top layer) were exchanged on the 5th day of culture to ensure a sufficient nutrient support to the cells. After 7 days of cell culture the bioreactor was opened for imaging.

While opening the PDMS channel the GM coming out was partially milky and also the bubble trap had some milky sedimentation on the bottom. This milky culture media can also be observed when looking at the pictures of the gel in Figure 60 indicating an infection of the culture. The infection can be seen throughout the pictures and is highlighted by a blue rectangle around it.

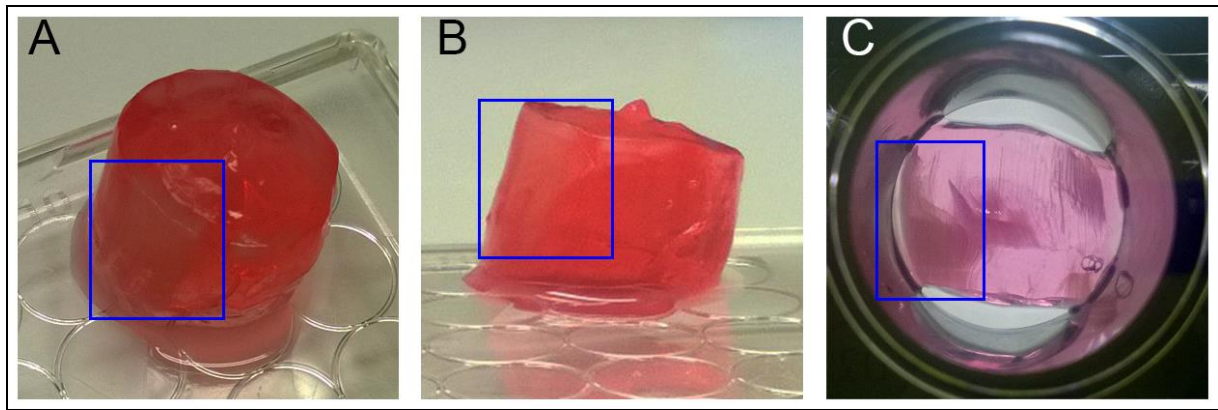


Figure 60: A and B) Showing the alginate gel right after taking it out from the PDMS channel; C) a slice of the gel in a multi-well plate; The blue boxes indicate the infection inside the scaffold; The gel size as described in Chapter 4.4.3

Interesting to note is the clear contrast of the capillaries in the gel being flown through by the culture media. This proving that flow through the capillaries is possible even over prolonged culture times.

The gel stiffness had decreased a lot during the culture period. It was comparable to the PBS buffer treatment as in the surface modification experiment (Chapter 5.2.3). Thus the handling with the tweezers as well as the cutting prior to imaging was hard to perform without breaking the gel.

Figure 61 shows an image of a capillary stitched together from multiple exposures. What it shows us is the inside of a capillary with micro sized objects and fluid flowing through. Under the microscope the small objects have been observed to move in a self-propelled way once more confirming an infection of the culture. Calcium crystals have been observed to form in the solution as well (see orange box).

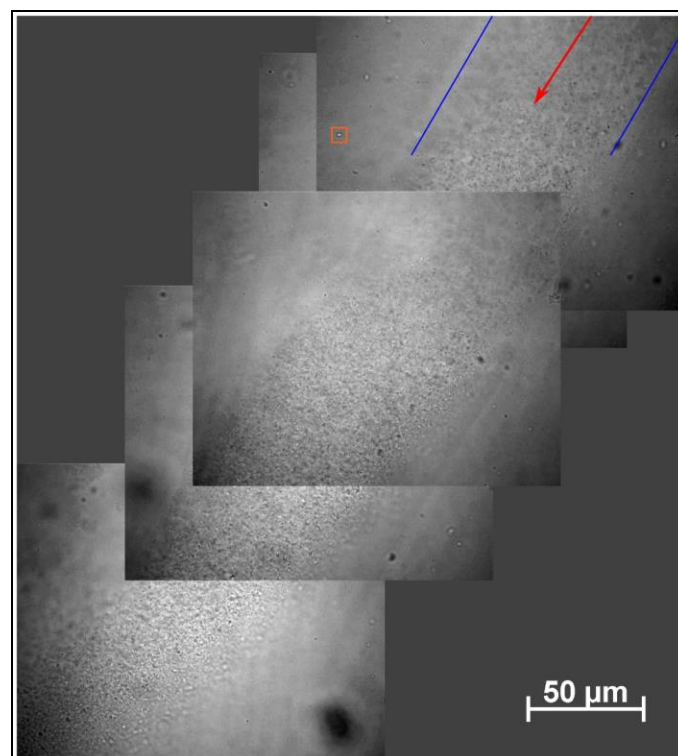


Figure 61: Stitched image of a single capillary in brightfield mode; blue lines indicating the capillary borders, red arrow showing the inside of the capillary and orange rectangle showing calcium crystals

Discussion

6.1 Bioreactor

6.1.1 Simulations

The main goal of the simulations in the terms of this project would have to be described as a tool in guiding the overall designing process of the bioreactor and specifically the PDMS channel. With this the design was changed from a rectangular to a conical design based on the flow distribution as presented in Figure 29 (Chapter 4.2.1). Furthermore, the estimation of the oxygen concentration in the middle of the bioreactor was of interest because in the conical design the wall thickness of the PDMS channel was increased. Therefore, it was necessary to judge if that would negatively affect the cell culture, which according to the results was not the case.

The main limitations of the model can be summarized in the following bullets:

- 2D Simulation
- Cells modelled in the middle of the capillaries only as O₂-sinks
- Missing the culture-dependent diffusivity and O₂-Consumption
- No deformations or mechanical stimuli from flow to other materials
- Disregarded surface properties e.g. printing and gel roughness
- Idealized capillary properties with regard to size, tube shape and distribution

Seeing that list of limitations gives a good idea of how challenging it is to make precise estimations with such a model system, especially about the internal processes in the bioreactor like oxygen concentration.

Finding reliable estimation of parameters like oxygen consumption has been problematic. Two different oxygen consumptions were given in literature and both were estimated with different measurement techniques. Furthermore, the choice of surrounding parameters e.g. glucose concentration in culture media or culture status is not always clear. In Nicholls et al. (Nicholls et al. 2010) different values for the oxygen consumption can be found therefore a parameter range was chosen in the first simulations. Eventually a discussion about the different possible factors for measurement variations in the oxygen consumption can be tied to this. As aforementioned the measurements were conducted in different ways, either with the Seahorse XF 96 analyser (Nicholls et al. 2010) or by using the Becton and Dickinson (BD) Biosensor system (Li et al. 2013). Albeit both measurement systems rely on fluorescence measurements the well-sizes and other dimensions can vary the culture conditions and impair the comparability of the two results. The oxygen consumption can also vary according to the stages of differentiation (Kislinger et al. 2005) or other metabolic changes caused by outer stimulants as shown by Nicholls et al. (Nicholls et al. 2010) or different concentrations of glucose can stimulate the metabolism as well (Li et al. 2013). Eventually there are a lot of factors to be considered but a difference of four orders of magnitude is still a very substantial change. When consulting other sources for different cell types one can find a publication by Kim et al. (Kim et al. 2013) about hepatocytes and human umbilical vein endothelial cells (HUVEC) whose oxygen consumption lies in orders of 10⁻⁹ and 10⁻¹⁰ respectively. Thus closer to the data given by Nicholls et al.

(Nicholls et al. 2010). With this the values for the modelling in Comsol Multiphysics 5.0 (Comsol Inc. 2015) was based on the data from Nicholls et al. (Nicholls et al. 2010).

The way the system is modelled at the moment sets the outer boundaries of the PDMS to be in contact with a constant supply of oxygen, an instream of oxygen saturated culture medium and a time-independent usage of the oxygen inside of the capillaries. After a steady stream between in and out flux is established the conditions will stabilize. Under culture conditions the oxygen consumption of the cells would fluctuate with increasing numbers, the cell fate and other biological variations in the metabolism. As indicated by Kim et al. (Kim et al. 2013) the diffusion through the cell culture layer should also be taken into account, which was disregarded here as well to limit the complexity of the model. Because the diffusivity would also change together with the cell culture state as mentioned before.

Eventually, simulations like this can be a useful tool in determining different changes and allow for visualisation like the flow field in the bioreactor. To set up a very precise model system remains very challenging as one also has to balance between computing power/time and to what extent the gained results are supposed to be used. As aforementioned the main purpose of the simulation was to justify design choices and to hint on problems in the geometry. The highly detailed implementation of the oxygen and glucose consumption could provide additional estimations of the culture status but would go beyond the goals of this prove-of-concept project.

6.1.2 Design of the Bioreactor

It was proposed in the half-time report to incorporate systems for measurement and parameter surveillance during the cell culture. No such system has been put in place to retrieve direct data about the culture status inside of the bioreactor. There were certain things that have been relied on, such as the colour indication of the GM as well as the transparent design of the bioreactor in general. This helped to investigate the status of the flow system, as bubbles could be observed and measures taken to reduce them. On the cellular level the indication of the GM can help to justify the oxygen levels as well as pH levels and give a rough estimation of the culture wellbeing. Although an infection cannot be observed in such a way. To observe infections, the bubble trap can be helpful as bacteria or other material starts accumulating at the bottom of the bubble trap. Here a differentiation between plain wash-out of the cells and accumulation of bacteria can be challenging at times as well.

The inclusion of a bubble trap has been speculated before as a future improvement of the bioreactor to give an additional mean to track the statuses of the culture, both visually and as an access path for taking media samples. It was implemented when longer 3D cell cultures with the bioreactor system were performed, because of previous problems with air leaking into the system. Additionally, the stop-cocks were exchanged for newly bought and pre-sterilized three-way stop-cocks. The old ones seemed to be one source of air leaking into the system. To avoid this problem in the future the trap was included but the trap proved itself useful for additional purposes. The system was planned to be used in a closed-loop fashion, thus the overall media content would be limited to roughly 1-2 ml. By adding the bubble trap an additional 5 ml reservoir was added to the system. Furthermore, a new mean of checking on the culture status was introduced and what turned out to be even more helpful was the possibility to exchange the culture media. As discussed later in the report (Chapter 6.3.1) at least a partial refreshment should be considered for longer cell cultures and when changing between different culture phases (proliferation to differentiation) the serum needs to be exchanged as well. This was all conveniently enabled with the inclusion of the bubble trap.

Another outlook from the half-time report has been the evaluation of the feasibility of the culture system by performing cell cultures with the whole bioreactor system assembled. This was performed during the seeding and culture experiments with the 3D alginate gels, hereby a lot of observations have been made and furthermore resulted in the protocol for the 3D seeding (see Appendix 14). Taking the result of the leakage experiments and the observations during the 3D cell cultures together a prolonged culture in the bioreactor system without leakage and even immense air bubble formation is possible whilst still maintaining flow through the alginate gel.

The shifting down of the alginate gels, resulting in the imprinting of the PDMS channel into the scaffold has raised some concerns about the dimensions of the bioreactor again. With respect to the pre-chamber before and after the gel in the culture chamber.

In the literature the distinction between batch and continuous feed bioreactors is established to divide between bioreactor systems that produce their results based on what has been given into the system at the beginning of the culture, batch bioreactor. The continuous feed bioreactor allows for a more active intervention throughout the cell culture by adding new media as well as removing overflow or waste (Ellis et al. 2005). The here presented bioreactor leans more towards the batch bioreactor side, with only little intervention when exchanging the media in the reservoir/bubble trap. As later discussed in Chapter 6.3.2 for finding a better operation mode of the system the further development of the bubble trap maybe to fulfil even more purposes. A concept drawing can be seen in Figure 62. This system would be put at the position of the bubble trap in a setup close to configuration 3 (Figure 25) because a direct pumping out of the bubble trap would be necessary in such an open bubble trap system. The media coming from the bioreactor would first go through a filter system, which could contain a sedimentation area were larger floating particles could sediment and be sucked away as waste. Additional filters could be used to get rid of the last particles remaining. Some more volume should be taken away to allow for the addition of new media in the reservoir.

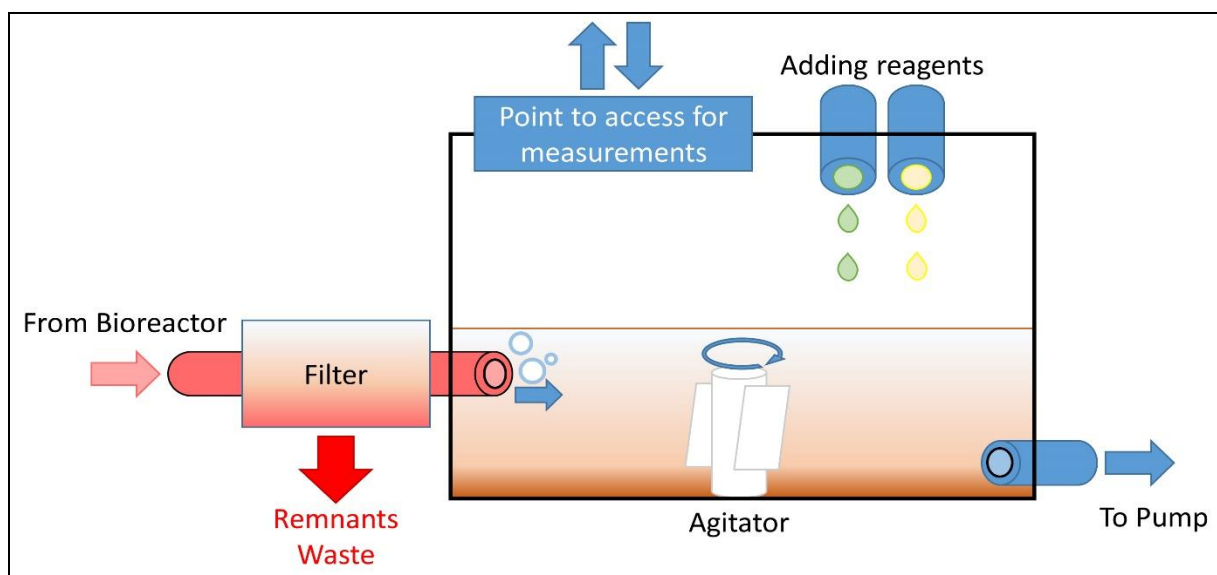


Figure 62: Concept of a new bubble trap & reservoir system

The media together with potential air is released in the tank where the bubbles can be released in the air. New media, other reagents or a culture media change can be performed through the nozzles dropping in different fluids. A slow turning agitator (<30rpm) in the middle of the reservoir could help to equalize media with the added reagents and dilute the potential unwanted leftovers from the filter system. Afterwards the pump can take the new media and deliver it to the bioreactor. An additional

access point for taking measurements of the media or add other reagents irregularly should be added to assess the status of the culture. A similar system might help to address some of the problems of the momentarily rather enclosed culture system.

6.2 Scaffold

6.2.1 Alginate a Feasible Scaffolding Material?

The capillary alginate used during this project has been investigated in pure form and has been modified with different materials. The overall goal has been to enable cells to attach and thrive on the alginate gel while being utilized in a flow through fashion. Therefore, the alginate also needs to enable the possibility of media flowing through and cells growing in. As we know from the background chapters about the cells, several cues need to be full-filled to allow the cells to attach well, proliferate or differentiate on a synthetic substrate. The evaluation what cues are more important than others or what set of criteria sets the minimum requirement has to be unravelled when developing a new scaffolding material. During the project it was in the main focus to bring down biologically effective modifications such as gelatin and GRGDSP on or into the matrix. During the culture experiments the elasticity and structural changes of the alginate has been observed as another crucial factor, which has not been accounted for in the planning of the project to a great extent.

The importance of mechanical stimuli on cell cultures for development is discussed by different sources (Chaudhuri et al. 2015; Palchesko et al. 2012) and specifically the influence on C2C12 cells is investigated (Sbrana et al. 2008; Grossi et al. 2011). Besides the specific modulations of the elastic moduli and various parameters more basic structural properties have to be taken into consideration. As aforementioned the alginate gel has been formed with the help of ionic processes, another way of crosslinking the alginate would be covalently binding the hydrogel. This process is more complex and a way of maintaining the capillary structure has to be found. Both fabrication methods result in hydrogels with the ability of stress relaxation but the characteristics are completely different (Zhao et al. 2010). The ionically crosslinked gel has the ability to dissociate the linkers and reform itself when stress is exerted thus displaying plastic behaviour. The covalently crosslinked gels react to stress by shifting the water concentrations within the gel and are able to fully recover from the deformation by shifting the water back into the network, described as elastic behaviour. (Zhao et al. 2010)

During the differentiation cycle of the C2C12 cells to functional skeletal muscle cells, spontaneous contractions of the fused fibres can be observed. The gel has to withstand these contractions and support the cells in their maturation process. Hydrogels with high plastic properties could not ensure a stable anchoring of the cells in the matrix when the cells gauge their substrate. Therefore, a “rip-out” from the matrix seems possible, too high stiffness on the other hand can lead to rupture of anchoring points because the substrate cannot give into the contractions of the cells. With this an ideal elastic modulus has to be found to allow for long-term cell cultures. Additionally the observations made by Palchesko et al. on C2C12 cultures on PDMS with varying elastic moduli where softer gels decreased the differentiation efficiency compared to the stiffer gels (Palchesko et al. 2012), making clear that the design of the alginate gel has to be performed more in concert with the cell’s requirements. It can be assumed that the C2C12 cells prefer a certain range of elastic modulus of substrate on which they can thrive best on. Previous reports on cells cultured on glass cover slips have not lead to successful differentiation, as the cells would already lift-off from the surface before reaching sufficient confluency (Wallin 2009). This is assumed to happen due to the lack of elastic properties of the glass surface.

What Palchesko et al. could not confirm is a difference in cell density caused by the different elastic moduli of the substrate. This is the line where the comparability of PDMS to alginate hydrogels has to

be drawn, as the PDMS will react in an elastic matter whereas the alginate strongly depends on the crosslinking process. (Palchesko et al. 2012)

The initial properties of the gel have to be considered with care, but to achieve a well-being of the culture the changes over culturing time have to be accounted for as well (Chaudhuri et al. 2015). For example a “rapid degradation upon incubation with cell culture medium” (Bernhardt et al. 2009) is described in the literature due to the dependence on divalent cations. This observation has not been confirmed in this project, as the gels seemed to regain stability by storage in the used GM. Which is supported by the results of Chaudhuri et al. where the Ca^{2+} in the DMEM of the culture media was used for crosslinking (Chaudhuri et al. 2015). This degradation effect was observed when the gels came in contact with a cell culture and cell culture medium, here it was speculated that exchange process in the gel occurred either through interactions with the cells, cations were “bound by medium compounds or exchanged with non-gel-inducing ions such as sodium and magnesium ions” (Bernhardt et al. 2009). In general, it is strongly depended on the mixture of the used culture medium, but the best way of avoiding any conflicts is refraining from the usage of divalent ions as crosslinking agent, specifically calcium ions.

Prang et al. performed the ionotropic crosslinking of the gel with copper nitrate solution utilizing the Cu^{2+} as a gelation agent (Prang et al. 2006). To compensate for the problems mentioned earlier the copper ions were exchanged by protons after retrieving the alginate gel. The gel was dehydrated by pure acetone several times, immersed in 10 % hexamethylene diisocyanate solution with the acetone soaked into the scaffold for 12 hours. Afterwards rinsed to eliminate remaining crosslinking solution and the gels were heated up to 70° C for 20 minutes in water. This way the gels were fixed and by rinsing with hydrochloric acid solution at 1 mol/l the copper ions were substituted. This process resulted in a metal-free hydrogel and it could withstand storage in sterile PBS at pH 7.4, confirming that no precipitation or dissolving of the gel occurs. Thus making it more suitable for cell cultures while still remaining the anisotropic capillary structure but also a lot more challenging to produce. Especially with the application as nutrition source or medical application the usage of a wide variety of chemicals will complicate the approval process.

Other sources report about using a strontium salt solution as a crosslinking agent to prevent the usage of calcium in the alginate gels (Thiele & Hallich 1957). It has been shown to be more stable in maintaining the anisotropic structure when in contact with culture medium as well as cell cultures. And it would be an easier method than proposed by (Prang et al. 2006). But it would not account for the mechanical differences between covalently and ionically bound gels, thus a cell culture could face potential problems with detachment in later stages of development as well.

Besides the problems with the cell attachment and well-being on the alginate hydrogels a softening of the gels reportedly impaired the feasibility of the bioreactor system. It is speculated that the decrease in inner strength increases the movability of the gel inside of the flow channel and as a result it blocks the outflow. Eventually leading to a stop of flow through most of the capillaries, blocking the overall sealing quality and a sufficient support of the cells in the gel is not possible.

One problem that came up during the discussion is the classification of the alginate gel properties depending on the crosslinking method, as aforementioned ionic linking results in plastic behaviour and covalent crosslinking in elastic gels (Zhao et al. 2010). But more importantly both gels have their own mechanism of stress relaxation (Zhao et al. 2010). Chaudhuri et al. on the other hand classified the gels into elastic for the covalently bound and stress relaxing gels for the ionically bound (Chaudhuri et al. 2015). The problem with that is that it neglects the forms of stress relaxation in covalently bound gels formerly observed. For the U2OS cells used in that study the proliferation and YAP expression had been

better on the ionically crosslinked gels, furthermore it was concluded that “stress relaxation can compensate for matrices with a lower stiffness” (Chaudhuri et al. 2015). If the results of the culture are solely explainable due to the different cell lines used is open for debate, but what it might emphasize is that proliferation and differentiation phase should be observed independent from each other. This ties in with the results of this project, as the PDMSFlatGelExperiment 1+7d showed the highest levels of survival on the used substrates. Therefore, the properties of the RGDA:alginate 1:5 might be more suitable for a differentiation phase.

To classify alginate as a suitable scaffolding material one has to investigate the biodegradability of the alginate gel as well. Because it interacts with the capability of maintaining a cell culture for prolonged periods. By utilizing the oxidizing capabilities of sodium periodate and varying the amount of low or high molecular weight alginate a controllable degradation of the alginate was achieved by Boontheekul et al. (Boontheekul et al. 2005). A decrease in tensile strength and weight loss has been investigated when keeping the gel in aqueous solution together with other parameters indicating degradation processes. If investigated further a tuning of the degradation process might be possible allowing for calibration of the degradation process with the development and shift in demands of the cell culture in mind. Eventually maybe even a total dissolution of the synthetic scaffold when the grown construct is strong enough. In the work by Boontheekul et al. the gels have been coupled with RGD and C2C12 cells were cultured on them (Boontheekul et al. 2005). This was just used to verify that no adverse effects of the degradation modification inflict with culture and differentiation of the cells. These both factors have been sufficiently proven by the results, but it raises concerns with respect to the observations made in this project and by Bernhardt et al. when the ionically crosslinked gels get in contact with actual culture media and a cell culture (Bernhardt et al. 2009). In the publication only the cells well-being has been investigated after cell culture, but not confirmed if the degradation processes have been that controllable in the culture condition as well as in the degradation experiments in the aqueous solution.

6.2.2 Scaffold Modifications

The positive influence of the modifications of the alginate gel has been observed in some cases like the PDMSFlatGelExp-1+7d (Table 10), but the most promising results have only been produced with the help of bulk modified alginate gels. Especially with the pre-coupled GRGDSP-alginate. These methods can be easily realized as they only include mixing of the respective solutions prior to crosslinking. The effectiveness with respect to cell interaction to the modification and the cost effectiveness is open for debate when using this rather crude method.

The surface modifications that have been performed with either collagen or GRGDSP did not result in gels displaying good attachment of the cells. The collagen has not been pursued further after the initial cell experiments of the project, but the RGD coupling was taken up in the later stages of the project to achieve a higher efficiency between protein content and cell availability. Thus improving the cell attachment as well as making it more controllable with regard to spatial distribution and concentration. A successful surface coupling could not be confirmed due to problems with the protocols used as well as the limited testing with the cells as single measure. The scaffold problems faced during the coupling process might be solvable by utilizing the gel preparation technique proposed earlier by Prang et al. making the gel more mechanically stable by removing the highly motile divalent ions. In addition to that a surface coupling allowing for axonal regrowth has been performed in this publication as well. The used method is straight forward as the alginate gel was placed in a solution containing laminin, collagen, fibronectin and poly L-ornithine for 12 hours. Here a healthy culture of adult neuronal progenitor cells was achieved and even axon regrowth was improved. (Prang et al. 2006)

Another aspect to consider is the RGD sequence that has been used during the project, the GRGDSP used during this project is assumed to be similar to the GRGDY peptide used in the first surface coupling protocol that has been followed (Rowley et al. 1999). Later papers indicate a switch towards a RGD peptide with more spacer units (G) either using the GGGGRGDY (Rowley & Mooney 2002) or the GGGGRGDSP sequence (Chaudhuri et al. 2015). This placing the bioactive component of the sequence further away from the surface and potentially increasing the availability to the cell culture. In the later process a similar process of carbodiimide coupling of the RGD to the alginate has been performed in solution before crosslinking, to our knowledge, a surface coupling as performed by Rowley et al. (Rowley et al. 1999) has not been published by the group afterwards again or been utilized by others.

Although the challenges faced during the surface coupling it is still highly advised to perform surface coupling for multiple reasons. First the modification is supposed to help the attachment of the cells on the surface on the gel does it needs to be available on the top. Secondly a surface modification is easier to control than a bulk modification in terms of amount, density and distribution in the gel. Bulk modifications are performed before crosslinking thus the interactions of the capillary formation with the modification material is unknown. The modification could end up buried in the gel due to phase separation processes. Mathematical estimations have been performed (see Appendix 16) showing that under the assumption of a 50 nm penetration depth (Rowley et al. 1999) the cells would only be able to access 0.03 % of the total gel and modification respectively, if an equal distribution is assumed. This shows how ineffective a bulk modification is, adding economic constraints to the proposed techniques as well as challenging the scientific discussion due to unknown availability to the cells.

The gelatin modification of the gel has certain merits and should be revisited for future investigations at least when aiming for a medical application. Remembering the results of the confocal microscopy performed on the gelatin:alginate 1:1 (5.2.2 page 56) an equal distribution throughout the gel had been achieved and it added to the structural properties of the hydrogel without interfering with the alginate structure according to the SAXS data (Appendix 15). In contrast to that it was able to support the capillary formation process when the gelatin:alginate 1:1 solution was autoclaved before the crosslinking process (Peng et al. 2014). Furthermore, it indicated to be beneficial for cell growth on the alginate gel as well. One way of utilizing the gelatin:alginate could be to use it in connection to other modification techniques. In that way an autoclavable solution could be achieved, the capillary formation process ensured and additional surface modifications could increase the effectiveness of the culturing overall. Future investigations towards mechanical properties, feasibility of covalently crosslinking the gel (dependence on ionic crosslinking) and the overall culture behaviour should be performed to progress with the gelatin.

The verification of the modification success has been performed by judging the attachment and well-being of the cell cultures on the gel surfaces. This has only been a strictly qualitative measure and showed to be challenging to assess during the project, as the well-being of the cells can be influenced by many different parameters.

In addition to that many other observations have been made like changing substrate stiffness or even the failure of the control cultures on the dishes (ControlFlatGelCulture GM/DM) which provided too little cell numbers for unknown reasons. Thus it is still challenging to keep the other parameters strictly confined between the different experiments or even the several dishes of one experiment.

If these other problems could be addressed and better controlled in the future, then methods like FTIR should be considered in verifying the success of the surface coating method. Here specifically looking out for the nitrogen in the amide bond of the RGD to the alginate or in the RGD sequence itself.

The bulk modification with gelatin has been tested with a confocal microscope by my collaborators and an even distribution of the gelatin throughout the scaffold has been confirmed. With this it got clear that the gelatin stays in the matrix and might potentially participate in stabilizing the gel as well as supporting the cell adhesion to the gel.

6.2.3 Optimization of the Protocols

The sterilization protocol of the scaffolds according to Stoppel et al. has proven to be sufficient in avoiding an infection of the cell cultures over the course of the project. The only time an infection was observed was during the second 3D cell culture experiment. But this cannot be linked to an insufficient sterilization method, as the possibilities for infection with the 3D cell culture experiments can be of multiple source. No signs of infection had been observed when taking the alginate gels stored in GM and in the incubator for several weeks prior to cell culture. Thus the sterilization method was also sufficient for the larger 3D alginate gels.

For the sake of the project other methods of sterilization might strongly be considered to progress with the culturing experiments and as shown now also to prevent further adverse interactions with the modification protocols. The group around Schuster et al. has been successful in performing the capillary forming procedure on autoclaved alginate, in our lab this has only been shown possible with the addition of gelatin to the solution. Thus the gelatin:alginate in a 1:1 weight ratio produced capillary hydrogels (Peng et al. 2014).

Bernhardt et al. sterilized the gels with gamma-irradiation prior to cell culture but this technique has been used to decrease the molecular weight in the alginate solution by Boontheekul et al. (Bernhardt et al. 2009; Boontheekul et al. 2005). With this it is open for debate if gamma-irradiation really serves as a suitable way of sterilizing the gel. The huge merit could be avoiding chemical reactions in the gel and the residing of the sterilizing agent in the gels especially in methods with ethanol emulsion (Stoppel et al. 2014; Prang et al. 2006). Furthermore Prang et al. placed the alginate gels in PBS after sterilization, thus a non-ionic crosslinking technique would be necessary for achieving subsequent washing (Prang et al. 2006).

When a full sterilization of the single constituents of the scaffold would be possible, it might be beneficial to perform the crosslinking in complete sterilize conditions from the beginning to rule out any after effects due to the sterilization. Then the crosslinking would have to be performed under sterile conditions but initial contaminations could be ruled out from the beginning.

6.3 Cells

6.3.1 Culturing Techniques

During the work with the project it got clear that one main focus in establishing future cell cultures has to be the scaffold development. Almost all of the cell experiments, besides the 3D cell cultures with the whole bioreactor system, have been designed to test the efficacy of the different modification and scaffold properties. Furthermore, most of the problems that arouse during those cultures have been linked back to the alginate behaviour in culture. For example, the not sufficient RGD modification of the gel or the changes in mechanical properties which lead to the loss in cell numbers. Nevertheless, during the hands on work with the many different cultures several observations were made that can lead to the development of culture protocols on and in the alginate gels.

One of those observations has been the decrease in cell number around day four on the alginate surface when cultured in GM. Originally, alginate slides of higher RGD content were seeded with cells and after 3 days the culture media was switched from GM to DM (during the PDMSFlatGelExp – 3+7 d). With this the possibility of differentiating C2C12 cells on RGD modified alginate was supposed to be tested. But here again the reduction of the cells during this proliferative phase in GM was observed until the switch to DM was performed. From this the idea to seed an even higher density of cells and switch to the DM after 24 hours of culture emerged (PDMSFlatGelExp – 1+7d). With this experiment the longest and most promising cultures have been achieved on the RGD modified flat gels. Therefore, it was speculated that maybe for future cell cultures in the capillary gel very high densities should be used and only the maturation steps should be performed in the capillary alginate. This would divide the proliferation and maturation phase completely but might have merits for later applications as well. Ways to produce high cell numbers could be provided by cell cultures on microcarriers in stirred-tank bioreactors (Rafiq et al. 2013). Afterwards the cells could be harvested from there and be seeded into prepared capillary alginate gels for self-aligning and maturation. This could make way for an automated seeding process and reduce the high demands of human intervention during culture and especially during the differentiation process. The method introduced by Mark J. Post includes a lot of handling of the cells themselves in small quantities and the maturation process for one single muscle fibre takes approximately three weeks. After that the assembly process to a full meat product is performed (Mark J. Post 2014). Here the idea of culturing cells in large tanks and sub sequentially mature them is pitched as well (Mark J. Post 2014).

The optimization of the seeding protocol has been tried for the flat gel experiments to allow for a better comparability between the different experiments and over the whole culture time. Furthermore, first experiments on the seeding techniques for the capillary alginate have been performed. As hinted for the seeding on the flat gel this was a mean to improve comparability and significance of the conclusions from the imaging. Focusing more on the seeding in the capillary gel the usage of the flow bioreactor in connection with the pump system resulted in a good distribution of the cells in the alginate gel. Cells were found throughout the whole volume of the alginate gel showing that a flow through is possible and allows for cell deposit in the gel.

One outlook in the half time report was to adjust the cell numbers for the seeding processes on flat as well as capillary alginate gels. Depending on the planned culture times the cell numbers were seeded to be confluent (~ 500 cells/mm²) when leaving the proliferation phase. For the capillary alginate gels high numbers as possible were used to get as many cells as possible into the construct as a counter measure to the speculated loss during seeding, not fully optimized attachment and death due to seeding stress. Together with the previous discussion in the case of producing the high cell numbers outside of the bioreactor the seeded cell numbers should be adjusted to allow for a confluent cell culture in the capillary gels. Estimating the cell numbers (see Appendix 17) based on the model alginate used in the calculations for this project we estimated that at least four million cells are necessary to fill the alginate gel with skeletal muscle fibres (Peng et al. 2014; Bruusgaard et al. 2003). Disregarding the remaining satellite cells in the fibres as well as only limiting to muscle cells. Overall a lot more cells and cell types will be necessary for a tissue mimic in the future.

Many challenges remain until a functional method exists for producing tissue engineering for various applications. When coming from the area of cultured meat one huge interest would be to substitute the currently used serum (e.g. FBS (Brunner et al. 2010)) contributing to animal welfare, thus cutting out animals completely from the production chain. Besides the ethical problems there lies profound scientific interest in reducing the usage of serum in culture media all-along (Brunner et al. 2010). As a product harvested from animals it has inherent batch-variation in form of quality and quantity of the

constituents (Brunner et al. 2010) thus it is an “ill-defined medium supplement” (Gstraunthaler 2003). The challenges in substituting serum completely lies in addressing the wide range of functions the serum provide in a cell culture where growth factors and hormones are just one small stepping stone. Brunner et al. summed up some of the additional roles like providing amino acids, vitamins and trace elements, protease-inhibitors, detoxification, osmotic pressure and even more (Brunner et al. 2010). Finding reagents to take over those functions will be a huge undertaking but can contribute greatly to the nearer understanding of the cells in culture. Our methods and scientific question narrow down further and further to even single cell assessment and interactions are studied on so small scales that possible variations as the lot-to-lot quality of serum just do not seem appropriate for future proceedings anymore.

In connection to the aspiration towards serum-free cultures some argued that the usage of FBS could even increase the risk of microbial infections or even virus transmission (DORMONT 1999; Eloit 1999). To address the problems of microbial infections the usage of antibiotics is advised as performed in this project as well. In the boundaries of the lab and during culture experiments it helps to prevent infections during the whole processing but when the methods are supposed to be devised for applications the reduction of antibiotics should be considered. As of now we already have problems regarding the rise of multiresistant bacteria (Dennesen et al. 1998) and the amount of antibiotics used in food production seems to be one factor for increasing the number of resistant bacteria stems (Perreten et al. 1997). Furthermore, the food could serve as a carrier for spreading those newly bred bacteria. A problem that will also have to be addressed when designing future culture techniques in tissue engineering. The aforementioned virus transmission is not solvable with antibiotics and especially when aiming to use the cultured products from farm animals for nutritional applications the transfection of viruses passing over species boundaries might be a problem that would have to be faced in the future.

On top of the technical issues to be solved one should keep in mind what would be necessary for approving future applications of tissue engineered constructs. Quality standards that have to be kept very high and batch variation should be almost non-existent. Applying that to cells we would have to make sure that especially in the proliferation phase the cues one single cell is exposed to be similar to every other cell in the culture. This criteria would have to be addressed by a good mechanism to keep up the suspension (Rafiq et al. 2013) or when using the microcarriers one concern raised is the quality and uniformity of the carriers. Maybe small debris of synthetic material could end up on the inside of the cell or in the final products, which would raise the hurdles for approval. Taking up the previously discussion on serum usage in cell cultures it was mentioned that it displays a lot of batch variations. Trying to approve a product for food or medical application where the quality and quantity of one constituent cannot be assured within reasonable boundaries will be challenging in the future.

6.3.2 Operations Mode

During the performance of the seeding and culture experiments with the capillary gels several observations have been made towards the future operation mode of the bioreactor. One major result of that is the 3D Seeding protocol (found in the Appendix 14) giving a first guideline of how to work when using the designed system. Which utilized the bioreactor as a seeding device for seeding the capillary alginate gels.

In the 3D culture experiments the used flow speeds have been used up to 10 $\mu\text{l/s}$ (0.6 ml/min) which was the recommended minimum according to Dennis et al. (Dennis et al. 2009). This flow speed was used to avoid wash-out of the cells from the capillary gel. The bioreactors were operated in closed-loop during cell cultures because in open-loop the usage of the media would be extensive, with 36

ml/h and a three-day culture would already use up over 2.5 litre of culture media. Besides the huge amounts of culture media used there are several merits and drawbacks to either of the operating modes.

As we know from Chapter 3.4.2 the interactions between a cell and its surroundings are manifold, hence it is challenging to model the right environment for a cell to grow in. Besides the scaffold, the media is the main carrier of reagents and cues to the cells. Paracrine and autocrine signalling of the cells is a very important step for the overall culture development and for this the surroundings have to be suitable for that form of communication to occur. If we now run the cell culture in open-loop, we deprive the cell culture of those factors released. On the other hand, in closed-loop mode everything that is released from the cell culture will be exposed to the culture again. The induction of apoptosis through other apoptotic cells is not unheard of either (Pérez-Garijo et al. 2013). Thus a good balance between freshening up the media over the time of the culture should be found also with respect to other culture parameters like pH or oxygen content. A new reservoir was proposed in Chapter 6.1.2 to address some of those problems.

The cell yield of bioreactors, culturing techniques or other specific parameters is at the focus of interest of many groups (Rafiq et al. 2013; Shipley et al. 2011; Ellis et al. 2005). At the forefront is to reduce the amount of culture media for producing reasonable quantities of cells with for example hollow fibre bioreactors (Shipley et al. 2011). Tying in with the previous experiences gathered during this project there are many things to consider when discussing the cell media handling during a cell culture. The typical cultures kept in the lab environment are performed on flat stackable T-flasks which are easy to handle. But in the culture medium itself gradients of gases, nutrients, pH and temperature will emerge due to the limited agitation and the gas exchange effectively happening at one side of the flask. Additionally the amounts estimated for growing a complete organ in T-flasks are not feasible for applications (Ellis et al. 2005). Perfusion bioreactors like the hollow fibre bioreactor (Ellis et al. 2005) are presented as an alternative for increasing the cell yield while reducing the amount of used media. Hewitt et al. is using stirred-tank bioreactors for scaling up purposes of human mesenchymal stem cells to tackle the gradient problematic in larger cell cultures (Rafiq et al. 2013). These systems hold promises for the production of large cell numbers and could be combined with the aforementioned ideas. In producing high cell quantities outside of the system and use the proposed bioreactor with scaffold to address the need for higher orders of culture by creating three-dimensional constructs for maturation.

6.3.3 Sterility during the cell culture

The sterility in connection to the scaffolding techniques has been discussed before. But maintaining sterility is not solely based on the sterile scaffolds. Every single component used needs to be sterilized, here ethanol sterilization has been performed quite often. This technique has shown to be efficient in most of the cultures, and has to be kept for the 3D printed parts made from ABS or other techniques like EtO sterilization (Medical Device & Diagnostic Industry 1997) should be considered to achieve longer shelf lives. The other components like PDMS channel, tubings, screws etc. could be put together to “culture kits” and autoclaved together for equally long storage.

For the future it would be beneficial to migrate more processes into the LAF bench to allow for a better controllable sterility conditions. Measures should be taken to allow better moving of the culture system between incubator and LAF bench, thus reduce the risk of infections during the culture time.

Summary and Conclusions

In this project a bioreactor system has been designed to culture muscle progenitor cells in a capillary scaffold. It was mainly divided into three main compartments, the bioreactor design, the scaffold development and the cell cultures with their respective culturing methods. These three parts were developed either individually or in concert with each other if possible. For example, the cell cultures were performed on the alginate gels, thus gaining insight into culturing techniques as well as supporting the scaffold development.

At the beginning modelling and simulation of the bioreactor was performed to assess the flow through and simulate the conditions during cell culture. The flow profile together with the spatial distribution of the oxygen concentration was of main interest during those simulations. The model served as a good tool to develop the system further. The flow profile resulted in changes of the bioreactor design and the flow through experiments have shown the improved flow distribution through the culture chamber. The oxygen simulations showed no sign of too low oxygen concentration during the cell culture, but the limitations of the current model do not allow for full prediction of the real cell culture conditions. The simulation of the diffusion pathways into the system over the PDMS further helped in developing the bioreactor system justifying the mesh like structure of the retainer.

A bioreactor setup was realised, which allows for perfusion cultures inside of the culture chamber of the PDMS channel. A leakage free operation was achieved and the pump system used allows for highly controllable flow rates during the culture. A bubble trap was introduced into the system to eradicate air bubbles in the system, allowing for media exchange and partial assessment of the culture status.

Hydrogels with parallel aligned capillaries have been formed from alginate and have been successfully modified with gelatin as well as RGD as bulk modification. These modifications showed positive effects when the C2C12 cells were cultured on them compared to the pure alginate gels with or without capillaries. Especially the capillary RGDA:alginate 1:5 displayed the densest cell cultures and allowed for the longest culture time up to eight days. Furthermore, the spatial orientation of the cells along the capillaries has been the best observed in this project. The surface modifications of the alginate gels with collagen or GRGDSP have not resulted in enhanced cell growth on the alginate gels. The modification with GRGDSP resulted in structural changes of the alginate gels thus impairing the usability and cell culture results. More structural changes have been observed after longer cell culture experiments on or within the alginate gels. The alginate started to lose tensile strength and parts broke off during handling. It was speculated that this prevents the cells from successfully attaching to the substrate.

All parts were put together in a perfusion 3D culture experiment. The bulk modified capillary RGDA:alginate 1:5 was seeded with the C2C12 cells inside of the bioreactor system. The bioreactor showed good results when used for seeding of the capillary gels. The cells were cultured for 24 hours in closed-loop perfusion at a flow speed of 5 $\mu\text{l/s}$. After this culture cells could still be found in the capillaries throughout the alginate gel. A total perfusion experiment without leakage and air bubbles build up in the system was possible under the same conditions for up to seven days.

Eventually, the project developed a prove-of-concept bioreactor allowing for future investigations. It helped to characterize the three main stages and delivers proposals for future experiments. The alginate scaffold should be developed further as a basis for future advances.

Future Outlook

The development of the alginate as a scaffold material was evaluated as the highest priority for progressing with the presented project. The alginate together with the RGD modification should be addressed first before progressing with any other part of the system. For future experiments the scaffold should be developed with the elastic modulus in mind and for this different crosslinking agents should be considered. In concert with this the possibility of covalently crosslinking the gels after formation of the capillary gels should be considered allowing for potentially beneficial changes of the mechanical properties. The switch from ion-dependant binding of the scaffold should increase the stability towards surface modifications and broaden the possibility of efficiently coupling the alginate gels. As shown in the project, the surface modifications should strongly be kept in focus from both a scientific and economical point-of-view. Especially the RGD modification as it has shown the best culture improvements when used as bulk modification. Other techniques of surface modification with laminin, collagen and fibronectin should be considered to further increase the amount of stimulations beneficial for cell attachment and development. After achieving a successful culture, the individual effects of the materials as surface coatings on the alginate can be investigated. Besides the cells as indicator surface analysis like FTIR should be considered to assess the modification efficacy of the alginate gels.

Regarding the elastic moduli and stress-relaxation behaviour of the substrate the cells might need different mechanical cues during different times of their developmental stage. Cell experiments with well-defined elastic moduli should be considered to unravel the needs of the cell culture. Together with this the degradation processes of the alginate gels (with different modifications) should be investigated to indicate limits of cell culture times.

The development of the scaffold should be performed while considering new sterilization methods. A sterilization of the components before scaffold formation is beneficial to not alter the properties of the finished construct. As long as the capillary formation can be assured.

After these in-depth investigations of the capillary alginate different progression could be:

- Development of alginate gels for specific developmental stages
- Remembering the discussion on seeding high cell numbers to solely utilize the aligning and 3D orientation support by the alginate gel
- Inclusion of co-culture especially when performing the differentiation of C2C12 cells with e.g. endothelial cells
- Development of protocols to degrade the alginate faster and allow for laydown of ECM by the cultured cells
- Trying to establish serum free cultures of the C2C12 cells, for scientific advantages and to enable applications for cultured meat production
- Further development of the bioreactor system,
Change the culture chamber by increasing the pre-chambers
Inclusion of the further developed reservoir/bubble trap

All the aforementioned ideas could spawn many new projects performed on the basis of the proposed system. But several side projects are imaginable resulting from the overall thesis project that not necessarily contribute to the achieving of the aims of the project.

One project could be the development and investigation of the capillary gelatin:alginate as a biomaterial maybe for more medical oriented applications. The interactions of both materials could be studied, especially with respect to the formation of capillaries. This could help to unravel the amount of contribution of the gelatin to the alginate mesh. A closer investigation of the storage process of the gelatin in the alginate mesh could be another focus of that work. This project could be enhanced with the inclusion of collagen as the pre-product of gelatin.

Another project could be performed solely on the started simulations to develop the model further. This could allow for a more dynamic modelling where the population growth of the cells could be included or the alginate modelled in a less computing power demanding way allowing for more reasonable simulation times or the addition of more complexity. This model could be developed further to allow for easier estimations in industrial upscaling projects.

Bibliography

- Abbott, A., 2003. Biology's new dimension. *Nature*, 424, pp.870–872.
- Abouna, G.M., 2008. Organ Shortage Crisis: Problems and Possible Solutions. *Transplantation Proceedings*, 40(1), pp.34–38.
- Atala, A., 2013. New body parts – the shape of things to come? Available at: http://www.wipo.int/wipo_magazine/en/2013/06/article_0004.html [Accessed December 8, 2015].
- Autodesk Inc., 2014. AutoCAD. Available at: <http://www.autodesk.com/> [Accessed September 15, 2015].
- B. Braun, 2015. Materials. Available at: <http://www.bbraun.se/> [Accessed September 15, 2015].
- BACHEM, 2015. Materials. Available at: <http://www.bachem.com/> [Accessed September 14, 2015].
- Baysal, K. et al., 2013. Chitosan/alginate crosslinked hydrogels: preparation, characterization and application for cell growth purposes. *International journal of biological macromolecules*, 59, pp.342–8.
- BD Biosciences, 2015. Protocols. Available at: <http://www.bdbiosciences.com/eu/home> [Accessed April 24, 2015].
- Bernhardt, A. et al., 2009. Proliferation and osteogenic differentiation of human bone marrow stromal cells on alginate-gelatin-hydroxyapatite scaffolds with anisotropic pore structure. *Journal of Tissue Engineering and Regenerative Medicine*, 3(1), pp.54–62.
- Bian, W. & Bursac, N., 2008. Tissue engineering of functional skeletal muscle: challenges and recent advances. *IEEE engineering in medicine and biology ...*, (October), pp.109–113.
- Binder, M.D., Hirokawa, N. & Windhorst, U., 2009. *Encyclopedia of Neuroscience* 1st ed., Springer-Verlag Berlin Heidelberg.
- Blanpain, C. & Fuchs, E., 2009. Epidermal homeostasis: a balancing act of stem cells in the skin. *Nature Reviews Molecular Cell Biology*, 10(3), pp.207–217.
- Blau, H.M., Chiu, C.-P. & Webster, C., 1983. Cytoplasmic activation of human nuclear genes in stable heterocaryons. *Cell*, 32(4), pp.1171–1180.
- van Blitterswijk, Clemens Thomsen, P., Lindahl, A. & Et.al., 2008. *Tissue Engineering* C. van Blitterswijk et al., eds., Burlington: Academic Press.
- Blokhuis, T.J. et al., 2000. Properties of calcium phosphate ceramics in relation to their in vivo behavior. *The Journal of trauma*, 48(1), pp.179–186.
- Boontheekul, T. et al., 2008. Quantifying the relation between bond number and myoblast proliferation. *Faraday discussions*, 139, pp.53–70; discussion 105–128, 419–420.
- Boontheekul, T., Kong, H.-J. & Mooney, D.J., 2005. Controlling alginate gel degradation utilizing partial oxidation and bimodal molecular weight distribution. *Biomaterials*, 26(15), pp.2455–2465.
- Brunner, D. et al., 2010. Serum-free Cell Culture : The Serum-free Media Interactive Online Database. , (December 2009), pp.53–62.

-
- Bruusgaard, J.C. et al., 2003. Number and spatial distribution of nuclei in the muscle fibres of normal mice studied in vivo. *The Journal of physiology*, 551(Pt 2), pp.467–478.
- Burattini, S. et al., 2004. C2C12 murine myoblasts as a model of skeletal muscle development: Morpho-functional characterization. *European Journal of Histochemistry*, 48(3), pp.223–233.
- Chaudhuri, O. et al., 2015. Substrate stress relaxation regulates cell spreading. *Nature Communications*, 6, pp.1–7.
- Chodorowski, A., 2014. Image Analysis (SSY095). Chalmers University of Technology.
- Comsol Inc., 2015. Comsol. Available at: <https://www.comsol.com/>.
- De Coppi, P. et al., 2005. Angiogenic gene-modified muscle cells for enhancement of tissue formation. *Tissue engineering*, 11(7-8), pp.1034–1044.
- Crawford, G.N.C., 1954. An experimental study of muscle growth in the rabbit. *Journal of Bone & Joint Surgery, British ...*, 36 B(2), pp.294–303.
- Datar, I. & Betti, M., 2010. Possibilities for an in vitro meat production system. *Innovative Food Science & Emerging Technologies*, 11(1), pp.13–22.
- DeHart, C., Geer, B. & Riutta, S., 2006. Inducing Smooth Muscle Differentiation in Mouse Embryonic Stem Cells using a Biological Circuit.
- Dennesen, P.J.W., Bonten, M.J.M. & Weinstein, R.A., 1998. Multiresistant bacteria as a hospital epidemic problem. *Annals of Medicine*, 30(2), pp.176–185.
- Dennis, R.G. et al., 2009. *Bioreactor Systems for Tissue Engineering* C. Kasper, M. van Griensven, & R. Pörtner, eds., Berlin, Heidelberg: Springer Berlin Heidelberg.
- Despang, F., Dittrich, R. & Gelinsky, M., 2011. Novel Biomaterials with Parallel Aligned Pore Channels by Directed Ionotropic Gelation of Alginate : Mimicking the Anisotropic Structure of Bone Tissue. In *Advances in Biomimetics*. pp. 349–372.
- DiMasi, J. a., Hansen, R.W. & Grabowski, H.G., 2003. The price of innovation: New estimates of drug development costs. *Journal of Health Economics*, 22(2), pp.151–185.
- Discher, D.E., Mooney, D.J. & Zandstra, P.W., 2009. Growth factors, matrices, and forces combine and control stem cells. *Science (New York, N.Y.)*, 324(5935), pp.1673–1677.
- DORMONT, D., 1999. Transmissible spongiform encephalopathy agents and animal sera. *Developments in biological standardization*, (99), pp.25–34.
- Dow Corning, 2014. Materials. Available at: <https://www.dowcorning.com/> [Accessed April 30, 2015].
- Drury, J.L., Dennis, R.G. & Mooney, D.J., 2004. The tensile properties of alginate hydrogels. *Biomaterials*, 25(16), pp.3187–99.
- Dynalab Corp, 2014. Acrylonitrile butadiene styrene. Available at: http://www.dynalabcorp.com/technical_info_abs.asp [Accessed December 18, 2014].
- Ehrlich, P.R. & Holdren, J.P., 1971. Impact of Population Growth. *Science*, 171(3977), pp.1212–1217.
- Ellis, M., Chaudhuri, J. & Al-Rubeai, M., 2005. *Bioreactors for Tissue Engineering* J. Chaudhuri & M. Al-Rubeai, eds., Dordrecht: Springer Netherlands.
- Eloit, M., 1999. Risks of virus transmission associated with animal sera or substitutes and methods of control. *Developments in biological standardization*, 99, pp.9–16.

- Emergent BioSolutions Inc., 2015. BioThrax. Available at: [http://emergentbiosolutions.com/news?page=releasetxt&id=2117340&pubdate=November 24%2C 2015](http://emergentbiosolutions.com/news?page=releasetxt&id=2117340&pubdate=November%2024%2C%202015) [Accessed November 26, 2015].
- FDA - U.S. Food and Drug Administration, 2015. Animal Rule Summary. Available at: <http://www.fda.gov/emergencypreparedness/counterterrorism/medicalcountermeasures/mcregulatoryscience/ucm391665.htm> [Accessed November 26, 2015].
- FMC BioPolymer, 2014. Materials. Available at: <http://www.fmcbiopolymer.com/> [Accessed April 22, 2015].
- Forsythe, J. a et al., 1996. Activation of vascular endothelial growth factor gene transcription by hypoxia-inducible factor Activation of Vascular Endothelial Growth Factor Gene Transcription by Hypoxia-Inducible Factor 1. *Molecular and cellular biology*, 16(9), pp.4604–4613.
- Gatenholm, P., 2014. Tissue Engineering I (KPO065). Chalmers University of Technology.
- Genes, N.G. et al., 2004. Effect of substrate mechanics on chondrocyte adhesion to modified alginate surfaces. *Archives of Biochemistry and Biophysics*, 422(2), pp.161–167.
- Gillies, A. & Lieber, R., 2011. Structure and function of the skeletal muscle extracellular matrix. *Muscle & nerve*, 44(3), pp.318–331.
- Goldthwaite, C. a, 2006. Chapter 10. The Promise of Induced Pluripotent Stem Cells (iPSCs). *Regenerative Medicine. U.S. Department of Health and Human Services.*, pp.97–104.
- Grossi, A. et al., 2011. Mechanical stimuli on C2C12 myoblasts affect myoblast differentiation, focal adhesion kinase phosphorylation and galectin-1 expression: a proteomic approach. *Cell Biology International*, 35(6), pp.579–586.
- Gstraunthaler, G., 2003. Alternatives to the use of fetal bovine serum: serum-free cell culture. *Altex*, 20(4), pp.275–281.
- Hopkins, P.D. & Dacey, A., 2008. Vegetarian meat: Could technology save animals and satisfy meat eaters? *Journal of Agricultural and Environmental Ethics*, 21(6), pp.579–596.
- Huis, A. van et al., 2013. *Edible insects. Future prospects for food and feed security*,
- Humphries, J.D., Byron, A. & Humphries, M.J., 2006. Integrin ligands at a glance. *Journal of Cell Science*, 119(19), pp.3901–3903.
- Imaging Technology Group, 2015. Light Microscopy Basics. *Beckam Institute for Advanced Science and Technology*. Available at: <http://virtual.itg.uiuc.edu/> [Accessed November 20, 2015].
- John Innes Centre, 2015. Microscopy @ JIC. Available at: <https://www.jic.ac.uk> [Accessed November 16, 2015].
- Kim, M.-C. et al., 2013. Mathematical analysis of oxygen transfer through polydimethylsiloxane membrane between double layers of cell culture channel and gas chamber in microfluidic oxygenator. *Microfluidics and Nanofluidics*, 15(3), pp.285–296.
- Kislinger, T. et al., 2005. Proteome dynamics during C2C12 myoblast differentiation. *Molecular & cellular proteomics : MCP*, 4(7), pp.887–901.
- Kjær, M., 2004. Role of extracellular matrix in adaptation of tendon and skeletal muscle to mechanical loading. *Physiological reviews*, 84(2), pp.649–98.
- Kosnik, P., Dennis, R. & Vandenberg, H., 2003. Tissue engineering skeletal muscle. *Functional tissue engineering*, pp.377–392.

-
- Lawler, J., 1988. Cell attachment to thrombospondin: the role of ARG-GLY-ASP, calcium, and integrin receptors. *The Journal of Cell Biology*, 107(6), pp.2351–2361.
- Li, W. et al., 2013. Response of C2C12 myoblasts to hypoxia: The relative roles of glucose and oxygen in adaptive cellular metabolism. *BioMed Research International*, 2013, pp.326–346.
- Magidson, V. & Khodjakov, A., 2013. Circumventing Photodamage in Live-Cell Microscopy. In *Methods in cell biology*. pp. 545–560.
- Makerbot Industries, 2014. Materials. Available at: <http://www.makerbot.com/> [Accessed April 22, 2015].
- Marcu, A. et al., 2015. Analogies, metaphors, and wondering about the future: Lay sense-making around synthetic meat. *Public Understanding of Science*, 24(5), pp.547–562.
- Maschmeyer, I. et al., 2015. A four-organ-chip for interconnected long-term co-culture of human intestine, liver, skin and kidney equivalents. *Lab Chip*, 15, pp.2688–2699.
- Mattick, C.S. & Allenby, B.R., 2012. Cultured meat: The systemic implications of an emerging technology. *2012 IEEE International Symposium on Sustainable Systems and Technology (ISSST)*, pp.1–6.
- Medical Device & Diagnostic Industry, 1997. The Effects of High-Energy and EtO Sterilization on Thermoplastics.
- Mehmetoglu, U., Ates, S. & Berber, R., 1996. OXYGEN DIFFUSIVITY IN CALCIUM ALGINATE GEL BEADS CONTAINING GLUCONOBACTER SUBOXIDANS. *Artificial Cells, Blood Substances and Immobility Biotechnology*, 24(2), pp.91–106.
- Methe, K. et al., 2013. Characterization of Decellularized Porcine Hearts as Scaffolds for Tissue-Engineering. *The Journal of Heart and Lung Transplantation*, 32(4), p.S70.
- Millet, L.J. et al., 2007. Microfluidic devices for culturing primary mammalian neurons at low densities. *Lab on a chip*, 7(8), pp.987–994.
- Mondal, P.P. & Diaspro, A., 2014. *Fundamentals of Fluorescence Microscopy - Exploring Life with Light* 2014th ed., Dordrecht: Springer Netherlands.
- Murata, Y., 2000. Use of floating alginate gel beads for stomach-specific drug delivery. *European Journal of Pharmaceutics and Biopharmaceutics*, 50(2), pp.221–226.
- National Cancer Institute, 2014. Skeletal Muscle Structure Image. Available at: <http://training.seer.cancer.gov/anatomy/muscular/structure.html> [Accessed January 31, 2014].
- Naughton, G.K. & Tolbert, W.R., 1996. Tissue Engineering: Skin. In *Yearbook of Cell and Tissue Transplantation 1996–1997*. Dordrecht: Springer Netherlands, pp. 265–274.
- Neville, C. et al., 1997. Skeletal muscle cultures. *Methods in cell biology*, 52, pp.85–116.
- Nicholls, D.G. et al., 2010. Bioenergetic profile experiment using C2C12 myoblast cells. *Journal of visualized experiments : JoVE*, (46), pp.2–7.
- No, D.Y. et al., 2015. 3D liver models on a microplatform: well-defined culture, engineering of liver tissue and liver-on-a-chip. *Lab Chip*.
- Olausson, M. et al., 2014. In Vivo Application of Tissue-Engineered Veins Using Autologous Peripheral Whole Blood: A Proof of Concept Study. *EBioMedicine*, 1(1), pp.72–79.
- Oldfield, R.J., 1994. *Light Microscopy: An Illustrated Guide*, Elsevier Health Sciences.

- Organogenesis Inc., 2015. Dermagraft. Available at: <http://www.dermagraft.com/> [Accessed November 24, 2015].
- Palchesko, R.N. et al., 2012. Development of Polydimethylsiloxane Substrates with Tunable Elastic Modulus to Study Cell Mechanobiology in Muscle and Nerve. *PLoS ONE*, 7(12), p.e51499.
- Pannérec, A., Marazzi, G. & Sassoon, D., 2012. Stem cells in the hood: The skeletal muscle niche. *Trends in Molecular Medicine*, 18(10), pp.599–606.
- Pawar, K., 2010. *IN VITRO AND IN VIVO CHARACTERIZATION OF ALGINATE BASED ANISOTROPIC CAPILLARY HYDROGELS TO GUIDE DIRECTED AXON REGENERATION*. Doctoral Thesis.
- Péault, B. et al., 2007. Stem and Progenitor Cells in Skeletal Muscle Development, Maintenance, and Therapy. *Molecular Therapy*, 15(5), pp.867–877.
- Peng, B. et al., 2014. *Skeletal muscle differentiation in 3D capillary alginate hydrogels*, Gothenburg.
- Pérez-Garijo, A., Fuchs, Y. & Steller, H., 2013. Apoptotic cells can induce non-autonomous apoptosis through the TNF pathway. *eLife*, 2, pp.1–18.
- Perreten, V. et al., 1997. Antibiotic resistance spread in food. *Nature*, 389(6653), pp.801–2.
- Post, M.J., 2014. An alternative animal protein source: cultured beef. *Annals of the New York Academy of Sciences*, 1328(1), pp.29–33.
- Post, M.J., 2014. Cultured beef: medical technology to produce food. *Journal of the Science of Food and Agriculture*, 94(6), pp.1039–1041.
- Post, M.J., 2012. Cultured meat from stem cells: challenges and prospects. *Meat science*, 92(3), pp.297–301.
- Prang, P. et al., 2006. The promotion of oriented axonal regrowth in the injured spinal cord by alginate-based anisotropic capillary hydrogels. *Biomaterials*, 27(19), pp.3560–9.
- Puleo, D.A. & Bizios, R., 2009. *Biological Interactions on Materials Surfaces* D. A. Puleo & R. Bizios, eds., New York, NY: Springer US.
- Rafiq, Q.A. et al., 2013. Culture of human mesenchymal stem cells on microcarriers in a 5 l stirred-tank bioreactor. *Biotechnology Letters*, 35(8), pp.1233–1245.
- Ratner, B.D. et al., 2012. *Biomaterials Science: An Introduction to Materials in Medicine* Third Edit., Academic Press.
- Rowley, J. a., Madlambayan, G. & Mooney, D.J., 1999. Alginate hydrogels as synthetic extracellular matrix materials. *Biomaterials*, 20(1), pp.45–53.
- Rowley, J. a. & Mooney, D.J., 2002. Alginate type and RGD density control myoblast phenotype. *Journal of Biomedical Materials Research*, 60, pp.217–223.
- Sbrana, F. et al., 2008. Role for stress fiber contraction in surface tension development and stretch-activated channel regulation in C2C12 myoblasts. *AJP: Cell Physiology*, 295(1), pp.C160–C172.
- Schuster, E. et al., 2014. Microstructural, mechanical and mass transport properties of isotropic and capillary alginate gels. *Soft matter*, 10(2), pp.357–66.
- Scientific Volume Imaging B.V., 2015. Scientific Volume Imaging. Available at: <https://www.svi.nl> [Accessed November 15, 2015].
- Seahorse Bioscience, 2015. Materials. Available at: <http://www.seahorsebio.com/> [Accessed April 24, 2015].

-
- Shiple, R.J. et al., 2011. A strategy to determine operating parameters in tissue engineering hollow fiber bioreactors. *Biotechnology and Bioengineering*, 108(6), pp.1450–1461.
- Sigma Aldrich, 2015. Materials. Available at: <http://www.sigmaaldrich.com/sweden.html> [Accessed April 22, 2015].
- Stoppel, W.L. et al., 2014. Terminal sterilization of alginate hydrogels: efficacy and impact on mechanical properties. *Journal of biomedical materials research. Part B, Applied biomaterials*, 102(4), pp.877–84.
- Sun, Z.-C., Qun-Li, Y. & Lin, H., 2015. ScienceDirect The environmental prospects of cultured meat in China. *Journal of Integrative Agriculture*, 14(2), pp.234–240.
- Tanaka, H., Matsumura, M. & Veliky, I.A., 1984. Diffusion characteristics of substrates in Ca-alginate gel beads. *Biotechnology and bioengineering*, 26(1), pp.53–8.
- Tedesco, F.S. et al., 2010. Repairing skeletal muscle: regenerative potential of skeletal muscle stem cells. *The Journal of clinical investigation*, 120(1), pp.11–9.
- Temenoff, J.S. & Mikos, A.G., 2008. *Biomaterials: The Intersection of Biology and Materials*, Pearson Education.
- The Anatomical Travelogue LLC., 2014. Semi-striated muscle tissue. Available at: <http://www.thevisualmd.com/> [Accessed November 21, 2014].
- Thermo Fischer Scientific & Life Technologies, 2015. Materials. Available at: <https://www.lifetechnologies.com/se/en/home.html> [Accessed April 22, 2015].
- Thiele, H. & Hallich, K., 1957. Kapillarstrukturen in ionotropen Gelen. *Kolloid-Zeitschrift*, 151(1), pp.1–12.
- Tortora, G.J. & Derrickson, B., 2012. *Essentials of ANATOMY and PHYSIOLOGY* 9th editio., John Wiley & Sons.
- Trotter, J. & Purslow, P., 1992. Functional morphology of the endomysium in series fibered musdes. *Journal of Morphology*, 212(2), pp.109–122.
- Tuomisto, H.L. & de Mattos, M.J.T., 2011. Environmental impacts of cultured meat production. *Environmental science & technology*, 45(14), pp.6117–23.
- Wallin, P., 2009. *Tissue engineering skeletal muscle on elastic fibers - A new bioreactor system for mechanical stimulation*. Chalmers University of Technology. Master of Science Thesis.
- Wegerhoff, R., Weidlich, O. & Kässens, M., 2006. Basics of Light Microscopy & Imaging. , p.56.
- Wild, D.G., 2013. *Immunoassay Handbook - Theory and Applications of Ligand Binding, ELISA and Related Techniques* 4th Editio., Elsevier.
- Willenberg, B.J. et al., 2006. Self-assembled copper-capillary alginate gel scaffolds with oligochitosan support embryonic stem cell growth. *Journal of biomedical materials research. Part A*, 79(2), pp.440–50.
- YAFFE, D. & SAXEL, O., 1977. Serial passaging and differentiation of myogenic cells isolated from dystrophic mouse muscle. *Nature*, 270(5639), pp.725–727.
- Yan, W. et al., 2007. Tissue Engineering of Skeletal Muscle. *Tissue Engineering*, 13(11), pp.2781–2790.
- Zhao, X. et al., 2010. Stress-relaxation behavior in gels with ionic and covalent crosslinks. *Journal of Applied Physics*, 107(6).

Appendices

1 List of Materials

FMC BioPolymer:

- Alginate Protanal RF6650 (food grade)
- Novatech MVG GRGDSP peptide-coupled alginate

Sigma Aldrich:

- Calcium Chloride (CaCl₂)
- Gelatin
- Collagen
- C2C12 cell line
- Fetal Bovine Serum (FBS)
- Horse Serum (HS)
- Dulbecco's Modified Eagle Medium (DMEM)
- sNHS
- EDC
- HEPES buffer
- PBS buffer
- MES buffer
- Rhodamine Phalloidin (RP)
- DAPI
- Triton-X 100
- Ethanol
- Glutaraldehyde
- 0.25 % trypsin EDTA
- Mercaptoethanol
- Sodium Phosphate (Na₃PO₄)

BACHEM:

- GRGDSP - H-Gly-Arg-Gly-Asp-Ser-Pro-OH H-7630

Dow Corning:

- PDMS Sylgard 184
- Sylgard 184 – Silicone Elastomer Curing Agent

Makerbot Industries:

- ABS filament

Thermo Fischer Scientific & Life Technologies:

- lifetechnologies NucBlue live staining

B. Braun:

- Discifix C – three-way stop cock (16494CSF)

2 PDMS Protocol

PDMS moulding

Adapted from Patric Wallin, Chalmers Göteborg

Reagents:

Sylgard 184 PDMS
Sylgard 184 Silicone Elastomer
Curing Agent

Material:

Mixing beaker
Pipette (single use)
Vacuum pump
ABS mould
Petri dish

Protocol:

1. Mix the PDMS and the curer in a 10:1 ratio into the mixing beaker
2. Carefully steer the mix with pipette until the viscosity is equal
3. Degas the mix in the vacuum pump for **1 hour**
4. Place ABS moulds in Petri dishes for easier handling
5. Pour in PDMS into the moulds, start slowly with the delicate structures and then fill up the rest. Carefully prevent additional bubble formation!
6. Let it sit in the fume hood over night to let it slowly degas more and fill in the gabs of the moulds
7. If necessary fill up the moulds to full amount
8. Bake the PDMS for **1 h at 90 °C**
9. Let it cool off
10. Extract PDMS from the mould

3 Sterilization Protocol

Source: Stoppel et al. (Stoppel et al. 2014)

Terminal sterilization of alginate hydrogels

Adapted from Stoppel et al. (PMID: 24259507)

<p>ASEPTIC TECHNIQUES</p> <p><u>Reagents:</u></p> <p>Sterile MilliQ</p> <p>Ethanol 70 %</p>	<p>ASEPTIC TECHNIQUES</p> <p><u>Material:</u></p> <p>1x 50 ml Tube (Waste)</p> <p>1000 µl Pipette (Blue)</p> <p>Well plate (Washing)</p>
--	---

Best performed before cell culture

Protocol:

1. Add alginate gels to the well plate
2. Add ethanol for the gel to immerse fully (*use similar amount for MilliQ washing steps*)
3. Incubate for **20 min at room temperature (RT)**
4. Aspirate media carefully
5. Add MilliQ ► Incubate for at least **5 min at RT**
6. Aspirate media carefully
7. Add MilliQ ► Incubate for at least **5 min at RT**
8. Aspirate media carefully
9. Add MilliQ ► Incubate for at least **10 min at RT**
10. Leave the gels in sterile MilliQ until application
11. If stored for later usage sterile storage conditions have to be ensured

4 Capillary Alginate Protocol

Formation of Capillary Alginate Hydrogels

Do not move the beaker after filling in CaCl₂ *Do not move the beaker after filling in CaCl₂*

Adapted from Ström & Schuster, (personal communication)

Reagents:

MilliQ
Alginate sol. 1.5 % w/w (3 % w/w stock)
Alginate Modification (optional)
CaCl₂ sol. (≤1M)

Material:

Glass beaker
Spray nozzle
Syringe

Protocol:

1. Fill in a small amount of alginate 1.5 % solution in the Glass beaker
2. Turn and tilt the beaker to cover all surfaces; let the excess trip out (turn upside down)
3. Place the beaker in the oven ► at least **1 h at 140 °C**
4. If alginate is dried completely, let beaker cool off
5. Cover with Parafilm, if stored for longer time-period
6. Prepare Alginate solution according to wanted ratios (decrease bubbles)
7. Fill in beaker, e.g. 30 ml in 100 ml sized beaker
8. Spray vertically on top of the alginate solution with CaCl₂ sol.,
3 sprays for 100 ml sized beaker
9. Let beaker sit until a meniscus is observed on the top layer ► **30 mins at RT**
10. Fill up the rest of the beaker to an equal amount as the alginate with CaCl₂ sol.,
Carefully with the syringe to not disrupt meniscus
11. Seal with Parafilm and let it sit for ► **48 hours at RT**
12. Extract gel from beaker and wash it with MilliQ
13. Put it to storage in the fridge or use it for application

Formation of non-capillary alginate can be performed in a similar way omitting the steps 1-5!

5 Two-Step coupling of Proteins Using EDC and NHS or Sulfo-NHS

Source: Life Technologies (Thermo Fischer Scientific & Life Technologies 2015)
<https://www.lifetechnologies.com/se/en/home.html>

Thermo
SCIENTIFIC

Procedure for Two-step Coupling of Proteins Using EDC and NHS or Sulfo-NHS

The following protocol, adapted from a procedure described by Grabarek and Gergely, allows sequential coupling of two proteins without affecting the second protein's carboxyls by exposing them to EDC. This procedure requires quenching the first reaction with a thiol-containing compound.

The activation reaction with EDC and Sulfo-NHS is most efficient at pH 4.5-7.2; however, the reaction of NHS-activated or Sulfo-NHS-activated molecules with primary amines is most efficient at pH 7-8. For best results, perform the first reaction in MES buffer (or other non-amine, non-carboxylate buffer) at pH 5-6, then raise the pH to 7.2-7.5 with phosphate buffer (or other non-amine buffer) immediately before reaction to the amine-containing molecule. For quenching the first reaction, use 2-mercaptoethanol, or the excess reagent can be simply removed (as well as the reaction pH adjusted) by buffer-exchange with a desalting column.

Materials Required

- Activation Buffer: 0.1M MES, 0.5M NaCl, pH 6.0
- Coupling Buffer: Phosphate-buffered saline (PBS), 100mM sodium phosphate, 150mM NaCl; pH 7.2 (Product No. 28372)
- Protein # 1: Prepared in Activation Buffer at 1mg/mL
- Protein # 2: Prepared in Coupling Buffer
- NHS or Sulfo-NHS (Product No. 24500 and 24510, respectively)
- 2-Mercaptoethanol (Product No. 35600)
- (Optional) Zeba™ Spin Desalting Column (Product No. 89891) or other gel filtration column
- Hydroxylamine•HCl (Product No. 26103)

Procedure

1. Equilibrate EDC and NHS to room temperature before opening bottles.
2. Add 0.4mg EDC (~2mM) and 0.6mg of NHS or 1.1mg of sulfo-NHS (~5mM) to 1mL of protein #1 solution and react for 15 minutes at room temperature.
3. Add 1.4μL of 2-mercaptoethanol (final concentration of 20mM) to quench the EDC.
4. Optional: Separate the protein from excess reducing agent and inactivated crosslinker using a desalting column that has been equilibrated with Coupling Buffer (PBS).
5. Add protein #2 to the activated protein at an equal molar ratio with protein #1. Allow the proteins to react for 2 hours at room temperature.
6. To quench the reaction, add hydroxylamine to a final concentration of 10mM. This method hydrolyzes nonreacted NHS present on protein #1 and results in hydroxamate. Other quenching methods involve adding 20-50mM Tris, lysine, glycine or ethanolamine; however, these primary amine-containing compounds modify carboxyls on protein #1.
7. Remove excess quenching reagent using a desalting column.

6 Collagen Coating Protocol

The Collagen coating is adapted from BD Biosciences (BD Biosciences 2015):

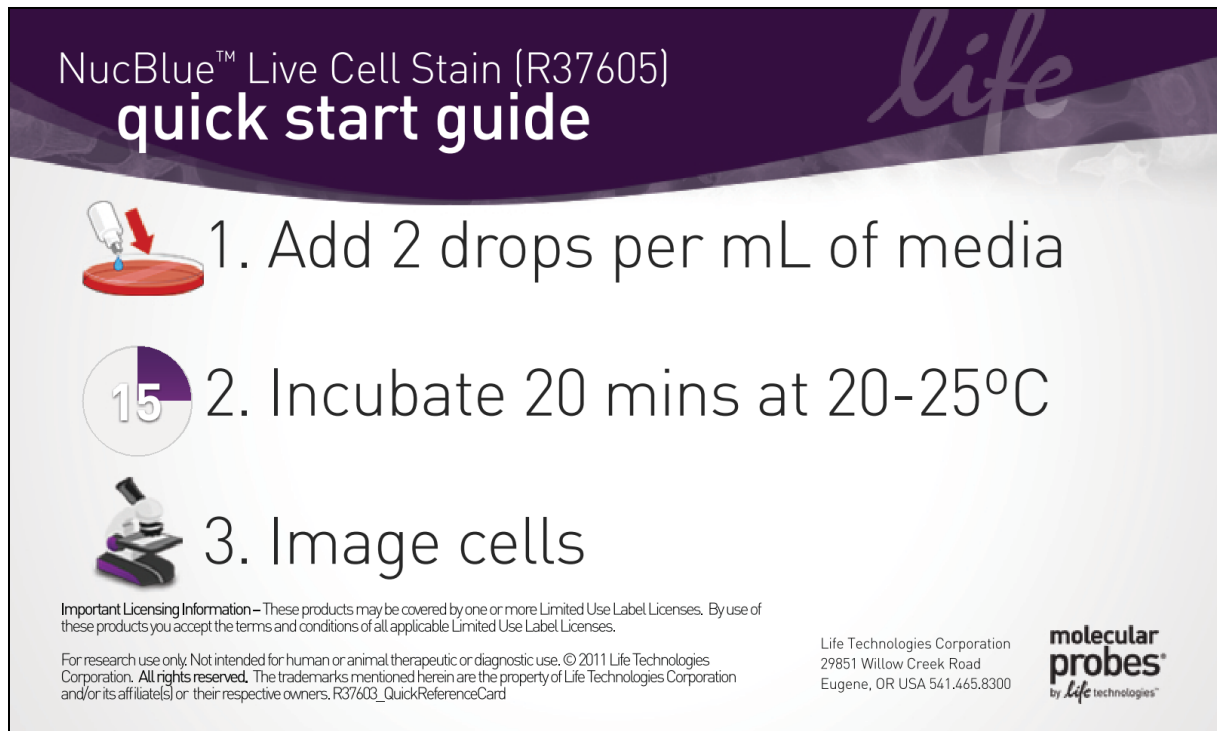
Thin Coating- We recommend using collagen as a thin coating at 5 ug per cm^2 . Please use this as a guideline for determining the optimum concentration for your application.

- 1) Dilute material to 50 ug/ml using 0.02N acetic acid. Collagen is insoluble at neutral pH.
- 2) Add enough diluted material to coat dishes with 5 ug/cm^2 .
For example: A 35mm dish has a surface area of approximately 10 cm^2 . One to two ml of the above solution would be sufficient to cover the dish.
- 3) Incubate at room temperature for one hour.
- 4) Carefully aspirate remaining solution.
- 5) Rinse well to remove acid, using PBS or serum free medium.
- 6) Plates may be used immediately or may be air dried. They may be stored at $2-8^\circ\text{C}$ for up to one week under sterile conditions.

7 NucBlue Protocol

Source: Life Technologies (Thermo Fischer Scientific & Life Technologies 2015)
<https://www.lifetechnologies.com/se/en/home.html>

NucBlue™ Live Cell Stain (R37605)
quick start guide



The quick start guide features a purple header with the product name and 'quick start guide' in white. Below the header, three steps are listed with corresponding icons: 1. Add 2 drops per mL of media (pipette icon), 2. Incubate 20 mins at 20-25°C (timer icon), and 3. Image cells (microscope icon). The background of the guide is light gray with a faint 'life' logo in the top right corner.

1. Add 2 drops per mL of media
2. Incubate 20 mins at 20-25°C
3. Image cells

Important Licensing Information – These products may be covered by one or more Limited Use Label Licenses. By use of these products you accept the terms and conditions of all applicable Limited Use Label Licenses.

For research use only. Not intended for human or animal therapeutic or diagnostic use. © 2011 Life Technologies Corporation. All rights reserved. The trademarks mentioned herein are the property of Life Technologies Corporation and/or its affiliate(s) or their respective owners. R37603_QuickReferenceCard

Life Technologies Corporation
29851 Willow Creek Road
Eugene, OR USA 541.465.8300

molecular probes
by life technologies™

8 Cell Seeding Protocol

Source: Patric Wallin, Chalmers Göteborg

C2C12 seeding	
ASEPTIC TECHNIQUES	ASEPTIC TECHNIQUES
<u>Reagents:</u> Cell solution (with known concentration) Growth medium (GM) (Pre-heated to 37°C)	<u>Material:</u> 1x 50 ml Tube (Waste) 1000 µl Pipette (Blue) 100 µl Pipette (Yellow) (10 ml Transfer pipettes) (5 ml Transfer pipettes) (Pipette Boy)
<u>Protocol:</u>	
<ol style="list-style-type: none">1. Obtain the cell solution according to protocol “Cell passaging” and count the cells to calculate the cell concentration according to protocol “Cell counting”2. Handle all samples and surfaces that are used as cell culture substrates with aseptic techniques and sterilize them before use.3. Label all samples clear information (data, name, cell type, experiment...)4. Add the right amount of media on the cell culture substrate; see table “Culture volumes”.5. Mixing the cell solution regularly during the seeding procedure (shaking every ≈5th pipetting step) to ensure equal cell densities in all samples.6. Pipette the calculated amount of cell solution into each well.7. Gently shake the seeded samples at the end.8. Place the samples in the incubator	

9 Cell Passaging Protocol

Source: Patric Wallin, Chalmers Göteborg

ASEPTIC TECHNIQUES
C2C12 cell passaging
ASEPTIC TECHNIQUES

Reagents:

Phosphor Buffered Saline (PBS)

Trypsin/EDTA 1x (TE)

Fetal Bovine Serum (FBS)

Growth medium (GM) (Pre-heated to 37°C)

Material:

Microscope

1x T-25 Flask

1x 15 ml Tube

1x 50 ml Tube (Waste)

10 ml Transfer pipettes

5 ml Transfer pipettes

Pipette Boy

1000 µl Pipette (Blue)

100 µl Pipette (Yellow)

Protocol:

1. Start the laminar flow hood, wait until the correct speed is established and wipe the metal surface and pipettes with ethanol.
2. Wipe the microscope stage and incubator door with ethanol.
3. Take the cells out of the incubator and check them under the microscope.
4. Take the cells into the laminar flow hood.
5. Remove the media from the cell culture flask with a 10 ml transfer pipette and dispose it in the 50 ml waste tube.
6. Add ≈ 5 ml PBS (from the side, to not detach the cells), move the flask to wash away all remaining media and remove the PBS.
7. Add 1 ml Trypsin/EDTA with the blue pipette and make sure the surface off the flask is completely covered with TE.
8. Incubate the flask for 4 min at 37°C.
9. Shake the flask and make sure that the cells are detached from the surface. Use the microscope to inspect the cells.
10. Deactivate the Trypsin/EDTA by adding 1 ml FBS with the blue pipette.
11. Add 2 ml GM with a 5 ml transfer pipette. Pipette the cell solution up and down, wash the cells from the surface and transfer the solution into a 15 ml tube.
12. Count the cells using the hemocytometer according to protocol "Cell counting".
13. Label the new T-25 flask and add 6 ml GM with a 10 ml transfer pipette
14. Add the calculated amount of cell solution into the flask with the yellow pipette. Before pipetting the cell make sure that you have a homogenous cell solution by gently shaking the tube.
15. Move the T-25 flask to ensure equal cell distribution on the surface and place the flask in the incubator.
16. Clean the laminar flow hood, switch it off and make sure that everything is as it should be before leaving the lab.

10 Cell Counting Protocol

Source: Patric Wallin, Chalmers Göteborg

ASEPTIC TECHNIQUES

Cell Counting

ASEPTIC TECHNIQUES

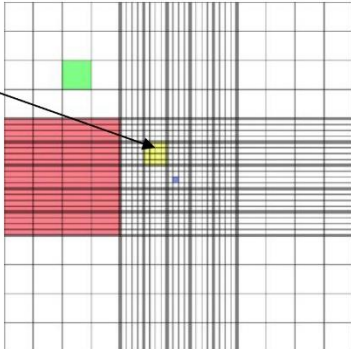
Reagents:
Cell solution

Material:
Microscope
Hemocytometer
20 µl Pipette (Orange)

Protocol:

1. Obtain the cell solution according to protocol “Cell passaging”.
2. Clean the hemocytometer with ethanol and dry it carefully with a special microscope tissue (the hemocytometer is more expensive than it looks like).
3. Wet the outer rim for the top glass slide and place it on top of the hemocytometer slide.
4. Mix the cell solution before pipetting.
5. Add 10 µl cell solution on each side; add the solution slowly to ensure that it is filling the space between the two glasses. Change tips in between the two pipetting steps.
6. Take the hemocytometer to the microscope and focus on the cells/grid.
7. Count at least 2 squares on each side. If there are strong differences between counts on one side count additional squares. If there are strong differences between the two sides repeat the whole preparation and mix cell solution more thoroughly. In cases where the cell density is high it might be beneficial to dilute the cell solution to simplify counting. The number of cells per square should be between 30 and 70.
8. Counting:
 - a. Each square is defined by a triple line and contains 4x4 small compartments.
 - b. All corners of the square should be visible in one field of wide before counting.
 - c. The usual practice is to include cells overlapping the top and left lines, but not those overlapping the bottom or right lines.
 - d. Write down the cell count for the square and count the next one.
9. Calculation:
 - a. Calculate the average from all cell counts.
 - b. Multiply the number by 10.000 that is the number of cells per ml
 - c. Multiply this number with the amount of cell solution (normally 3-4 ml), in order to know the total number of cells
10. Clean the hemocytometer with ethanol and put it back in the box.

Counting Square
with 4x4 compartments



11 Cell Fixation Protocol

Source: Patric Wallin, Chalmers Göteborg

Cell Fixation	
ASEPTIC TECHNIQUES	ASEPTIC TECHNIQUES
<u>Reagents:</u> Phosphor Buffered Saline (PBS) Paraformaldehyde 4% (Fixative solution) (cold)	<u>Material:</u> Microscope 1x 50 ml Tube (Waste) 1000 µl Pipette (Blue)
<u>Protocol:</u> <ol style="list-style-type: none">1. Start the laminar flow hood, wait until the correct speed is established and wipe the metal surface and pipettes with ethanol.2. Wipe the microscope stage and incubator door with ethanol.3. Take the cells out of the incubator and check them under the microscope.4. Take the cells into the laminar flow hood.5. Remove the media from the sample and dispose it in the 50 ml waste tube.6. Add PBS, similar amount as culture medium, to wash the sample and remove the PBS after gentle shaking.7. Add 4% fixative solution, use as much as you need to cover the whole sample.8. Incubate for 20 min at 4°C.9. Remove the fixative and dispose it in the 50 ml waste tube.10. Wash the sample with PBS:<ol style="list-style-type: none">a. Add PBS, similar amount as beforeb. Remove PBSc. Add PBS, similar amount as befored. Remove PBSe. Add PBS, the amount should be sufficient to ensure that the sample does not dry out too fast.11. Store the sample at 4°C for up to several weeks before staining and imaging. Check regularly if PBS needs to be added to avoid drying.	

12 Cell Staining Protocol

Source: Patric Wallin, Chalmers Göteborg

Working in the dark	Cell Staining	Working in the dark
<p><u>Reagents:</u> Phosphor Buffered Saline (PBS) Staining solution (pre-heated)</p> <ul style="list-style-type: none">- DAPI 1:1000- Rhodamin/Phalloidin 1:400- 0.1% Triton-X 100- PBS		<p><u>Material:</u> 1x 50 ml Tube (Waste) 1000 µl Pipette (Blue)</p>
<p><u>Protocol:</u></p> <ol style="list-style-type: none">1. Pre-heat and mixed the staining solution by putting it in the Sonicator for 20 min.2. Remove the PBS from the sample and dispose it in the 50 ml waste tube3. Add staining solution to sample, use just enough to cover it (it is expensive).4. Incubate for 30 min at room temperature.5. Remove the staining solution and dispose it in the 50 ml waste tube.6. Wash the sample with PBS:<ol style="list-style-type: none">a. Add PBS, similar amount as was in the sample beforeb. Remove PBSc. Add PBS, similar amount as befored. Remove PBSe. Add PBS, the amount should be sufficient to use the immersion lens.7. Store the sample wrapped in aluminum foil to avoid photo bleaching at 4°C.8. Image the sample with the Zeiss fluorescence microscope according to protocol "Cell imaging".		

13 MHC Staining Protocol

Working in the dark**Myosin Heavy Chain
staining C2C12****Working in the dark**

Adapted from Patric Wallin, Chalmers Göteborg

Reagents:

Phosphate Buffered Saline (PBS)

Fixative 4 % Formaldehyde in PBS (ice-cold)**Blocking solution:**

- 3 % Milk Powder
- 0.1 % Triton-X 100
- PBS

Primary antibody:

- 1:1000 Anti-Myosin MY32 produced in mouse M4276 Sigma

Secondary antibody:

- 1:2000 Anti-mouse Alexa Fluor 488 or Alexa Fluor 594

Staining Solution:

- Rhodamin:Phalloidin 1:400
- DAPI 1:1000
- 0.1 % Triton-X 100
- PBS

Material:

1x 50 ml Tube (Waste)

1000 µl Pipette (Blue)

Protocol:

1. Remove media
2. Wash with PBS 1x
3. Fixate cells with ice cold fixative ► Incubate for **30 min at 4 °C**
4. Wash with PBS 1x
5. Add blocking solution ► Incubate for **10 min at room temperature (RT)**
6. Aspirate the solution
7. Add primary antibody 1:1000 in blocking solution ► Incubate for **1 hour at RT**
8. Wash with blocking solution 3x
9. Add secondary antibody 1:2000 in blocking solution ► Incubate for **1 hour at RT**
10. Wash with PBS 3x
11. Add Staining solution ► Incubate for **30 min at RT in the dark**
12. Wash with PBS 3x
13. Add mounting media carefully (optional step)
14. Keep the samples in the dark & Image

14 3D Cell Seeding Protocol

Aseptic techniques

3D Cell Seeding

Aseptic techniques

Material:

4x Three-way stop cocks
Pump with Luer-lok connectors
5 ml Eppendorf
with tubing + Luer-lok connectors (2x)

Syringes:

- 2x 10 ml syringes
- 2.5 ml syringe

Sterilized components:

- Culture Stand
- PDMS channel (bottom and top part)
- ABS retainer
- Screws (4x), washers (8x), nuts (8x)
- Overflow cup (250 ml)

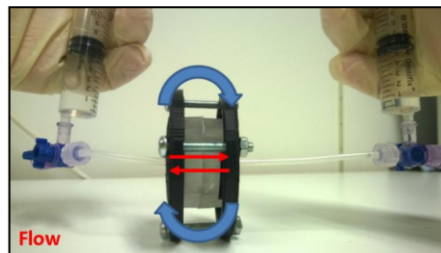
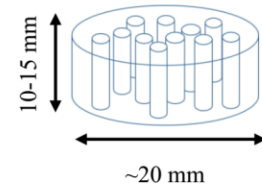
Reagents:

Ethanol 70 %
Sterile MilliQ
Growth Media (GM)

Protocol:

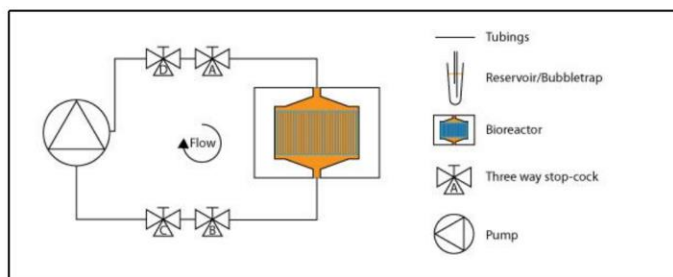
1. Cut the capillary alginate generously for the culture chamber,
Test capillary flow through by dropping on water, otherwise re-cut
2. Sterilize according to the Alginate Sterilization Protocol
3. Suspend alginate gel in GM ► Incubate overnight **12 hours at 37 °C**
4. Work in LAF bench;

Place alginate in PDMS channel and assemble the bioreactor around plus three-way stop cocks

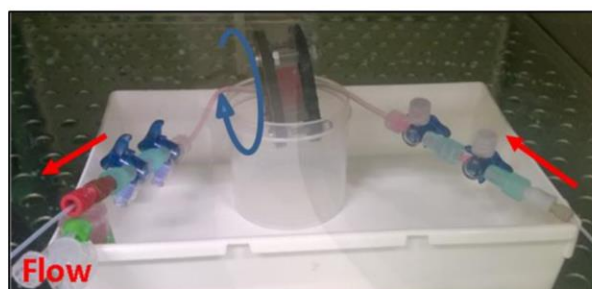


5. Fill two 10 ml syringes with ~5 ml GM , flush with alternating direction until air is out of the system, close stop cocks and place it in the incubator until used further

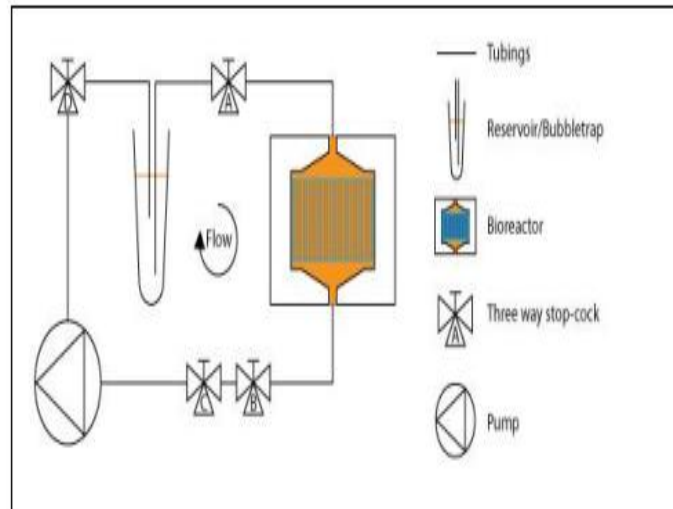
6. Prepare the pump + set up computer, connect two three-way stop cocks to the ends of the tubing on each site clean the pump (Ethanol ► sterile MilliQ)



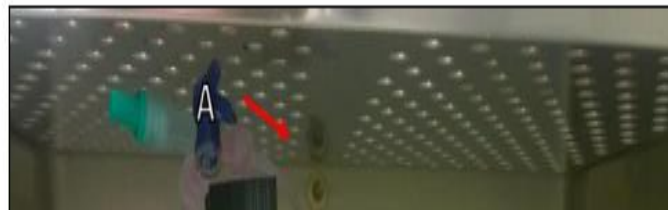
7. Take bioreactor from the incubator, place in culture stand and connect as shown in the schematic above
8. Flush between the connectors D-A and C-B with GM with the help of syringes
9. Connect 10 ml syringe with 10 ml GM to connector B and one empty syringe on A
10. Turn on the pump to flush the left half of the system with GM,
Make sure that every air bubble is out of the system until proceeding!!!
11. Prepare 2.5 ml syringe with cell solution for seeding
12. Connect a waste syringe to D and connect syringe with cell solution to A
13. Let the pump draw in cell solution ► **10 µl/s (~3 min)**
14. When the syringe at A is empty switch to closed loop, let it run for at least another 3 min and turn of the flow



15. Place it in Incubator as shown above ► **Incubate for 30 min at 37 °C**
 16. Closed loop ► **5 µl/s for 5 min**
 17. Turn bioreactor 90° according to rotation in picture above
 18. **Incubate for 1 hour at 37 °C**
 19. Place bioreactor in culture stand
- } Repeat four times
Turn back in original position before last waiting times



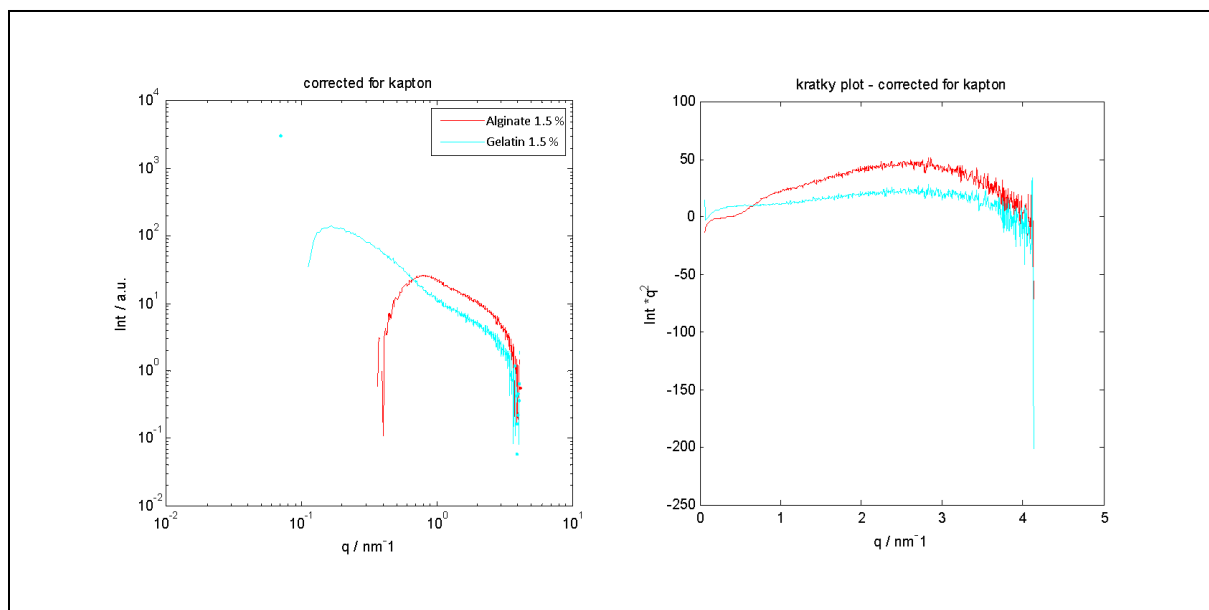
20. Add in bubble trap (5 ml Eppendorf tube), fill with GM and flush the tubing from connector D and A ► make sure that no air reaches the bioreactor from connector A
21. Place the set-up in the incubator like in the figure below



15 SAXS results

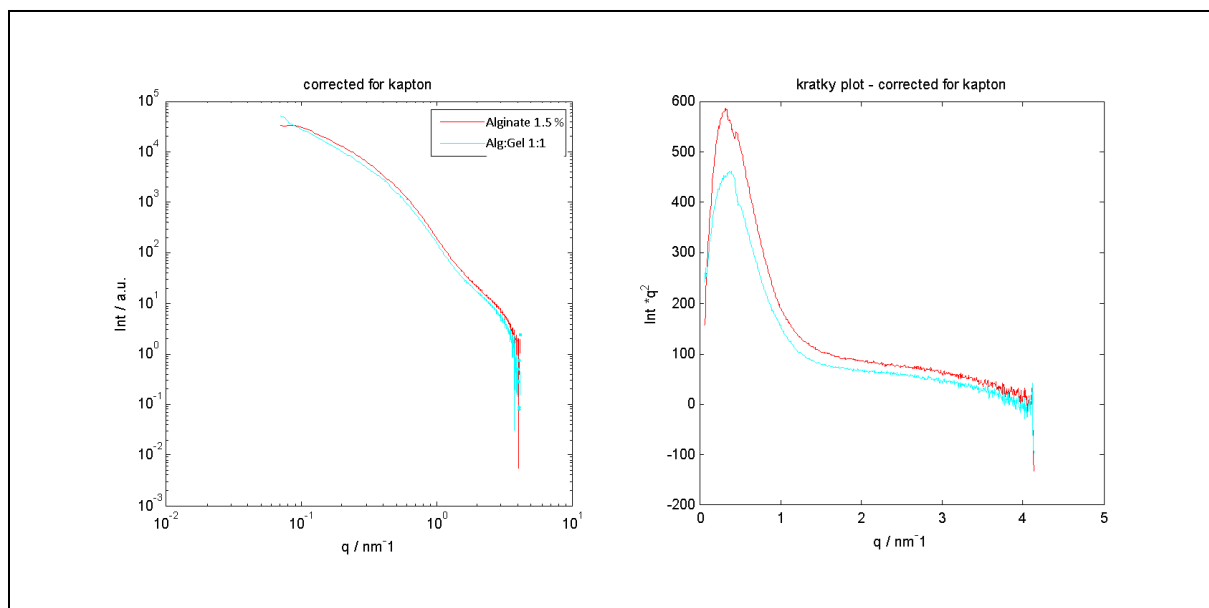
Reference solutions measured

1.5 % w/w alginate and 1.5 % w/w gelatin



Capillary gel measured

1.5 % w/w alginate capillary gel and gelatin:alginate 1:1 capillary gel



16 Estimation of the Relative Amount of Surface Interaction

Pore size (Peng et al. 2014):

$$d_{pores} = 78\mu m \quad (4)$$

Pore density (Peng et al. 2014):

$$\rho_{pores} = 30 \text{ pores/mm}^2 \quad (5)$$

Scaffold size:

$$\begin{aligned} h &= 10mm \\ d &= 17.5mm \end{aligned} \quad (6)$$

Penetration depth (Rowley et al. 1999):

$$p = 50nm \quad (7)$$

Total amount of pores in the gel:

$$\begin{aligned} n_p &= A_g \cdot \rho_{pores} \\ n_p &= \pi \cdot \left(\frac{d}{2}\right)^2 \cdot \rho_{pores} \\ n_p &= \pi \cdot \left(\frac{17.5mm}{2}\right)^2 \cdot 30 \text{ pores/mm}^2 \\ \underline{\underline{n_p}} &= \underline{\underline{7216 \text{ pores}}} \end{aligned} \quad (8)$$

Active volume of a singular capillary:

$$\begin{aligned} r_{pores} &= d_{pores} \div 2 \\ r_{pores} &= 78\mu m \div 2 \\ \underline{\underline{r_{pores}}} &= \underline{\underline{39.00\mu m}} \end{aligned} \quad (9)$$

$$\begin{aligned} R_{pores} &= r_{pores} + p \\ R_{pores} &= 39\mu m + 50nm \\ \underline{\underline{R_{pores}}} &= \underline{\underline{39.05\mu m}} \end{aligned} \quad (10)$$

$$\begin{aligned} A_{active} &= \pi(R^2 - r^2) \\ A_{active} &= \pi((39.05\mu m)^2 - (39\mu m)^2) \\ \underline{\underline{A_{active}}} &= \underline{\underline{12.26\mu m^2}} \end{aligned} \quad (11)$$

$$\begin{aligned}
 V_{active} &= A_{active} \cdot h \\
 V_{active} &= 12.26\mu m^2 \cdot 10.00mm \\
 \underline{\underline{V_{active} &= 0.1226mm^3}}
 \end{aligned} \tag{12}$$

Active volume of all capillaries:

$$\begin{aligned}
 V_{total} &= V_{active} \cdot n_p \\
 V_{total} &= 0.1226mm^3 \cdot 7216pores \\
 \underline{\underline{V_{total} &= 884.6816mm^3}}
 \end{aligned} \tag{13}$$

Total volume of gel:

$$\begin{aligned}
 V_{gel} &= V_{outer} - V_{capillaries} \\
 V_{gel} &= \left[h \cdot \pi \left(\frac{d}{2} \right)^2 \right] - \left[h \cdot \pi \left(\frac{d_{pore}}{2} \right)^2 \cdot n_p \right] \\
 V_{gel} &= \left[10mm \cdot \pi \left(\frac{17.5mm}{2} \right)^2 \right] - \left[10mm \cdot \pi \left(\frac{39\mu m}{2} \right)^2 \cdot 7216pores \right] \\
 V_{gel} &= 2405.28mm^3 - 86.20mm^3 \\
 \underline{\underline{V_{gel} &= 2319.08mm^3}}
 \end{aligned} \tag{14}$$

Relative volume accessible by the cells:

$$\begin{aligned}
 V_{rel.} &= \frac{V_{total}}{V_{gel}} \cdot 100\% \\
 V_{rel.} &= \frac{884.6816mm^3}{2319.080mm^3} \cdot 100\% \\
 \underline{\underline{V_{rel.} &= 0.0381\%}}
 \end{aligned} \tag{15}$$

17 Estimating the cell numbers for a confluent seeding

Pore size (Peng et al. 2014):

$$d_{pores} = 78\mu m \quad (16)$$

Pore density (Peng et al. 2014):

$$\rho_{pores} = 30 \frac{pores}{mm^2} \quad (17)$$

Scaffold size:

$$\begin{aligned} h &= 10mm \\ d &= 17.5mm \end{aligned} \quad (18)$$

Total amount of pores in the gel:

$$\begin{aligned} n_p &= A_g \cdot \rho_{pores} \\ n_p &= \pi \cdot \left(\frac{d}{2}\right)^2 \cdot \rho_{pores} \\ n_p &= \pi \cdot \left(\frac{17.5mm}{2}\right)^2 \cdot 30 \frac{pores}{mm^2} \\ \underline{\underline{n_p}} &= \underline{\underline{7216 pores}} \end{aligned} \quad (19)$$

Cell nuclei density of a skeletal muscle fibre (Bruusgaard et al. 2003):

$$d_{nuclei} = 50 \text{ Nuclei}/mm \quad (20)$$

Initial cell amount for maturation process:

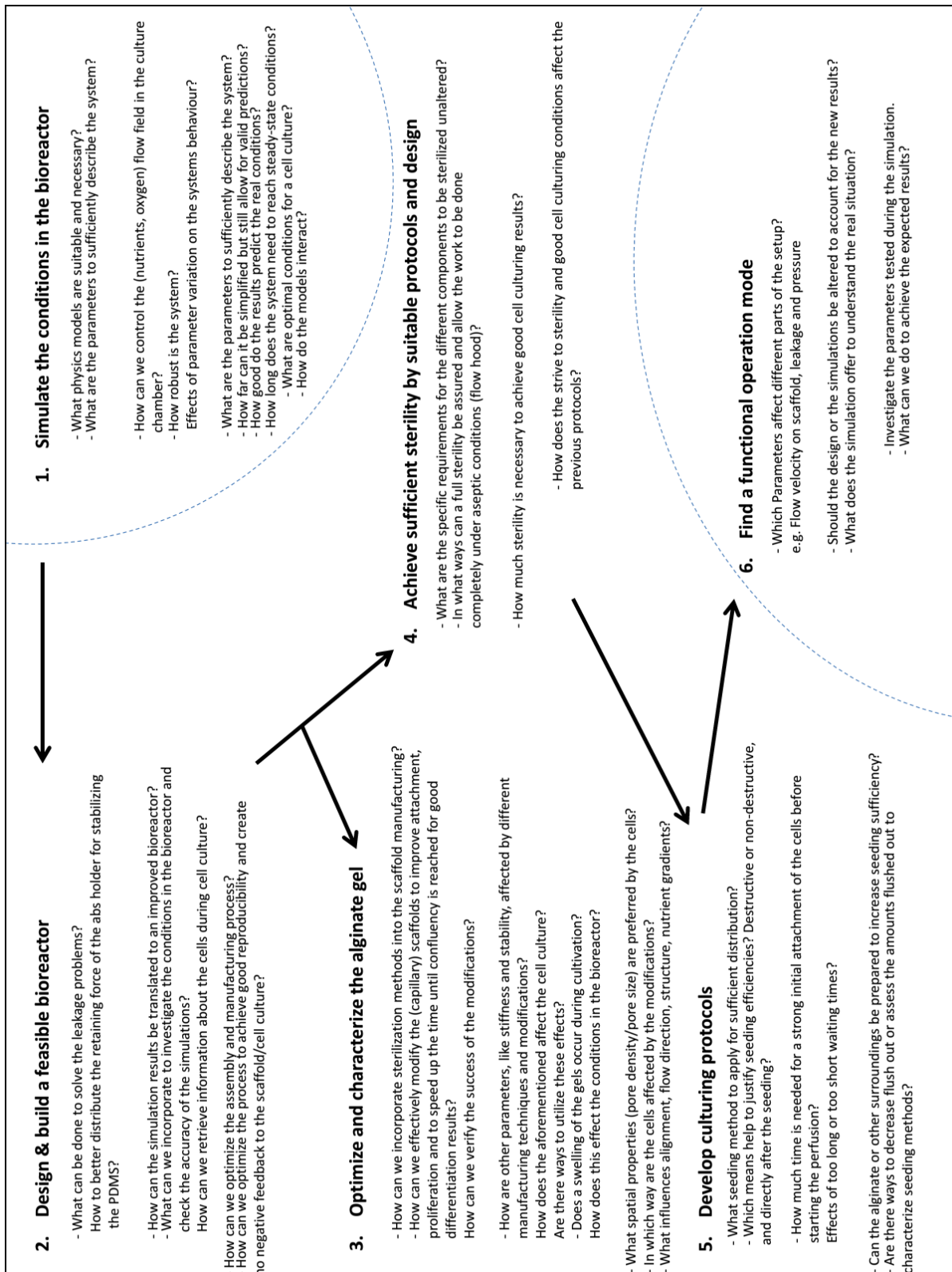
$$\begin{aligned} n_{cells} &= d_{nuclei} \cdot n_p \cdot h \\ n_{cells} &= 50 \frac{\text{Nuclei}}{mm} \cdot 7216 \text{ pores} \cdot 10mm \\ \underline{\underline{n_{cells}}} &= \underline{\underline{3,608,000 cells \approx 4,000,000 cells}} \end{aligned} \quad (21)$$

Revision after half time report

Project Week	24	25	26	27	28	29	30	31	32	33	34	35	36	37	38	39	40
Dates	May			June			July			August			Sep				
Calendar week	19	20	21	24	25	27	28	29	30	31	32	33	34	37	38	39	40
Task and Milestones																	
Report Writing																	
Final Report																	
Simulation																	
Add nutrient simulation																	
Re-visit simulation and adjust																	
Material																	
Adjust RGD content																	
Surface modifications																	
Flat Gel Experiments																	
Cultures on RGD-modified Alginate																	
Investigate the alignment on cap. Gels																	
Imaging																	
Capillary Gel Experiments																	
Conduct first experiments																	
Develop & evaluate seeding protocols																	
Proliferation & Differentiation testing																	
Assessing the culture status																	
Investigate culturing times																	
Imaging																	

19 Questions to be Addressed

Collection of Questions to be addressed for the project, from the planning report. Used for planning and visualising the contents of the project.



20 Overview Mind map

The mind map showing categorizing the different experiment into their respective categories. Used for planning during the half time report.

